UNIVERSITY OF LINCOLN

School of Engineering
College of Science

The Design and Realisation of a 3D-Printed Myoelectric Prosthetic Arm for Toddlers Utilising Soft Grippers

Daniel Richard De Barrie

MSc by Research

January 2020

The Design and Realisation of a 3D-Printed Myoelectric Prosthetic Arm for Toddlers Utilising Soft Grippers

Daniel Richard De Barrie

A thesis submitted in partial fulfilment of the requirements of the University of Lincoln for the degree of MSc by Research

January 2020

Abstract

A prosthetic device aims to improve an amputee's ability to perform activities of daily living, by mimicking the function of a biological arm. The use of a prosthesis has also been shown to minimise some of the issues facing amputees, such as poor posture and muscular skeletal pain. Active, myoelectric-controlled prosthetic arms have primarily focused on adults, despite evidence showing the benefits of early adoption in reducing the rejection rates and aiding in proper motor neural development.

This work presents SIMPA, a low-cost 3D-printed prosthetic arm with a soft-gripper based end device. The arm has been designed using CAD and 3D-scaning and manufactured using predominantly 3D-printing techniques. This all serves the aim of reducing cost and lead-time, both crucial aspects for prosthetic manufacturing, particularly with the rapid growth rates of young children.

A voluntary opening control system utilising an armband based (surface electromyography) sEMG has been developed concurrently. This simple control system acts as a base for more advanced control structures as the child develops. Grasp tests have resulted in an average effectiveness of 87%, with objects in excess of 400g being securely grasped. Force tests have shown that the arm is performing in line with current adult prosthetic devices. The results highlight the effectiveness of soft grippers as an end device in prosthetics, as well as viability of toddler-scale 3D-printed myoelectric devices.

Acknowledgements

Statements and Declarations

Declaration of Originality

This dissertation contains no material which has been accepted for a degree or diploma by the University or any other institution, except by way of background information and duly acknowledged in the dissertation, and to the best of my knowledge and belief no material previously published or written by another person except where due acknowledgement is made in the text of the dissertation, nor does the dissertation contain any material that infringes copyright.

Signed:

Date: 31/01/2020

Statement of Ethical Conduct

This project presented no issues requiring Ethical Approval and was self-certified by the project supervisor. The research was carried out in compliance with the University's ethical guidelines for library/desk/laboratory/studio-based research, with Health and Safety regulations, and with all other relevant University policies and procedures.

Table of Contents

List of Figures

List of Tables

1 Introduction & Significance of Study

The aim of this project is to design and realise a 3D-printed prosthetic arm for toddlers. This introduction will go over some background information and look at the significance of this study. An overview of the appropriate healthcare systems and relevant literature will also be reviewed, with the goal of defining the project further.

1.1 Background Information

Congenital upper limb reduction defects occur in 4.1-5.0 per 10,000 births [1], with transverse deformities effecting around 2.9/10,000 [2]. Other non-congenital deformities also affect infants, though there is limited work identifying the proportion effected; a 1988 to 1996 study found that dysvascular[1], trauma-related, and cancer related conditions had a respective frequency of 2.25, 2.65, and 0.15 per 100,000 between the ages of 0-14 years [3].

Upper limb amputation[2] can be categorised based on the severity of the reduction, this ranges from transphalangeal (where part of one or more of the digits on the hand are missing) to forequarter (where the whole arm, including the shoulder socket is missing). For this project, the focus is on near elbow amputations, specifically high-level transradial, elbow dislocation and low-level transhumeral. Amputations are also categorised as unilateral (where a limb is missing from only side of the body), or bilateral (where both limbs exhibit a reduction defect).

---

[1] Amputations that are caused or acquired due to a limb's poor vascular condition.
[2] In this work the term "amputation" will refer to both congenital and traumatic limb loss.
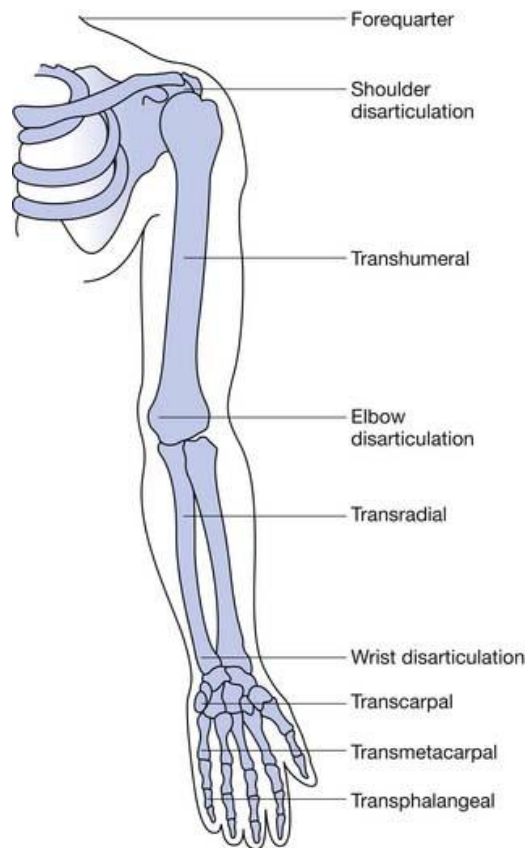
Figure 1.1 Types of upper extremity amputations [4]

In cases of limb amputation, a prosthetic device is often used to replicate the function and/or appearance of its biological counterpart. For upper limbs, prosthetics can be classified as passive or active. A passive prosthetic hand is mostly used for cosmetic reasons [5], and as such will not typically have any grip functionality. Passive devices may also come in the form of tools, rather than a hand, and are designed to be specialised for certain tasks, such as griping the handlebar of a bicycle [6].

Figure 1.2 Ottobock Passive Arm Prosthetic [7]

Conversely, active devices allow for end device to dynamically grasp an object. Active devices can broadly be defined into three subcategories [8], body-powered, myoelectric, and hybrid. A body-powered device utilises the movement of the individual's remaining limb and/or torso to open and close the end device. This end device may be hook like or designed to appear more like a human hand.
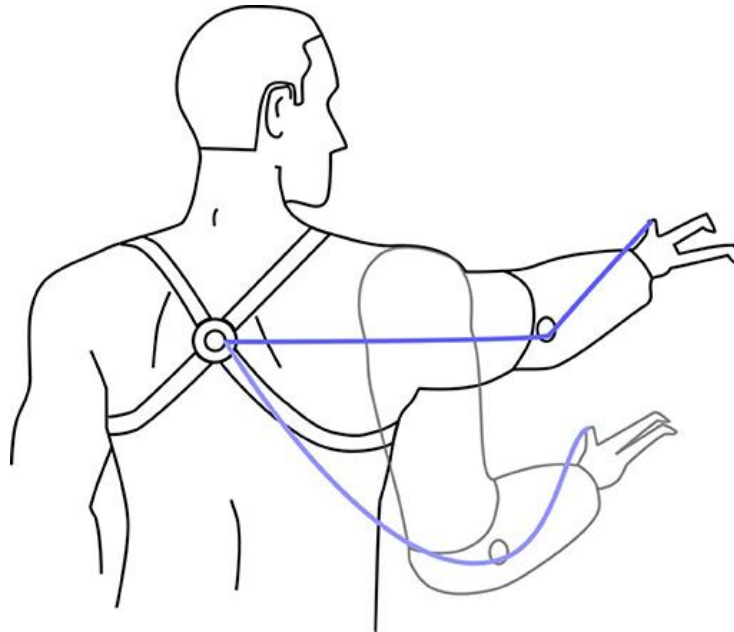
Figure 1.3 Example of a Cable Driven Body Powered Device [9]

An externally powered device is driven by an external source (i.e. a battery), rather than by the mechanical movement of the individual's body. These devices are often controlled via electromyography[3] (EMG), these are known as myoelectric prosthetics. These have the advantage of not requiring a complex system of straps/harnesses and are generally more discrete. Myoelectric devices are also often capable of performing a range of grasping gestures.

---

[3] The recording of the electrical activity of muscle tissue.
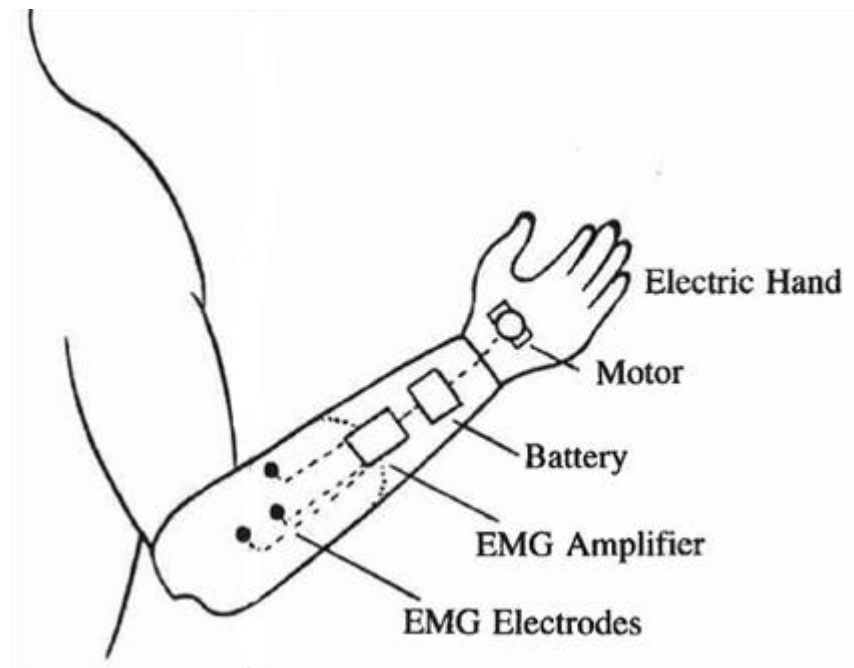
Figure 1.4 Overview of a Myoelectric Prosthetic Device [10]

The final type of active device is hybrid prosthetics, these utilise a mixture of both external and body-powered components, such as a body-powered elbow and a battery-powered end device. Typically, this style of prosthetic is used with high level amputation (transhumeral and above).

1.2 Background Literature

Congenital upper limb deficiencies, without the aid of a prosthetic, results in the patient recognising the stump as the end of the limb. This in turn during early childhood develops the motor neural skills and proprioception up to the base of the stump, resulting in the child developing their own methods of grasping objects [11], with later difficulty adapting to methods using a prosthetic device.

Physical conditions as a result of limb loss are also present. Muscle atrophy occurs in cases where a lack of activity causes the muscle to weaken and reduce in size; this is apparent in amputees as the affected limb will normally be used less frequently and bare no or minimal load [12]. Targeted physiotherapy can reduce muscle atrophy, although this is not always readily available [13] and may be unworkable depending on the receptiveness of the child. The fitting of a prosthetic that allows functionally, such as grasping and lifting objects, can aid in the natural development of these muscles, though some reduction in muscle mass will likely still be present. This development can also provide a muscular base for the eventual fitting of a larger adult prosthetic.

In the long term, amputation may also cause issues with posture and muscular-skeletal pain [14] due to an overreliance on the residual limb and off balance centre of mass [15][16]. This in adulthood can cause deformation of the spine, affecting many aspects of life. B. Greitemann [17] examined instances of unilateral upper limb amputation have been shown to result in asymmetrical posture and musculature,

concluding that properly weighted prosthetics can offset this tendency. If this is done in infancy, it may help to prevent such issues from ever occurring, as opposed to being corrective later in life. Furthermore, the fitting of an active prosthetic can take the strain off the residual limb side and promotes a more natural, balanced approach to grasping activities.

According to [18], 20% of congenital limb deficiency (CLD) patents studied experienced phantom limb pain (PLP), with 42% of young amputees (under age 6 at time of amputation) reporting PLP. This study refutes the notion that congenital deformities are not subject to PLP and goes further to show that PLP is more commonly felt whilst not wearing a prosthetic, indicating a correlation between prosthetic use and reduced PLP in cases of CLD and young age amputation. The study does not explore this fully and further work would serve to highlight the true scale of the correlation; a focus on this as well as the effect different prosthetics have on PLP, could then feasibly provide meaningful data to aid in the design process. M. V. Johnston [19] references PLP being associated with neural plasticity, as the brain is developed areas prior to amputation that now must adjust; the disparity seemingly causing the pain. This could explain the reduction in PLP from prosthetic use seen in [18], however this study does not comment on it and it is thought no research on the subject has been published.

Though the consensus across the literature is that wearing a prosthetic device is beneficial, there are still counter arguments that the generalised devices (rather than task specific tools) provide little day to day benefit, outside of helping with social acceptance [20]. It should be noted that this study only looked at children unilateral congenital below-the-elbow deficiency, and its findings may not be relevant for other higher level or bilateral cases. An estimated 90% of daily living tasks (ADLs) can be performed unilaterally [21], [22]. This may also point to why in one study found that 89% of those surveyed who rejected a prosthetic felt that they were "simply more functional without the prosthesis" [23].

Still the consensus remains that prosthetic use is beneficial, however despite this prosthetic rejection rates are high, with various studies showing around 20% of upper limb amputees across all ages reported not using any prosthetic device [24], [25]. Looking across all prosthetic device types, there is a general consensus that early fitting reduces reduction rates [26]–[28]. This reduction is seemingly quite significant, with one study showing a rejection rate for fitting before and after the age of 2 years of 22% and 58% respectively [29]. A 2002 study covering the use of myoelectric infant prosthetics [30], also found a correlation between early adoption and duration of daily use. The level of amputation was also found to influence the acceptance rate, with transhumeral correlating with increased usage compared to transradial.

The question of whether a myoelectric device specially reduces rejection in comparison to a body powered or passive device is difficult to fully answer. A review of North American clinics showed a preference for fitting a passive device at 6 months, followed by an active device around 18 months [31].

It is noted however that few clinics use objective tests to measure outcomes of fitting and does not cover the topic of rejection rates. One review study [24] found there was a mean rejection rate in paediatric populations of 45% and 35% for body powered and myoelectric devices respectively. This would suggest that from rejection rate standpoint, there is a benefit to fitting a myoelectric device. However, a long-term study from 2002 [32] in which patients were provided with a variety of prosthetic options at a young age, showed that only 15% selected the myoelectric device as their primary prosthesis. This study however, like many which look at this topic, was conducted over a decade ago and may not be relevant with more modern myoelectric prosthetics. A review study also concluded that there is insufficient evidence to conclude that myoelectric devices have a significant general advantage compared to body powered devices [33].

One of the key factors in reducing rejection rates seems to be the child's and family's perception of the device as functional [34]. If there is a perceived benefit to using the device, and an adequate level of comfort is achieved, then the likelihood of rejection is reduced [25], [27]. An ongoing study in collaboration with the National Health Service (NHS) England, claims that function is the primary factor in rejection [35]. It also states that cost is the primary limiting factor and is exploring the use a new lower-cost 3D printed myoelectric device for patients aged 8 to 18 exhibiting transradial limb reduction.

In comparison to passive devices, there is a substantial amount of maintenance and support needed to operate a myoelectric device, such as fitting the prosthetic, changing the batteries and encouragement to use the powered prosthesis. This family support, alongside clinical training appears to be a key factor in whether or not the child will accept the device in the long term [28]; it was also shown in [30] that an intense training program significantly influences the acceptance rate. This study also showed that issues of weight, reliability and battery life of a myoelectric prosthetic were a primary concern for the parents surveyed. This points to how myoelectric devices can often be perceived as being too complex, expensive and heavy, particularly with young children. With the advent of more advanced manufacturing techniques such as 3D-printing, alongside improved electrical components and batteries, these apprehensions to myoelectric devices may be countered. This is evident in the UK with NHS England's recently policy update to "cover future production of smaller child appropriate multi grip hands and digits" [36], along with the ongoing study into the feasibility of additively manufactured paediatric prosthetics [35]. The proposed prosthetic arm in this work aims to highlight how these advancements could be used to produce a lightweight and functional myoelectric upper limb prosthetic for young children.

1.3 Healthcare Systems

1.3.1 UK Healthcare Systems

For the vast majority of people in the UK, the primary healthcare provider is the NHS. This is a universal public healthcare system that is segregated between the UK's four countries. NHS England is the largest and will be the primary focus in this work. The policies between all countries typically quite similar due the budgetary restrictions in place at a UK level. In the UK, private healthcare makes up a small amount of the overall healthcare system, with it mostly being used for elective procedures, or by those unwilling to wait to have the procedure with the NHS. With regards to prosthetics, Bupa, one of the main private providers, does offer prosthetic and orthotic support [37], though this has a negligible impact compared to the NHS

There are currently a number of systems in place within the NHS to provide care to those with limb deformities, with spending of around £60 million per year on these services [38]. Approximately 55,000 – 60,000 patients make use of the prosthetic services, across 35 centres throughout England.

The cost of a prosthetic currently is very high, as such the NHS is reluctant to provide them to infants, due to the rapid growth rate. This is particularly true for active prosthetics, with the cost being considerably higher than for a simple passive device. It is unlikely with the current political climate that a significant increase in NHS funding will become available [39], hence cost reduction is the most effective way to provide adequate support.

As of 2017, NHS England began a trial using 3D-printed bionic limbs. The £5,000 limbs took just a single day to manufacture [40], compared to traditional active prosthetics that cost up to £80,000 and at least 12 weeks to be produced [41], [42]. A second trail is planned with SBRI Healthcare. The NHS also recently allocated funding for lower limb sports prosthetics, with an undeclared share of £750,000 also being spend on developing bionic upper limb prosthetics [43].

1.3.2 International Healthcare Systems

As this project will take place in the UK, the focus is naturally on the British healthcare system, however the nature of a cheap customisable prosthetic devices lends itself to healthcare systems in the low-income nations [44]. 3D-printing and CAD allows for decentralised design; in areas where proper infrastructure and access to medical resources are limited, this approach would allow much of the engineering to be carried out remotely, with the device only requiring fitting on location. The cost of an active prosthetic in high-income nations, such as the USA, is upwards of $20,000 [45], with even simple cosmetic options costing around $3000-$5000. In low-income nations an expense on this scale for a custom fit prosthetic device is totally unfeasible, especially with many families already facing hardship as a result of the amputation [46]. By reducing the cost of these devices with 3D-printing and other advanced manufacturing techniques, it is anticipated that developing nations will slowly adopt

these practices. Even in high-income nations such as Canada, Australia, and Japan only 35-40% use a myoelectric prosthetic due to cost-driven restrictions on their healthcare policies [47].

1.4   Additive Manufacturing Technologies

Additive manufacturing or 3D-printing has emerged in recent years as a viable technology for producing prosthetic devices. There is a growing interest in researching this topic due to the low material and labour cost, rapid production, and high geometric complexity that can be achieved using additive manufacturing technology. Literature mostly focusing on upper limb prosthetics has been reviewed here, along with a brief overview of some of the current 3D-printed devices that are being produced.

1.4.1   Literature Surrounding Upper Limb Prosthetics

Kate et al [48] provides an overview of the use of 3D-printing within the confines of prosthetic production. 58 devices are examined in total, with the work noting the lack of resources in peer-reviewed literature necessitating a wider scope, utilising websites and databases as sources. This same limitation is present within this literature review. Of the 58 devices looked at, 46 (79%) utilise fused deposition modelling (FDM), with the most common materials being acrylonitrile butadiene styrene (ABS) and polylactic acid (PLA). The study highlights how these materials are non-compliant, lacking the subtleness of human skin as a grasping surface, resulting in a poor grasp. The use of soft materials in the end grip device would likely help to improve grip performance. It is now possible to print with such soft materials, opening up new possibilities.

In [49] the design and realisation of a 3D-printed prosthetic hand is explored. The hand is predominantly made of 3D-printed components, with the rest of the arm being manufactured in a more traditional way. The scale is for that of an adult male and the hand has been given 6 degrees of freedom (DOF). The device has been tested on an amputee patient and reportedly is able to grasp a range of objects, though this is limited to 250g due to the grip strength.

Patrick Slade et al [50] developed an open source 3D-printed hand, that again is scaled for an adult. The design of this hand is somewhat similar, though no consideration is given to the rest of the arm. This focus on a high DOF adult size hand is common across literature, with studies such as [51] and [52] presenting very similar designs.

The process of designing, testing and manufacturing a custom prosthetic for a partial hand amputee patient in order to play the French horn was explored in [53]. The study notes how underutilised CAD and 3D-printing are within the development/manufacture of prosthetics in the UK, with 'hand skills' instead being preferred. The case report puts forward a process whereby 3D-scanning is first used, followed by 3D-modelling, finite element analysis (FEA), 3D-printing, and eventual product evaluation. The research highlights how in the UK a qualified person is responsible for specifying the design characteristics to the manufacturer of a custom prosthetic, who in turn is responsible for

producing appropriate documentation regarding design and performance. The use of CAD/computer-aided manufacturing (CAM) and FEA could streamline the process and show that a product it is fit for purpose before manufacturing has begun. The study claims that a competent person, through online resources, could learn the CAD techniques needed for the showcased project, underlining how current prosthetists could be retrained with relative ease.

Cabibihan [54] showcased a method of producing a 3D-printed passive prosthetic that closely matches the appearance of the residual limb. The study uses computer tomography (CT) images of the residual limb, mirrors them, and creates a detailed CAD model for the prosthetic. The stump on the affected limb is also imaged using a CT scanner so that a socket model can be created. The two models are combined to form a complete prosthetic design. The work argues the advantages of 3D-printings rapid specialised production and relative low cost are ideally suited to prosthetic design. Its most key aspect is the use of CT as a means of 3D-scanning a patient's limbs. In developed nations, such as the UK, CT scanners are commonplace in hospitals and could be utilised for this application, mitigating the need for additional 3D-scanning technology to be acquired. The study is primarily concerned with the appearance of the device and as such mostly focuses on passive technology.

Only one example of a myoelectric 3D-printed device with a life-like appearance has been found in literature. Yoshikawa et al [55], presented a 3D-printed prosthetic that has been shaped to match a human hand, allowing the fitting of a lifelike cosmetic glove. The design also features a socket suitable for transradial users. Tests centred on activities of daily living (ADL) showcased the viability of the system as a usable prosthetic. This device and many others in published literature focus on the low material and parts cost (US$1250 in this instance) but this fails to factor in the cost of labour and the cost of development and regulatory compliance; the "low-cost" aspect of such devices therefore should be scrutinised.

With almost all the literature reviewed here, the focus is on adult devices which by now are starting to achieve a level of sophistication. A simple body-powered hand for children is explored in [56]. The open source hand is very basic in its design, being powered by the user moving their wrist to pull on cables within the fingers, as such it is only suitable for those with transcarpal/transmetacarpal amputation. The study does not give any details regarding validating the functionality of the hand, nor discusses the durability of the device. The work also does not state the age range that such a device would be suitable for. Zuniga et al [57] also looked at the development of a paediatric device. This body-powered prosthetic has been designed for patients with shoulder dislocation. The device is fully 3D-printed and is one of few examples of a 3D-printed device featuring a shoulder joint. The device lacks the grip strength to be used unilaterally, however with bilateral tasks and as a transitionary device to prepare for a heavier more complex prosthetic, it appears to perform well.

Whilst there is a deal of excitement about the prospect of 3D printed prosthetics, it is important to look at them critically in the context being a viable medical device, rather than simply a research project or hobbyist creation. A 2018 review [58] looked at 8 papers which all reported human trials of 3D printed upper-limb prosthetics. The study found that whilst promising results have been shown, none of the trails have been conducted as long-term randomised trials, with most acting as a proof-of-concept rather than a rigorous assessment of the device. Metrics common for the analysis of traditional prosthetics, such as the Southampton Hand Assessment Procedure (SHAP), were not used in the validation of these 3D-printed devices. Similar criticism of current 3D printing trials is found in [59], with the work outlining its own methodology for a yearlong trial, with a focus on user reported usage of the device. The results of this study have yet to be published.

There are now a number of unregulated open-source devices which can be downloaded and produced by anyone with access to a 3D-printer. These open-source designs are not regulated and are often produced and fitted without the consultation of medical professionals [60]. Without this consultation and a strong regulatory framework, 3D-printed devices should not be considered acceptable alternatives to regulated devices. There is also a risk that a device may cause injury due to material failure, or that a user may be put off using a prosthetic because of inadequate support and training. The issue of manufacturer liability with 3D-printing is an ongoing debate [61], this potentially becomes even more problematic with medical devices such as prosthetics. This is yet another area which needs to be considered in greater detail, particularly with regards to the open-source movement.

1.4.2 Current 3D-Printed Paediatric Prosthetics

Currently there are several 3D-printed active prosthetic options commercially available for children, including both myoelectric and body-powered devices; some of these are shown in Table 1.1. The traditional method of prosthetic manufacturing typically involves an end device unit being manufactured in set sizes to then be fixed to a custom cast constructed socket. There are very limited options for young children, with manufacturers typically concentrating on the more profitable adult market. The Otto Block Electrohand 2000 [62] is one example of a product that can be used for infants as young as one and half years old, due to its small size. Its high cost, along with the additional expense of other electrical components, wrist unit, and the socket means that often it is an unaffordable option.

Table 1.1 Examples of Currently Available Paediatric Upper Limb Prosthetic Devices

Product name, manufacturer	Design	Actuation type	Custom fit?	Age range (years old)
Team UnLimbited	 *Figure 1.5 UnLimbited Arm* [63]	Body-powered	Yes	~5 onwards
Limbitless Arm, Limbitless solutions	 *Figure 1.6 Limbitless Arm* [64]	Myoelectric	Yes	~7 onwards
Hero Arm, Open Bionics	 *Figure 1.7 Hero Arm* [65]	Myoelectric	Yes	8 onwards

As a counter to the expensive traditional options, a number of small organisations have sprung up producing 3D-printed custom fit prosthetics, for both children and adults. All of these limbs are custom made and can be decorated to the user's preference, such as having superhero decals or a football team logo; this moves away from the lifelike appearance prosthetics tend to follow.

Team UnLimbited [63] is an open source charity organisation that provides tools to easily customise and manufacture their 3D-printed body-powered prosthetic. The design of the prosthetic is very simple and is attached to the affected limb with hook and loop straps. In cases where no other option is available, this device may prove useful, however the simplicity and relative flimsiness put into question the overall effectiveness of such a prosthetic. Without any form medical safety validation, there is a risk of injury present when using such a device Such a safety risk has been brought up in an opinion piece by the Professional Standards Officer for the Australian Orthotic Prosthetic Association [66], the piece goes on to cover the multi-faceted risks that hobbyist medical professionals can present.

The remaining two arms looked at in Table 1.1, the Limbitless Arm [64] and the Hero Arm [65] are both myoelectric controlled and present a sturdier socket design. Crucially both companies are working with governing medical bodies, in the USA and UK respectively, to ensure safety standards are met. Both showcase an affordable and functional prosthetic option, though there is still relatively little uptake as prosthetists are still unsure of the merits of additive manufacturing, though this appears to be slowly changing. The Hero Arm having been medically approved is now available in a number of high-income countries, including the UK, USA, and France. The cost of this device varies due to the custom nature

of each prosthetic, from between £3,000 ($4000) to around £10,000 ($13,300). This presents a substantial reduction from the $25,000-$70,000 (£18,500-£52,000) cost of other commercially available myoelectric hands [67], [68]. Unlike the papers reviewed in section 1.4.1, this is the actual market cost of the device; a rare but positive example of a 3D-printed device demonstrating a real cost reduction rather than one that is simply hypothesised from lower material/manufacturing costs.

Across all the 3D-printed designs looked at, none are producing limbs for children younger than 5 for body-powered and around 7 for myoelectric. This is likely due to the additional space and weight constraints, along with the increased support required to introduce a prosthetic to a young child. As discussed in section **Error! Reference source not found.**, early adoption is important for reducing rejection rates, with cost and lead times often being the primary factor in making infant myoelectric devices unviable. To this end a 3D-printed prosthetic aimed specifically at young children may be able to provide a functional and economically viable alternative to the current commercial devices.

1.5   Soft Grippers

A key aspect of upper limb prosthetics is the end grasping device; typically, this resembles a human hand, though this does not necessarily have to be the case. Work focusing on soft, flexible gripping devices that utilise 3D-printing and/or other advanced technologies has emerged, most of this focuses on robotics used within the agricultural sector.

Slesarenko et al [69] scrutinised various designs for 3D-printing a cable driven soft actuator. The 3D-printing method uses a multi nozzle print-head that allows for multiple materials to be printed together, this permits reinforcement at key points to ensure the cable deforms the gripper in the appropriate way. The study details different designs with slits and reinforcement, ultimately producing a gripper that maximised strength, whilst retraining a flexible grip. The work ends by demonstrating how the gripper can be used to pick up strawberries damage-free, without requiring a grip force feedback system, instead the design itself naturally applies a genital grip. The research does not mention a prosthetic application for such a system; however it is conceivable that such a technology could transfer over and provide a lightweight, flexible grasp device.

A design for a cable-driven soft gripper is presented in [70]. The device is powered by a DC motor and utilises three finger-like grippers. The cable, when pulled, closes the fingers, thus achieving a grasp; when the tension is released, the gripper returns to its previous state by releasing the elastic energy stored in the material during bending.
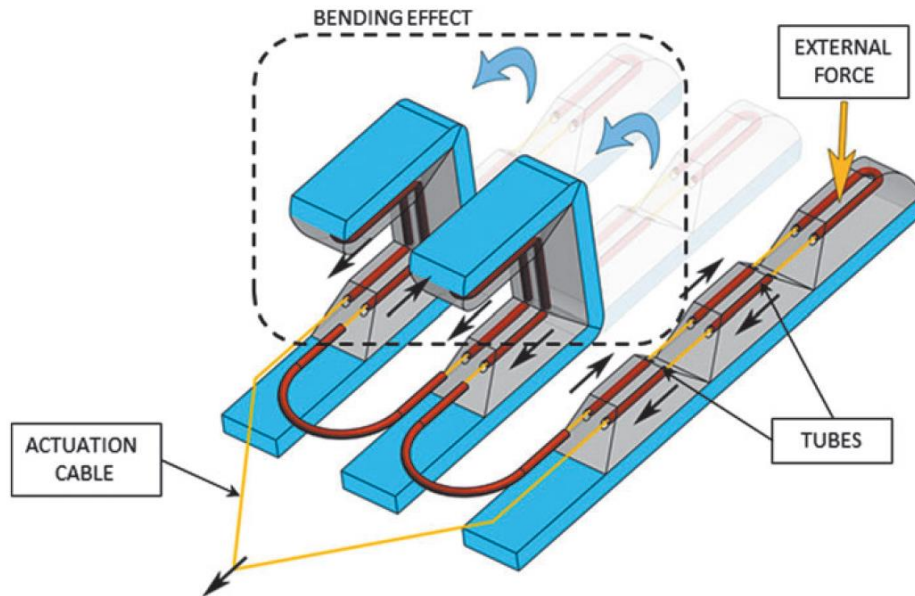
Figure 1.8 The adaptability of the soft actuator mechanism [70]

Tubes within the grippers allow the cable to move freely, this has the benefit of allowing one or more of the grippers to have a force acting upon it, whilst still allowing the other digits to move. This in practice allows for objects with non-uniform geometry to be grasped as the digits contract to various extents. The experimental procedure was designed to validate the performance of the device in achieving a stable grasp, with objects of various geometry being grasped successfully. Each digit has a 135mm length and total hand weight (excluding the DC motor) of 110g. Clearly this scale is outside the realm paediatric prosthetic devices, though as the paper references it could be scaled down.

Low et al [71] presented a soft actuator for use in prosthetics. The actuator created was 3D-printed and uses a pneumatic driven system. The design follows a pattern of reinforced segments to control the actuation. Pneumatic actuators, like those described in the study, could be integrated within a child's prosthetic, the need for compressed gas however makes it undesirable compared to an electrically driven design; the complex control system required for such a device is also problematic.

Polygerinos [72] explores hydraulic actuators. A glove was fitted with hydraulic actuators, to increase the wearer's grip strength. This system appeared to achieve good results; however, it required the user to wear a belt containing pumps and a fluid reservoir. No published research regarding the use of hydraulic actuators in prosthetics has been identified. Much like pneumatic devices, the use of a hydraulic gripper would necessitate a complex control system.

1.6   Control Systems

In this subchapter the control aspect of active prosthetic devices will be investigated. Typically, active devices will be controlled using electromyography (EMG), in conjunction with a micro controller. Alternative methods of control have been proposed, some working in combination with EMG, though

these have not seen wide scale adoption. Electromyography or EMG is the process of recording electrical signals produced by muscles under flexion. The technique has been widely adopted in medical applications [73], including prosthetic control [74]. The recording is most commonly conducted with sensors on the surface of the skin, this is known as surface electromyography (sEMG). Another approach is intramuscular electromyography, whereby wire/needle electrodes are threaded into the muscle tissue; this can result in a superior recording [75]. Surface EMG is generally favoured due to it being a non-invasive procedure, especially with paediatric devices. Surface EMG can be broken down further into four subcategories:

1. **Single-site, single-action:** this system uses a single detection site which once a single threshold is met preforms an action, e.g. opening a grasp.

2. **Single-site, multi-action:** this is the same as the previous system however here the amplitude of the signal is considered, e.g. different grasps for low, mid, and high-level signals.

3. **Multi-site, single-action:** here multiple sEMG sites are used to create a more robust detection system, only a single action would be performed with this method.

4. **Multi-action, multi-site:** this is the most advanced method of sEMG, whereby multiple sites are used, each with a different action, e.g. different grasp types, wrist or elbow actuation, etc.

Muzumdar [76] describes these methods as a potential paediatric EMG control systems. The recommendation for a child's first myoelectric prosthetic is to use a single point, single action system, known as the "Cookie Crusher". The method involves the hand being in a closed position by default, with the hand voluntarily opening with a detected muscle flex. Initially the sensitivity of the system can be set quite high, so that the child becomes aware of the hand's movement. As they begin to master the gesture, the sensitivity can be reduced. The more advanced systems such as "single site two level sensitive" (where the system can exist in low, mid-point, or high position) can be introduced later, by reprogramming the control unit. The work only looks at simple surface EMG and does not reference any studies backing up its effectiveness, though the simplicity of this method means that it is like to be the initial control system regardless of the potential sophistication of signal acquisition method. Other studies also point to the 'cookie crusher' being the preferred means of control [77] for an introductory myoelectric prosthetic.

Whilst sEMG prosthetic control is well adopted technique, many users find it difficult or frustrating [78], [79], with this potentially leading to rejection of the prosthetic. This frustration may be due in part to several factors, including inconstant EMG response. There is a notion that a user is able to develop an EMG skill, improving the reactiveness of their prosthetic. One study [80] proposed a framework to assess the EMG skill of a user and the unpredictability of the signal acquisition in

comparison to daily prosthetic usage. Through this procedure it hoped that issues from either user skill or the signal acquisition can be identified, with a corrective procedure then implemented.

The use of video games controlled via EMG to develop their 'EMG skill' has been examined [81]. The study compares 5 games, developed by visual art and design staff and students at the University of Central Florida. The games are controlled wholly or in part, through the use of a myoelectric sensor [82], with the aim being to teach children the appropriate muscle movements required for an 'action' signal to be registered. This 'action' signal would translate into a 'grasp' signal when using a single gesture prosthetic. The tests highlighted how players would often have trouble returning a muscle to a resting state, particularly with extended gameplay sessions. This requires more investigation but does seem to highlight the importance of training the muscle to relax as well as flex. A continuation of the study showed that child users of prosthetics indicated high usability and user enjoyment whilst controlling the games with EMG [83].

One of the primary issues with sEMG is the requirement for a clear muscle signal recording. In the case of young children with underdeveloped musculature or instances where part of the recorded muscle is missing (i.e. in cases of limb reduction), the signal may be too weak for reliable use in a control system. Ensuring proper electrode contact and selecting the correct placement site(s) can aid in this, though in some cases the recorded EMG may still be quite weak. This can be made worse in cases where the child is too young to understand verbal instruction to perform the flex/reaction needed. A proposed system whereby the threshold values of the EMG can be adjusted remotely has been shown to be effective, achieving 89% discrimination rate in children [84]. The system is design to aid in the critical training process and the adjustment can be performed parent of the user. As mentioned in section **Error! Reference source not found.**, a strong training period has been shown to reduce rejection rates. A system such as this where a parent or medical professional can make adjustments to the control system during this training phase, may aid in the process of configuring the prosthetic, whilst also demonstrating the devices value to the child.

1.7 Project Publications

The project has produced the three publications listed below:

- D. De Barrie, R.Margetts, K.Goher. "SIMPA: Soft-grasp Infant Myoelectric Prosthetic Arm", IEEE Robotics and Automation Letters (RA-L). (Published January 23rd 2019).

- D. De Barrie, R.Margetts, K.Goher. "SIMPA: Soft-grasp Infant Myoelectric Prosthetic Arm", International Conference on Robotics and Automation (ICRA 2020), Palais des Congrès de Paris, France, 31 May - 4 June 2020. (Accepted January 22th 2020).

- D. De Barrie, K.Goher. "Conceptual Design of 3d-Printed Active Prosthetic Arm with Soft Grippers for Toddlers", 22nd International Conference on Climbing and Walking Robots and the Support Technologies for Mobile Machines (CLAWAR 2019), Kuala Lumpur, Malaysia, 26-28 August 2019. (Published).

1.8   Chapter Summary

From exploring current literature, it is clear that there have been major advancements 3D-printed prosthetics, with some now starting to become commercially available. Despite this however, there has been little work focusing on devices for young children, despite evidence displaying the benefits of early adoption in minimising prosthetic rejection rates. A gap to investigate the feasibility of utilising these advancements and immerging technologies in the field of paediatric prosthetics has become apparent. The most up-to-date study on myoelectric prosthetic use in young children was conducted in 2002 [30], since then there has been very little academic or industrial work in this area.

The consensus across the published literature is that early adoption fosters a decrease in prosthetic rejection and an increase in the time spent in wearing the device. The limiting factors in ensuing early fitting identified include, but are not limited to, the following:

- High initial financial cost,
- Rapid replacement cycles due to the child's growth,
- Strict dimensional and weight restrictions,
- Long lead-times, and
- Limited functionality
- An ineffective/frustrating control system

This project's intention is to demonstrate that filling this gap for a myoelectric prosthetic for toddlers is possible with advanced manufacturing techniques, such as additive manufacturing, being utilised to overcome many of the restrictions that have traditionally held back the mass adoption of infant bionics. This project will deliver a functioning prototype of a 3D-printed myoelectric device to showcase the viability of motorised toddler prosthetics.

In the subsequent chapter the design process of the prosthetic arm and soft grippers will be covered, from the concept selection up to the realisation of the final prototype.

2   Prosthetic Design & Realisation

This chapter will cover the design and realisation of the prosthetic, with the proceeding chapter focusing on the control aspects of the device. The design was based on specifications determined from the literature review process, predominately focusing on grasp effectiveness, low-cost, and ease of use and suitability for young children. A concept selection matrix was used to select the most effective of the five produced concept designs. The selected design is then described in three segments: the gripper design, the main arm design, and the socket design. The design was predominantly conducted in Autodesk Inventor (Autodesk Inc.) with the components, including all the prototypes, being manufactured using the Ultimaker S5 (Ultimaker B.V.) 3D-printer.

2.1   Design Specifications

The below specifications are based around information gathered during the literature review. Focus is given on producing a device suitable for the target audience of young upper limb amputees, that meets the project criteria of utilising 3D-printing and advanced manufacturing techniques in an effort to demonstrate a potential reduction in lead-time and production costs.

- **The primary focus will be on high level transradial patients:** this is due primarily to available patient data. The original project outline was to conduct this research with a volunteer, this sadly was not fully realised, however the design still follows their biometrics. A transhumeral and elbow dislocation variant is considered but not developed.

- **The device must be suitable for children between the ages of 2 and 5 years old:** the biometrics used in the design are from a 4-year-old child, the final design should also be scalable to work with other young children within this range. This focus on early stage paediatric devices follows the findings presented in section **Error! Reference source not found.** regarding early adoption reducing rejection rates.

- **The weight of the arm should not exceed the weight of a biological counterpart:** for a 4-year-old child this is around 400g. The centre if mass should also be located close to the sump as to reduce the moment of force.

- **Demonstrate low production costs and lead times**: this should demonstrate as others have that 3D-printing techniques can offer low production costs. It is hoped that this could translate to a market cost saving compared to traditionally manufactured prosthetics as has been shown with the Hero Arm, though this is outside of the scope of this project. The low production cost is also with consideration for how the device could be utilised in low-income nations.

- **Wherever possible additive manufacturing is to be utilised**: the flexibility of design and rapidness of 3D-printing is to be taken advantage of for both for prototyping and with regards to final production specifications. This is in line with a growing body of work demonstrating the potential of 3D-printing prosthetic devices.

- **The arm will be printed as a single unit**: the main body is to be printed as one single part, resulting in a fixed wrist. This is done as to maximise the structural integrity of the arm and reduce complexity. An adjustable wrist would add weight and it is not seen as overly beneficial in a device aimed at young children.

- **CAD, 3D-scanning, FEA and other computer aided technology will be used primarily:** the project aims to show an alternative development and production method to casting and other traditional techniques. The digital design process also aims to demonstrate how a decentralised design may be used in cases where the user is unable to easily access a prosthetic clinic.

- **The prosthetic is to be controlled electronically via sEMG placed on the upper arm:** the project aims to produce a myoelectric device, as to deliver high grasping functionality. Whilst other control methods do exist, EMG is the most widely accepted and utilised. The sensor placement on the bicep is due to the level of amputation, it is assumed that the bicep will generate better EMG signal than the stump of the remaining forearm.

- **The control system will be voluntary opening:** the "cookie crusher" method as described in section 1.6, is the most wildly used for young children and acts as a starting point to accustom the user with myoelectric control.

- **Hand must be capable of grasping everyday objects**: as discussed in section **Error! Reference source not found.**, function is perceived as one of the most important factors in a prosthetic device. The hand should therefore be able to perform simple grasping tasks and basic tasks of daily living which would be typical for a young child.

2.2   Concept Selection

From the design specifications, five concept designs were produced. These designs exist only as basic free hand drawings, with the only the determined optimal design being worked on further, making the transition into a CAD model. All the below designs would have been produced using 3D-printing, with the electrical components being contained within the body of the arm once assembled. Similarly, all designs would be controlled by the user via EMG of some kind. The primary difference with all the designs is the end grasping device.

2.2.1   Concept A – Lever Driven Hand

This design utilises a DC motor driven spring-toggle joint, similar to those found in plasterboard fixtures, which would operate the gripper. The grippers would be fixed structures with no joints for flexibility. The spring toggle mechanism could likely not be 3D printed, though compliant mechanisms have shown some promise and could possibly be utilised in a design like this with some modifications of the spring-toggle concept [85].
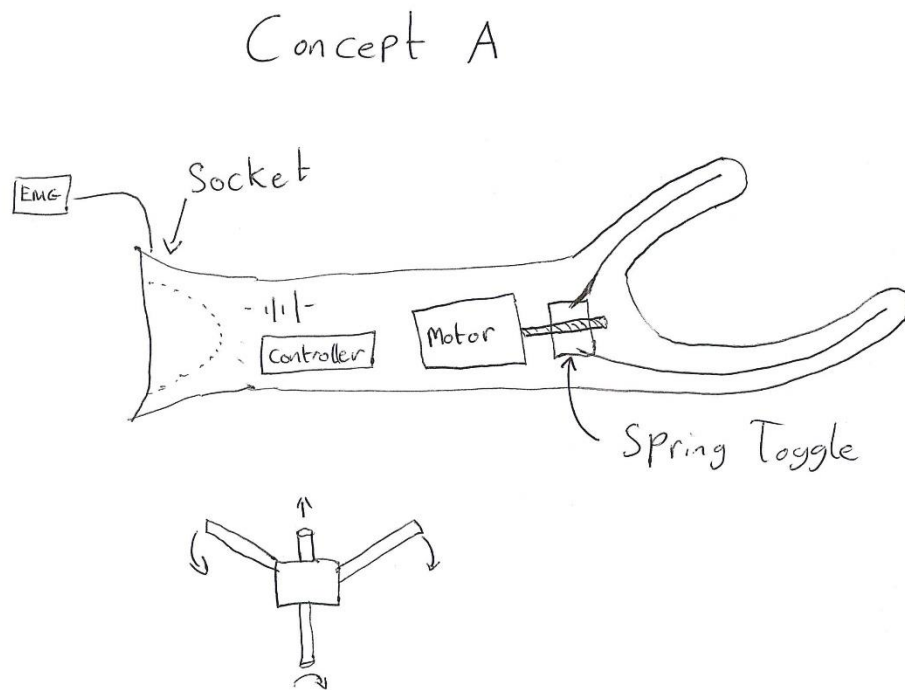
Figure 2.1 Concept Design A

2.2.2 Concept B – Cable Driven Thumb Grip

This concept would utilise a segmented "thumb". The gripper would be threaded with a wire/string that when pulled would cause the "thumb" to close against the palm and static "fingers", forming the grasp. An elastic material would be incorporated into the design of the gripper to return it to its extended state once tension is released. A second wire could also be used instead to drive the motor in the open position, though this method would not be preferred due to the additional complexity.
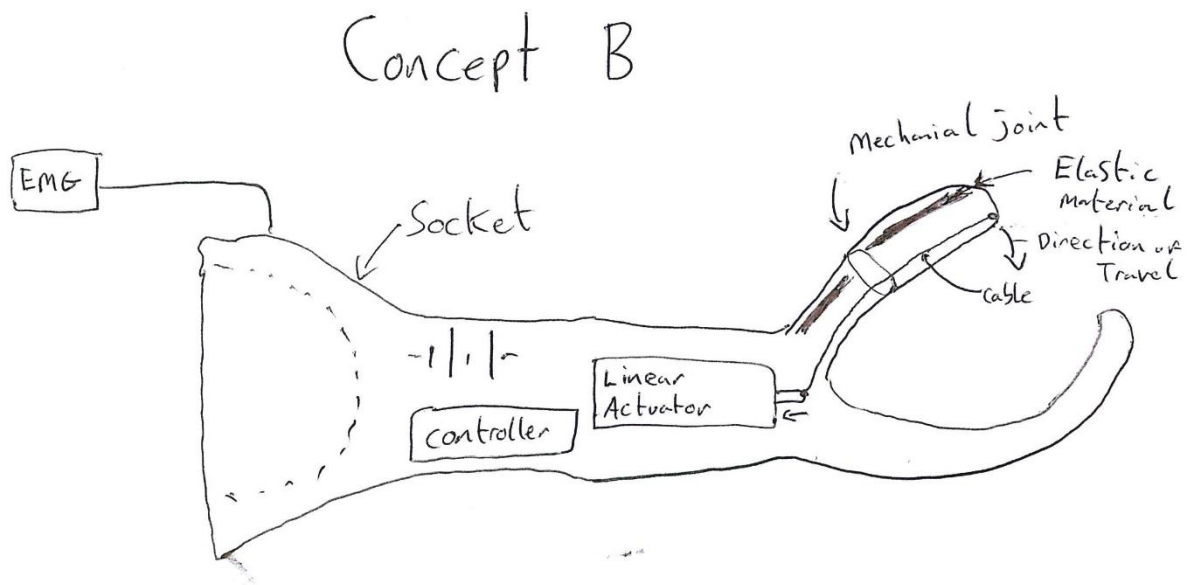
Figure 2.2 Concept Design B

2.2.3 Concept C – Multi-digit Cable Driven Grip

Concept C is a variation on Concept B, utilising a full set of articulated digits. The "thumb" design would remain the same, with a single joint at the midpoint of the gripper; conversely the "fingers" would have two joints, mimicking the design of human fingers. Two or four fingers could be utilised, giving a three- or five-digit hand. For cosmetic purposes, five digits would be preferred, though space restrictions may necessitate the use of a three-digit system. Once again, an internal elastic structure would likely be used to extend the grippers. The system could use one linear actuator for all the digits, or split the load between two actuators, one to drive the "thumb" and one for the "fingers".
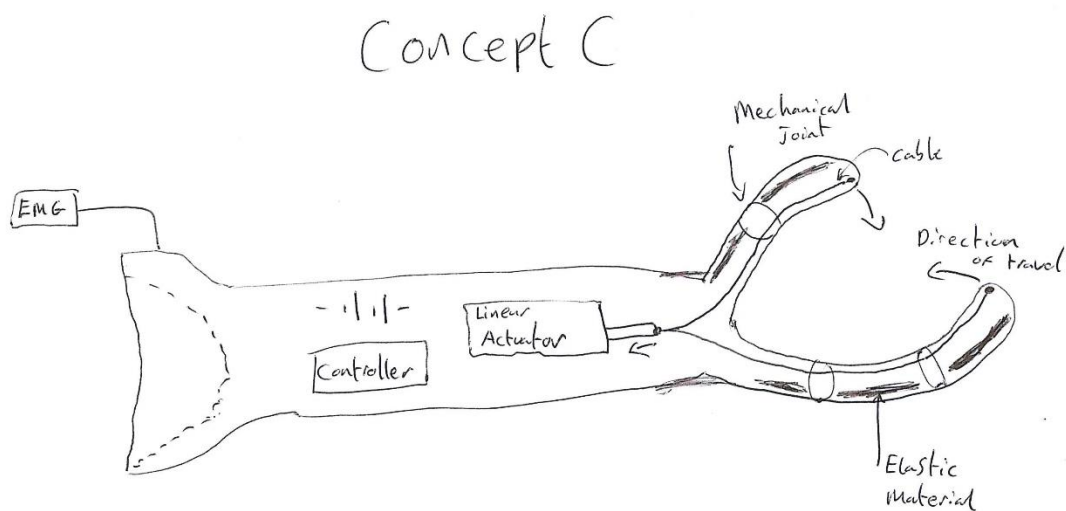
Figure 2.3 Concept Design C

2.2.4 Concept D – Cable Driven Soft Grippers

This fourth concept would use a similar approach to concepts B and C, incorporating a linear actuator(s) to pull on wires within the gripper. This design differs however as joints would not be used, instead the grippers would be made of a soft material, such as silicone rubber. The soft-grippers would be formed with 90° segments at ordinarily jointed points, to encourage bending around these points, similar to the design presented in [70]. As the grippers would already be made of a high-elasticity material, there would be no need for an additional mechanism to return the grippers to their extended state. A composite design could be incorporated using a tougher rubber on the outside face of the gripper to provide the additional elastic potential. The contact surface of the grippers should be subtle, with a feel mimicking human skin. This contact surface should have an increased performance compared to the use of jointed grippers, with hard contact pads. The soft grippers should also provide a flexible, highly adaptive grasp. Their use may also have a beneficial safety factor, due to the lack of pinch points in the joint-less design of these grippers.
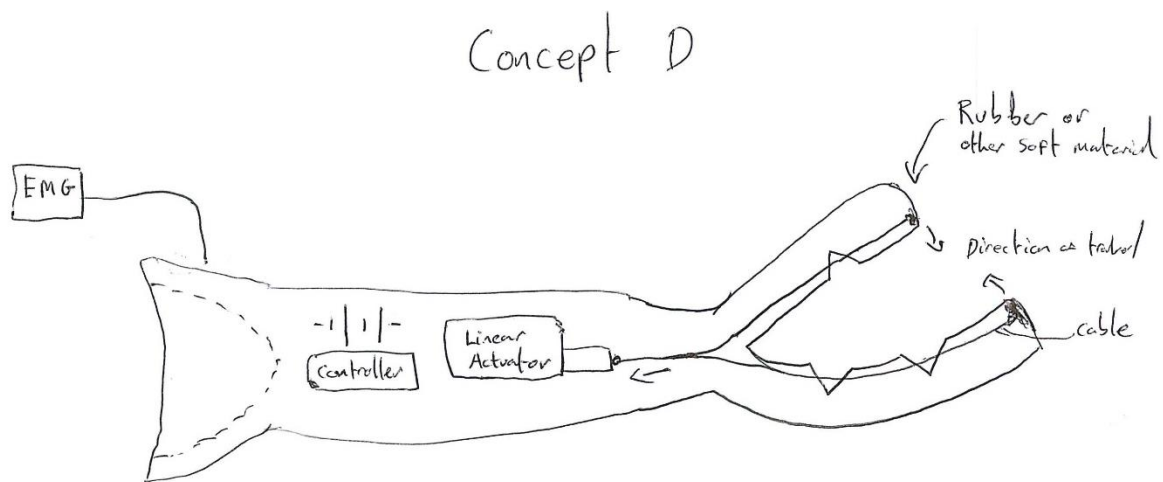
Figure 2.4 Concept Design D

2.2.5 Concept E – Pneumatic/Hydraulic Driven Soft Gripper

This final concept design would also look to incorporate soft grippers, though rather than using a cable driven system, hydraulic or pneumatic grippers would be used. These grippers would contain pockets where either a pressurised gas or liquid would be propelled in, causing the deformation of the grippers. This style of soft gripper has appeared in literature, such as in [86], though no literature seems to have incorporated this into an upper limb prosthetic end device; work on an soft pneumatic glove [87] has been conducted, though this acts as grip assist, rather than as an independent grasping device. The complex control system required, as well as the need for a hydraulic/pneumatic reservoir, impacts the suitability for such a device to be used in paediatrics. The device would also likely be heavier than the other concepts, due to this hydraulic/pneumatic components. Should these difficulties be overcome, the flexible grippers should have a high grasp effectiveness by encompassing the object, as seen in robotics. The contact surface too would be malleable, increasing contact area when grasping objects.
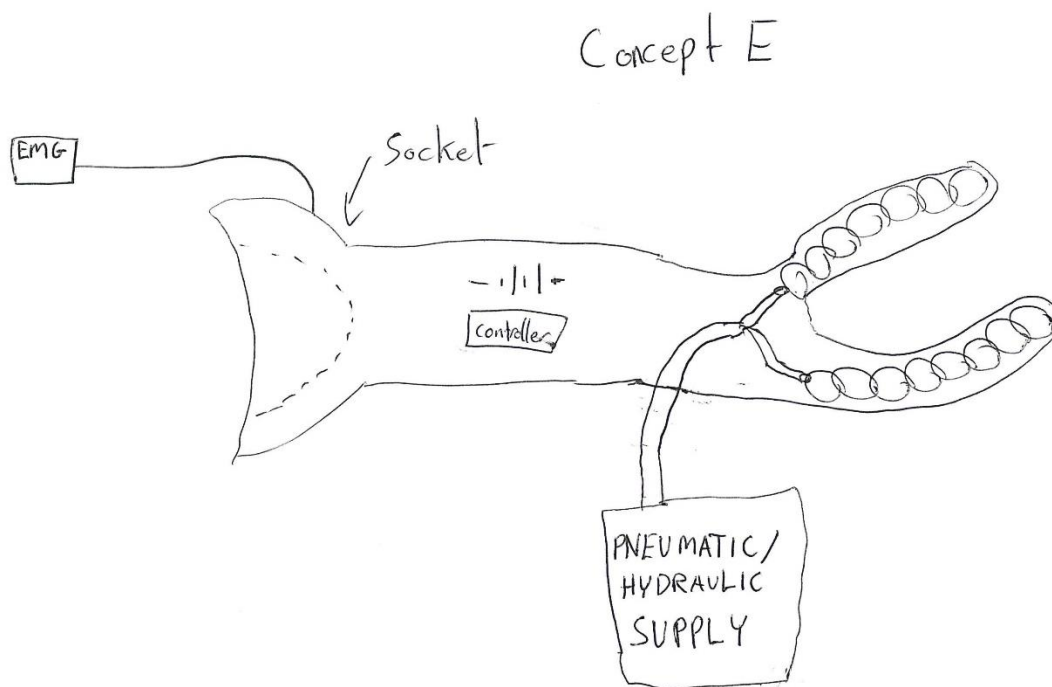
Figure 2.5 Concept Design E

2.2.6 Concept Selection Matrix

With the concepts designed, there is now a need to compare them in a systematic manner. To this end, a selection matrix has been utilised here to rank the designs based on several weighted performance categories (Table 2.1). These several categories cover a range of facets regarding functionality of the prosthetic, these are based on studies such as [27], where parents were surveyed regarding the factors that result in prosthetic rejection. The most important aspect of the design is deemed to be the grip functionality, as this is where the worth of the device will be shown; conversely the production time and ease of manufacturing are deemed less important as these will not directly affect the end user.

Table 2.1 Concept Selection Matrix Evaluation Criteria

Evaluation Criteria	Weighting
Close to bio-equivalent-weight	15.00%
Easily controllable	15.00%
Appearance (life-like or bionic styling)	5.00%
Low maintenance	10.00%
Long battery life	10.00%
Affordability	15.00%
Easy to manufacture	5.00%
Production time	5.00%
Grip functionality	20.00%

The designs were ranked on an unweighted 1-5 scale, with one being very poor and 5 being very good. Table 2.2 shows the rankings for each design concept, when determining the scoring, the weighting was not considered as this will be incorporated later. These criteria rankings are perceived, rather than based of measurable metrics. In some cases, there are relatively safe assumptions, such as concept E's complex fluid-based system resulting in a heavier device compared to simpler motor driven concepts. Based on this unweighted score, the weakest design is concept E, with the remaining designs scoring approximately equally.

Table 2.2 Unweighted Concept Ranking

Evaluation Criteria	Concept A	Concept B	Concept C	Concept D	Concept E
Close to bio-equivalent-weight	4	4	3	3	2
Easily controllable	4	4	4	4	2
Appearance	3	4	4	3	3
Low maintenance	3	3	3	4	2
Long battery life	3	3	3	3	3
Affordability	4	4	4	4	3
Easy to manufacture	4	4	4	3	2
Production time	3	4	4	4	3
Grip functionality	4	3	4	5	5
Total	32	33	33	33	25

Table 2.3 shows the results with the weightings into account. The frontrunner is concept D, the wire-driven soft-gripper. The reason is mostly due to the high importance that is placed on grasp effectiveness, which it is believed the soft grippers would excel at. The same data displayed on a radar chart can also be seen in Figure 2.6, to further reinstate the difference in the performance of each design.

Table 2.3 Weighted Concept Ranking

Weighted Evaluation Criteria	Concept A	Concept B	Concept C	Concept D	Concept E
Close to bio-equivalent-weight	0.6	0.6	0.45	0.45	0.3
Easily controllable	0.6	0.6	0.6	0.6	0.3
Appearance	0.15	0.2	0.2	0.15	0.15
Low maintenance	0.3	0.3	0.3	0.4	0.2
Long battery life	0.3	0.3	0.3	0.3	0.3
Affordability	0.6	0.6	0.6	0.6	0.45
Easy to manufacture	0.2	0.2	0.2	0.15	0.1
Production time	0.2	0.2	0.2	0.2	0.15
Grip functionality	0.6	0.6	0.8	1	1
Total	3.55	3.60	3.65	3.85	2.95
Rank	4th	3rd	2nd	1st	5th
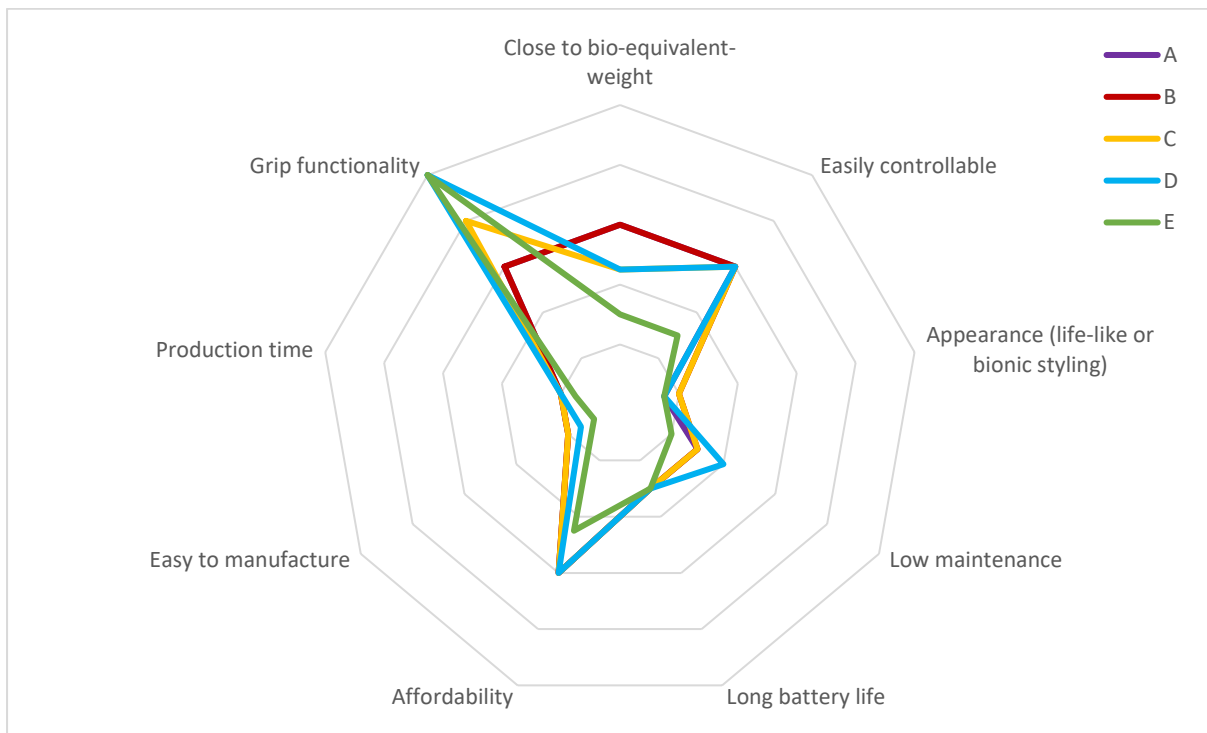
Figure 2.6 Radar Graph of Weighted Concept Ranking

As the soft gripper concept was selected as the optimal design, this will be the focus moving forward, with the proceeding subsections of this chapter focusing on the development and realisation of this design. It is worth noting that this selection process is bias to the authors assumptions taken from literature and does not present a wholly quantifiable process based on measurable metrics. A small change to the criteria rankings could easily result in a different concept being chosen. At the time of this selection process, no prosthetic device with fully soft grippers had been discovered in published literature; this too impacted the desire to explore concept D.

2.3 Gripper Design

In this subsection, the soft gripper design will be examined. This will cover the full development of the grippers from concept designs, to the final realised components.

2.3.1 Initial Design

The gripper design is loosely based on human fingers. The sizing of the gripper is based on measurements of a 4-year-old child's hand. The extruding section of each finger is 50mm long and is comprised of three segments. The base extends a further 20mm, though this is purely to house the gripper within the 'hand'.

The gripper contains within it hollow tubes that allow for a wire or string to be thread through. When the string is pulled back, the gripper will contract around the slots in the gripper. The total angular deformation of the tip is approximately 180°, due to the two 90° slots. Due to the nature of the flexible gripper, the exact deformation is difficult to fully quantify or model. Some lateral deformation is possible with this gripper, in cases where an obstruction occurs.
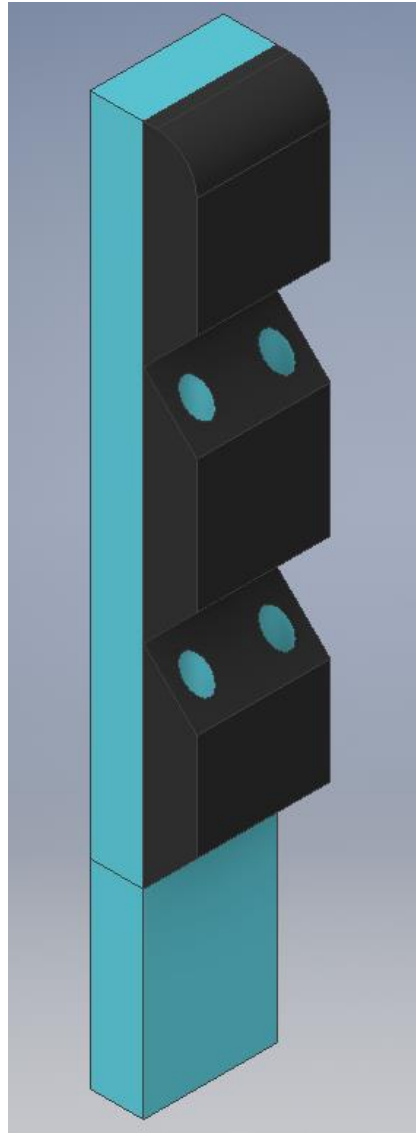
Figure 2.7 CAD Model of Soft-Gripper

It was decided that the grippers would be constructed as a composite. The gripper is 10mm wide and is effectively spit in half (Figure 2.7), with a malleable contact surface (shown in black) and a stiffer silicon rubber that acts as a reinforcement for the gripper, as well as an elastic energy store (shown in blue). For the contact area of the grippers, a malleable material with a feel resembling that of human skin is to be used. The justification for this is that the surface of the gripper would distort slightly around an object's surface during a grasp, thus increasing the contact surface area as shown in Figure 2.8. The material chosen for the contact surface was Dragon Skin™ 30 (Smooth-On, Inc.). This silicon rubber is used in prosthetic makeup for its skin like appearance and texture; this skin-like property should be well-suited for this application.
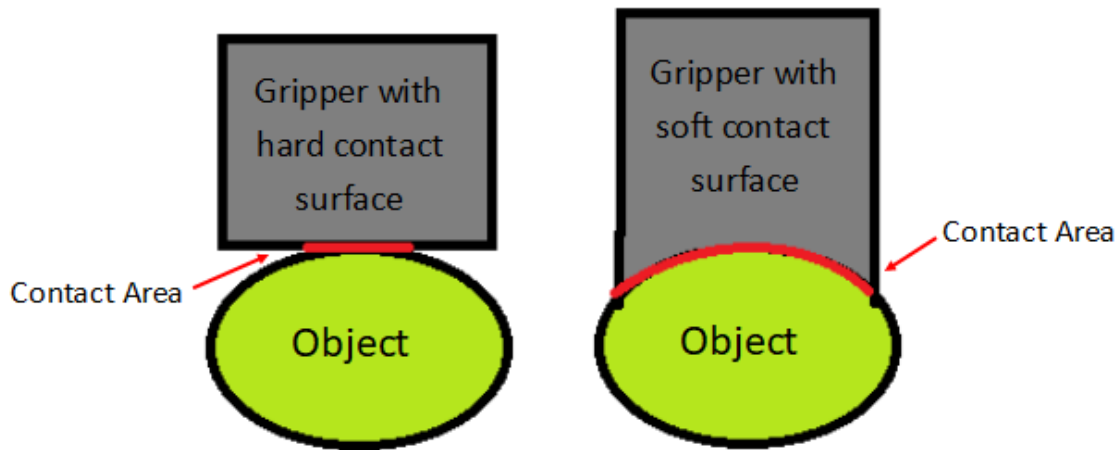
Figure 2.8 Exaggerated Surface Contact Comparison for Hard and Soft Grippers

The second component of the composite gripper is Smooth-Sil™ 960 (Smooth-On, Inc.). This material acts as an elastic energy store for returning the gripper back to its pre-deformation state. Smooth-Sil™ 960 is a more rigid silicon rubber than the Dragon Skin™ 30 and is not intended to come into contact with an object during a grasp. The material also acts as a reinforcement for the gripper, with the base extension also being made from this material so that the gripper may be securely slotted into the 'hand' of the prosthetic.

2.3.2 Prototyping

The printing capacity at the time of this work being conducted did not allow for direct printing in a flexible enough FDM filament, because of this, the aforementioned silicon rubbers were used instead. Additive manufacturing was however utilised to produce the moulds for the grippers. The design for the mould was produced on Autodesk Inventor, using the mould tool to automatically create an inverse of the gripper design. A 3-degree taper was applied on the edges of the gripper in order to ease the removal of the gripper from the mould.
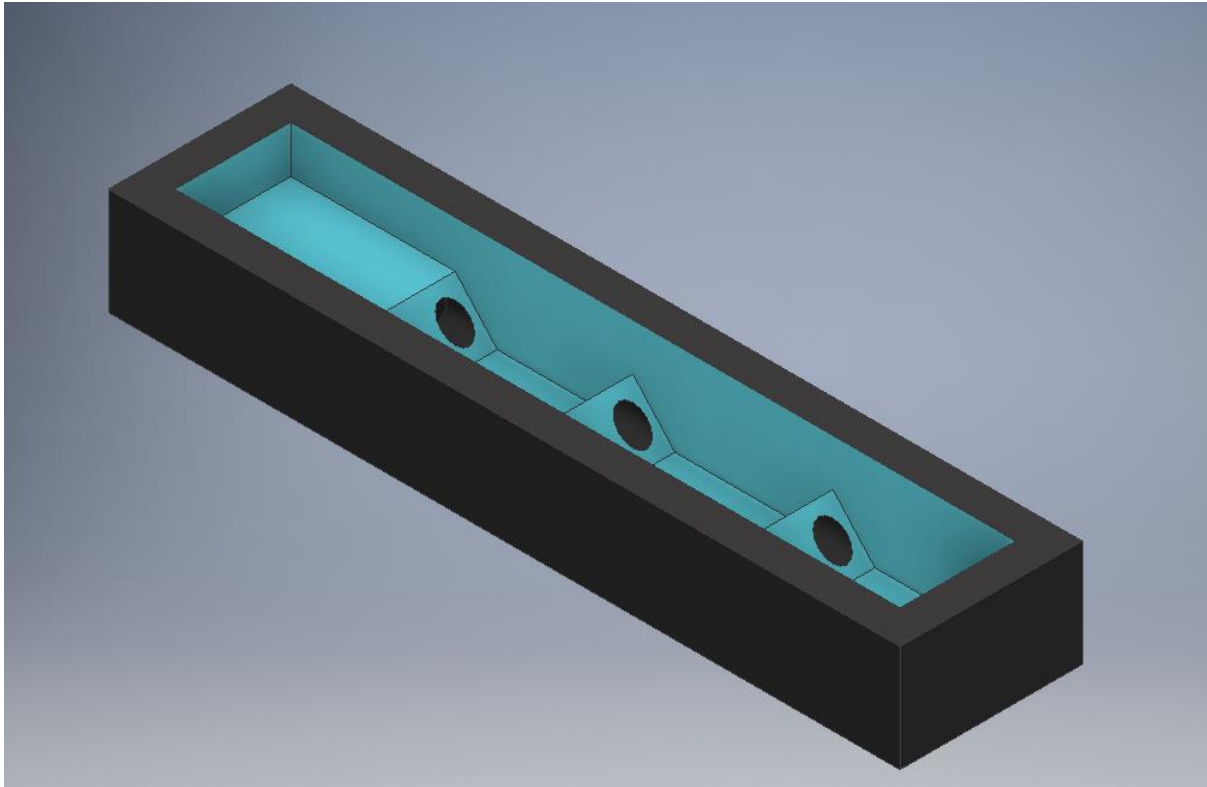
Figure 2.9 CAD Model of the Gripper Mould

The material used was Ulitmaker's TPU-95, a slightly flexible 3D-printerable material that allows the gripper to be removed easier than if the mould was completely rigid. An STL file was imported into Ultimaker Cura (Ultimaker B.V.), this software takes the geometry data and produces the g-code file that the printer will run. For this mould, the default settings were used, with a layer height of 0.1mm. The Ultimaker 2+ was used to produce the mould, as only a small build area and single material extrusion was needed.
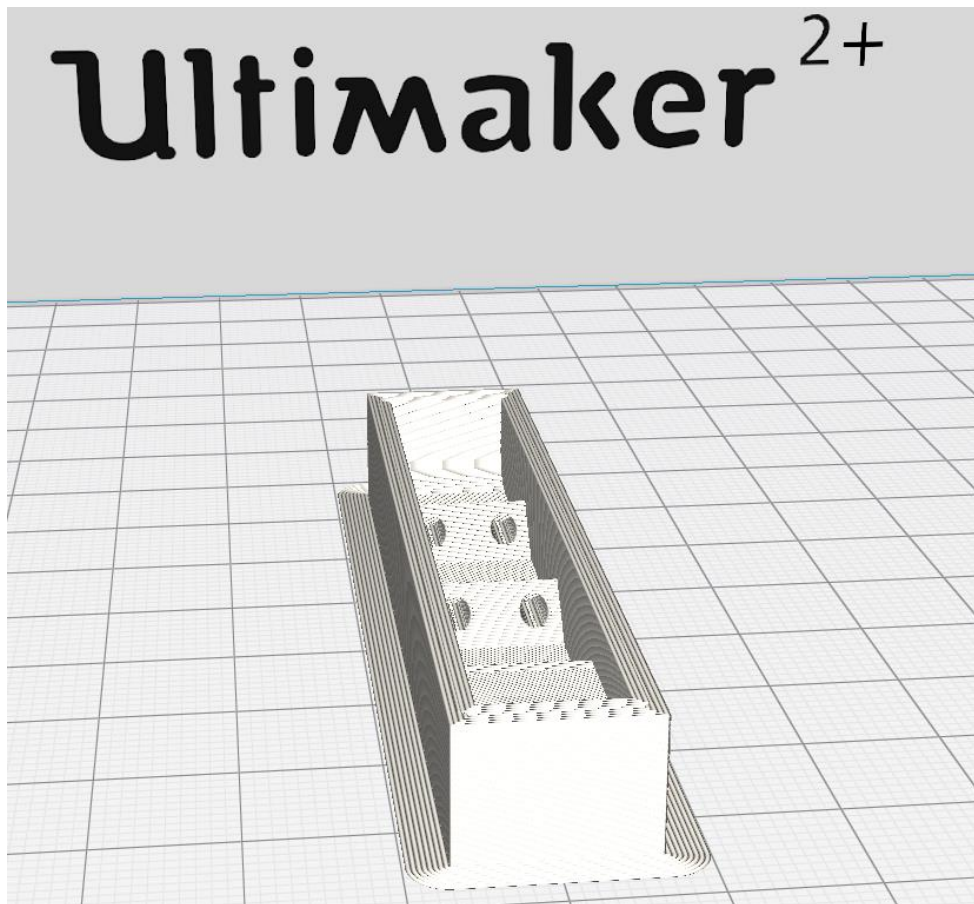
Figure 2.10 Gripper Mould Imported into Cura

The first stage of the moulding process is to insert plastic tubing into the holes within the mould. These will form the internal cavities in the grippers for the cable to be threaded through later. This procedure is extremely delicate and took a considerable amount of time complete. The loop at the end of the gripper was especially challenging, due to the small radius often causing the tube to buckle when bent.

The next stage involves first poring the Dragon Skin 30 up to the halfway point (the top of the wedges), once this has set, the Smooth-Sil 960 can be poured on top, filling the mould. The completed gripper is easily removed from the mould, some finishing techniques are required however; this mostly consists of removing material excess near the tubes.
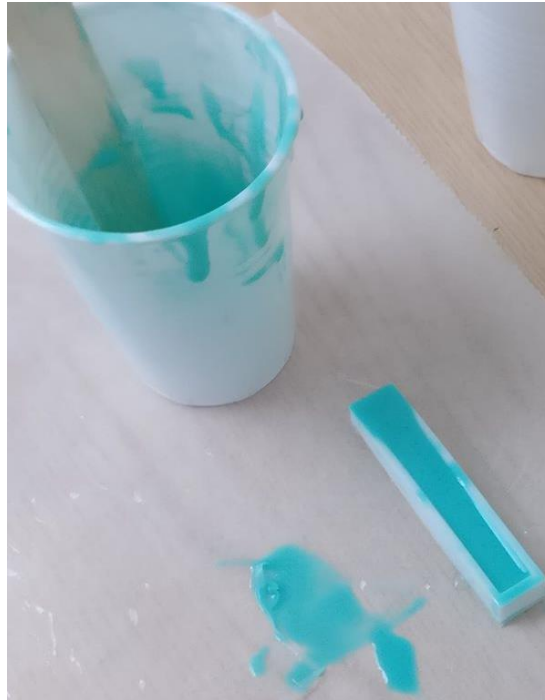
Figure 2.11 Silicon Rubber moulding Process

2.3.2.1   *Final Gripper Design*

Due to issues regarding the moulding and threading of the gripper (detailed in Appendix A1), design was altered so that the gripper width is doubled to 20mm. This larger width necessitates the need for 3 digits to be used, instead of 5. From an appearance perspective, the use of 3 grippers would have been preferable as anthropomorphic styling is typically preferred in the field of prosthetic design, mimicking the general aspects of the human hand [88]. Ultimately anthropomorphic styling is deemed as a secondary consideration in the design of this device, with the emphasis being placed on the grasp effectiveness of the prosthetic. From a grip functionality perspective, the use of 3 digits in robotics has been shown to provide a grasp effectiveness of 90% [89]. This three point contact was deemed effective enough to move forward with a three-digit system and produce the updated 20mm grippers.
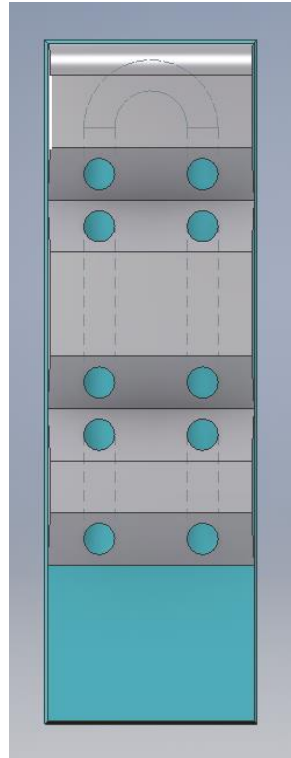
Figure 2.12 CAD Model of the 20mm Gripper

The CAD design process simply involved editing the dimensionality of the previous version. The mould design and 3D-printing likewise followed the same pattern as before, with no noteworthy incidents occurring. Inserting the tubes into the wider mould was considerably easier than with the previous 10mm version. The end loop did not tend to kink, and the plastic-coated wire was able to be threaded through the entire pathway, producing the first functional gripper. A slight air bubble is present in the gripper, this is likely from the pouring process. Slower pouring and lightly shaking the mould mostly negated this issue; ideally a vacuum chamber would be used in the future.
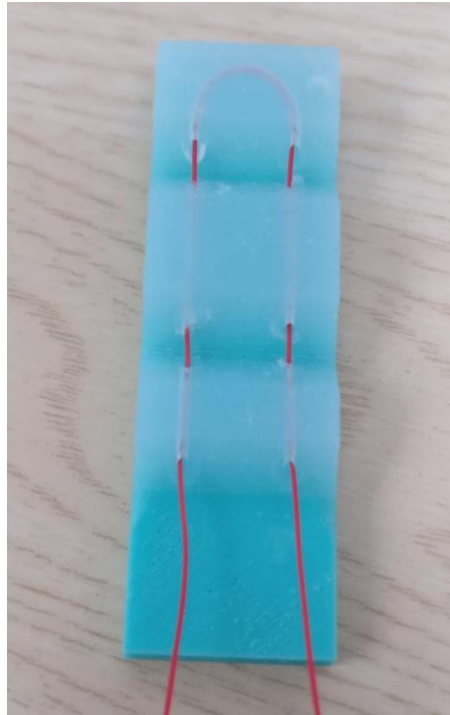
Figure 2.13 Threaded 20mm Soft-Gripper

2.3.2.2 'Thumb' Design

A variant of the gripper was produced, using the same CAD, 3D-printing and moulding process. This version has 2 segments, rather than 3, mimicking the style of a thumb. The main reasoning behind including this variant gripper was to improve the biomimicry of the 'hand' to make it more cosmetically appealing. This gripper would only be used as a 'thumb' with the remaining digits acting as 'fingers' with 3 segments. The use of a 2-segment and 3-segment thumb will be compared for grasp effectiveness in later chapters 4 and 5.
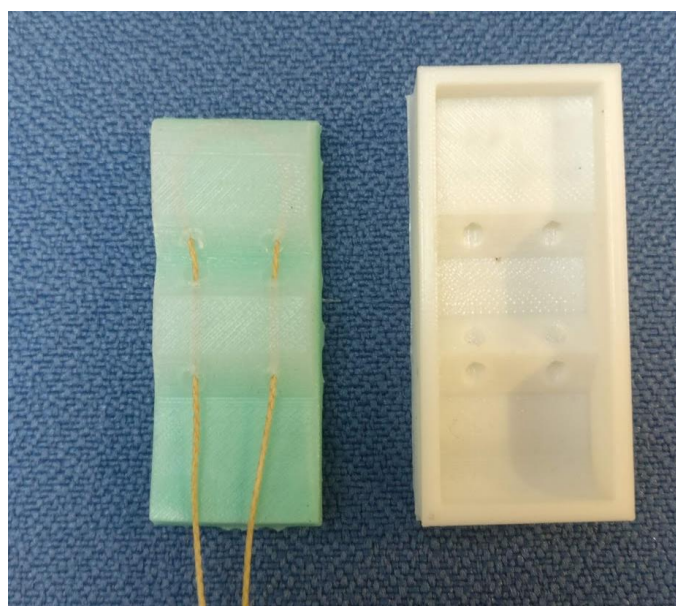
Figure 2.14 'Thumb' Style Gripper with Mould
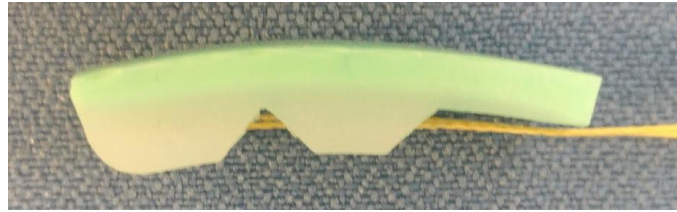
Figure 2.15 'Thumb' Style Gripper - Side View

This final gripper design will now directly feed into the design of the rest of the arm, particularly the hand. The proceeding subsection will focus on this.

2.4 Hand Design

The design of the arm is predominantly based on biomimicry, using the approximate dimensionally of the human arm to set the design parameters. Hand measurements were provided by a volunteer, giving the approximate hand dimensions of a 4-year-old male (Figure 2.16).
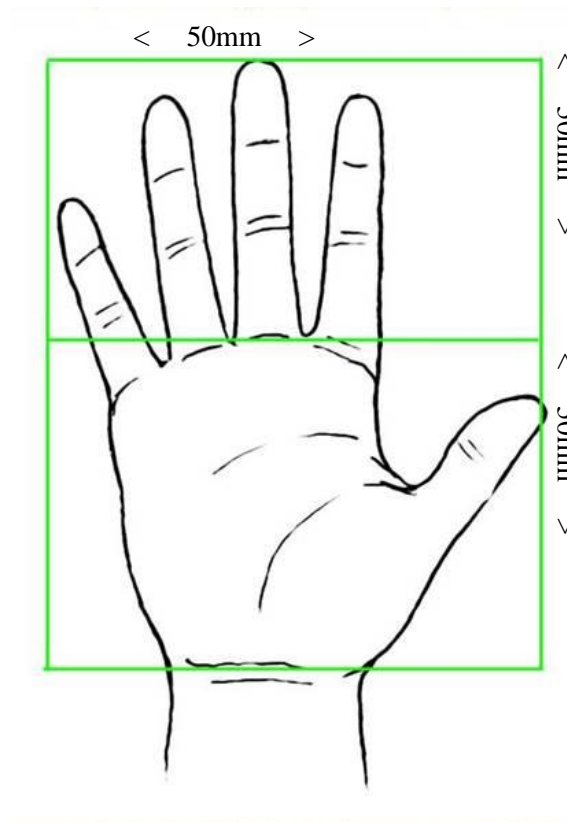
Figure 2.16 Approximate Dimensionality of a 4-Year-Old's Hand [90]

Further dimensionality of the arm was determined using reference data in [91]. Based on an average height of 105cm [92] and the proportionality of the arm, we get forearm length of 15.33cm. The width of the arm is based around the maximum width of the hand (50mm).

$$0.146 * 105cm = 15.33cm$$
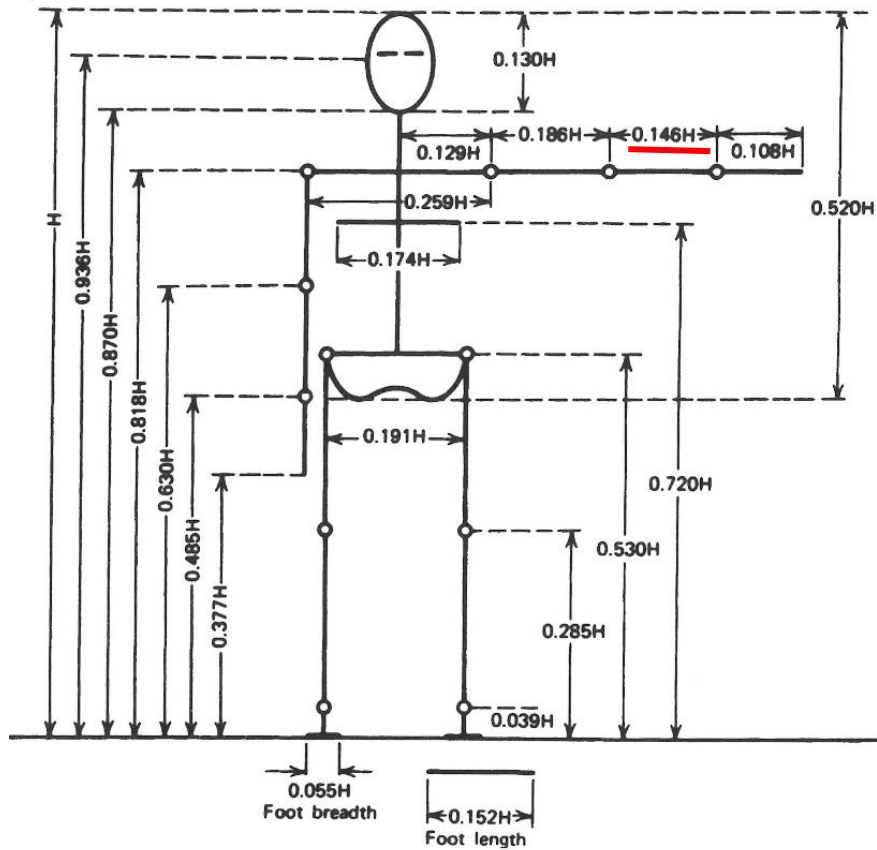
Figure 2.17 Proportionality of the Human Body [91]

The initial focus of the design is centred on the 'hand', with the rest of the forearm being constructed later; this approach was taken as the most significant feature of the prosthetic is the end grasping device. As previously covered, the 'hand' will use 3 soft-grippers. Of these 3 grippers, 2 of them act as the 'fingers', sitting side-by-side on the palm side of the 'hand'. The 'thumb' is offset from the palm by 45° in the initial design.

The soft-grippers are cable driven. The method of preforming this action will be to utilise linear actuators, located in the forearm; this necessitates tubes to be incorporated into the design for the cables to be threaded through, two tubes for each gripper. The CAD drawing in Figure 2.18, shows the initial design for the 'hand'. In this early stage, the cables were operated manually, in order to simulate the grasping mechanism of the hand.
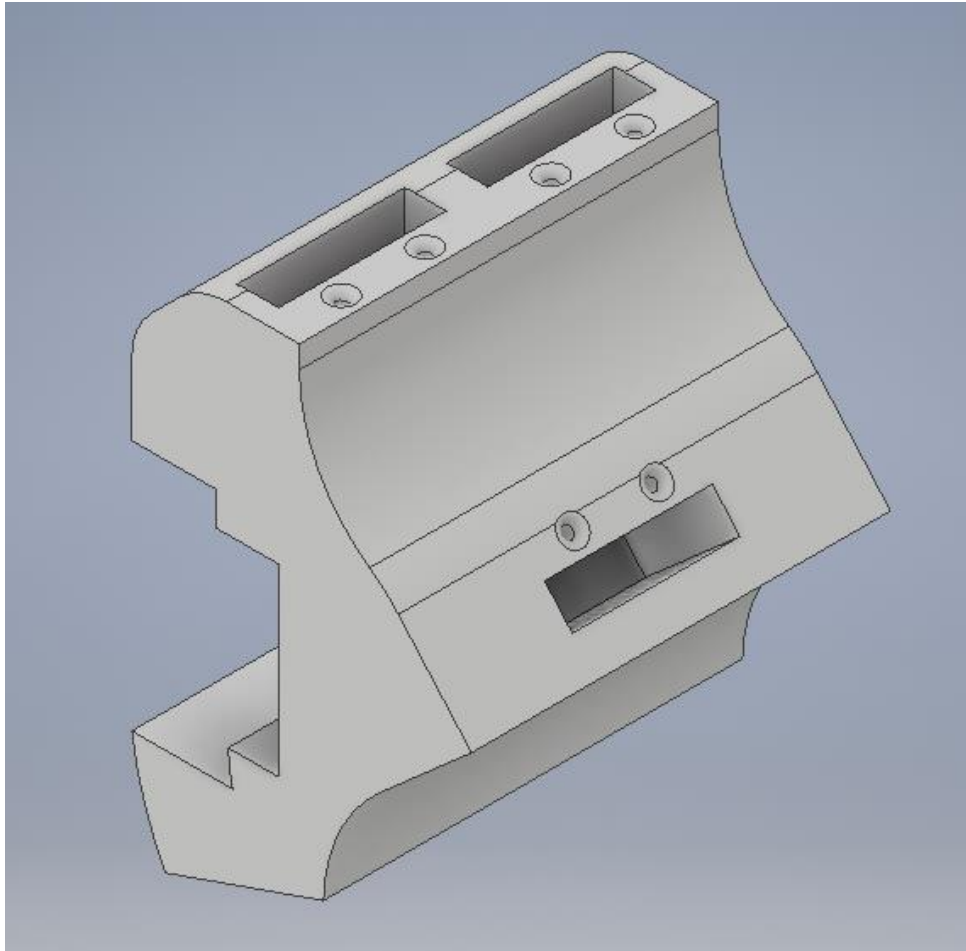
Figure 2.18 CAD Model of the Initial 'Hand' Design

This initial prototype was able to successfully grab some small objects (Figure 2.19) and helped to verify the design of the hand and grippers. The opening width of the hand however has proven to be a limiting factor in the effectiveness of the grasping mechanism. To counter the issue of a restrictive grasp width, the angle of the 'thumb' offset was adjusted to 90°, from an initial 45; this is detailed in Appendix A2. The rest of the design remained unchanged.

Figure 2.19 Prototype 45° Hand Grasping a Plastic Bottle

2.5   Component Selection

Before any more work was performed on the design, the external components needed to be selected and sourced; this primary considered of electrical components. The outline for the circuit (shown in Figure 2.20 and described in further in section 3.1) consists of a micro controller which takes input from an EMG sensor. This recording is processed and used to control two linear actuators, which in turn feedback to complete the control loop. The system is powered by a single rechargeable battery.
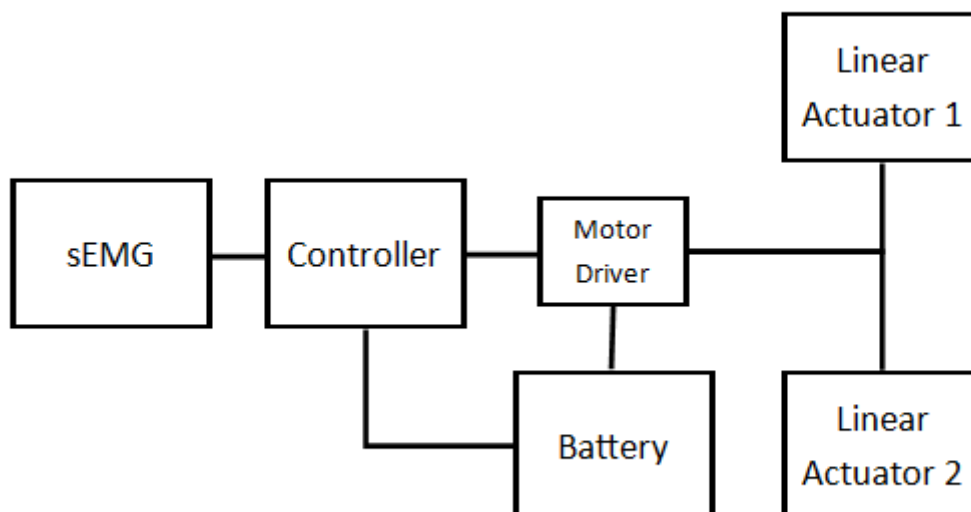
Figure 2.20 Outline of Major Control System Components

One of the first components selected were the linear actuators. The Actuonix PQ12-P Micro Linear Actuator (Actuonix Motion Devices Inc.) was chosen. This device is one of the smallest linear actuators currently on the market and has been used already in prosthetic hands, such as the Youbionic Hand [93]. The linear actuator has several configurations available, the one chosen utilises a built-in potentiometer that can be used to determine the extension of the shaft. This allows for the gripper extension/contraction to be accurately controlled. The gear configuration comes in 3 variants, with the 1:63 ultimately being chosen for its balance of extension speed and peak force. It was decided at this point that two actuators would be used, one for the 'thumb' and the other for the 'fingers'.

Figure 2.21 Actuonix PQ12-P Micro Linear Actuator [94]

For the micro controller the Arduino board is to be used. There are many different variants under the umbrella of Arduino. The ultimately the Arduino Nano, a small board with architecture comparable to the Arduino Uno, was chosen for the final design, primarily due to its compactness.
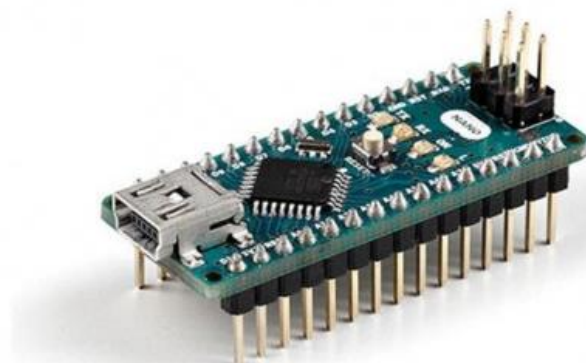
Figure 2.22 Arduino Nano [95]

As detailed in section 2.1, the sEMG system's sensor will be placed on the bicep. This ruled out the use of pads embedded in the socket directly. It was ultimately decided that an armband-based device, rather

than individual pads stuck to the surface of the skin would be used. The reasoning behind this is to minimise the discomfort of wearing the device, as well as making it easy to fit/remove. A few devices are available on the market that serve this function; the one chosen here was the OYMotion Gravity: Analog EMG Sensor (OYMotion Technologies, Inc.). The device is specifically designed to work with Arduino boards and comprises of two constituent parts. Firstly, the armband itself which has three contact pads on the under-side, these detect the voltage difference in the muscles. A 3.5mm jack cable is then used to connect to the second part, a filter board that amplifies and filters the single from the sEMG; this second board then connects to one of the Arduino's analog-input pins.

Figure 2.23 OYMotion Gravity: Analog EMG Sensor [96]

As the motor is rated 6V, the battery for the arm must at a minimum meet this voltage. The battery must also power the controller and EMG. A 7.5V Lithium Ion was utilised in the design. The battery has a capacity of 2.2Ah. The complete circuit draws approximately 2.5W when the motors are running and 0.5W when stationary. In order to determine an approximate battery life, we can covert the battery storage to Watt-hours.

$$Ah * V = Wh$$

$$2.2 * 7.5 = 16.5Wh$$

We can then determine how long the system should run with the motors running:

$$\frac{16.5}{2.5} = 6.6h$$

And when they are unpowered:

$$\frac{16.5}{0.5} = 33h$$

These calculations provide only an approximation and it is likely the actual performance will be lower than this; however, it verifies that the battery should, even under heavy use, be able to last a full day of operation between recharges.

Figure 2.24 Rechargeable 7.5V Lithium Ion Battery [97]

The other components purchased are detailed in Appendix D. The full list includes small parts, such as cable adapters and the motor controller. An overview of the circuit used will be covered in chapter 3.1. All these components feed into the design of the final prototype, which is detailed in the following subsections.

2.6   Arm Design

The rest of the arm was designed with the 'hand' as the basis, whilst incorporating the procured components. The arm has been designed in such a way as to keep all the electrical components within the structure of the prosthetic. The reasoning behind this is to reduce discomfort from having external components, for instance the battery being stored in backpack. The only component that is external is the sEMG armband, which would attach to the user's bicep, necessitating it to be external. As noted previously, two actuators would be used, one for the fingers and one for the thumb. This allows for independent control of the fingers/thumbs whilst also increasing the overall grasp strength. This will impact the weight of the device, however the actuators and other electronics used were selected to keep the arm under the design specified weight of 400g given in section 2.1.

Figure 2.25 shows a rough model of the complete system with the forearm cover removed. For this draft, the socket was modelled as a basic oval, to demonstrate how it would connect to the rest of the arm. The proceeding subsection 2.7 will focus on the socket design using a 3D-scan of a residual limb.
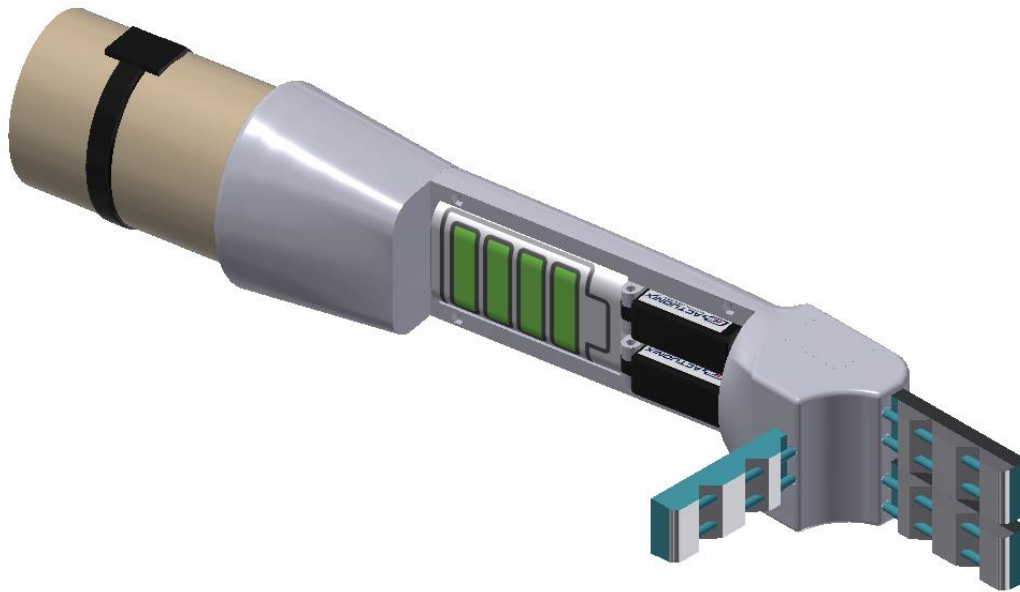
Figure 2.25 Early CAD Model of Full Prosthetic Arm

2.6.1 Prototyping

The design of the prosthetic arm must incorporate the features of the previously designed 'hand' as well as all the electrical components. The two main constituent parts will that be focused on here are the main arm structure (not including the socket) and the cover which is placed on the forearm of the device. There is also a small plate that fits on the back of the 'hand', though this will only be covered briefly.

2.6.1.1 Arm

The design presented here, took the 90° 'thumb' offset 'hand' presented previously and adds a forearm to the CAD Model. It was decided to use a fixed wrist, rather than an adjustable one. The justification for this is due to the intention for the device to be a child's first active prosthetic, there therefore is a desire to keep the mechanisms as simple as possible. An adjustable wrist would add an additional layer of complexity to the device, which may frustrate the user. The small scale of the device and the desire to utilise 3D-printing, also adds attentional difficulties in producing an adjustable wrist. Some small-scale passive wrist units are available on the market such as Ottobock's MyolinoWrist 2000 [98] and work has been conducted on designing an active wrist mechanism [99], though this remains outside of the scope of this project. The fixed wrist segment of the arm was offset from the hand by a 10° angle.
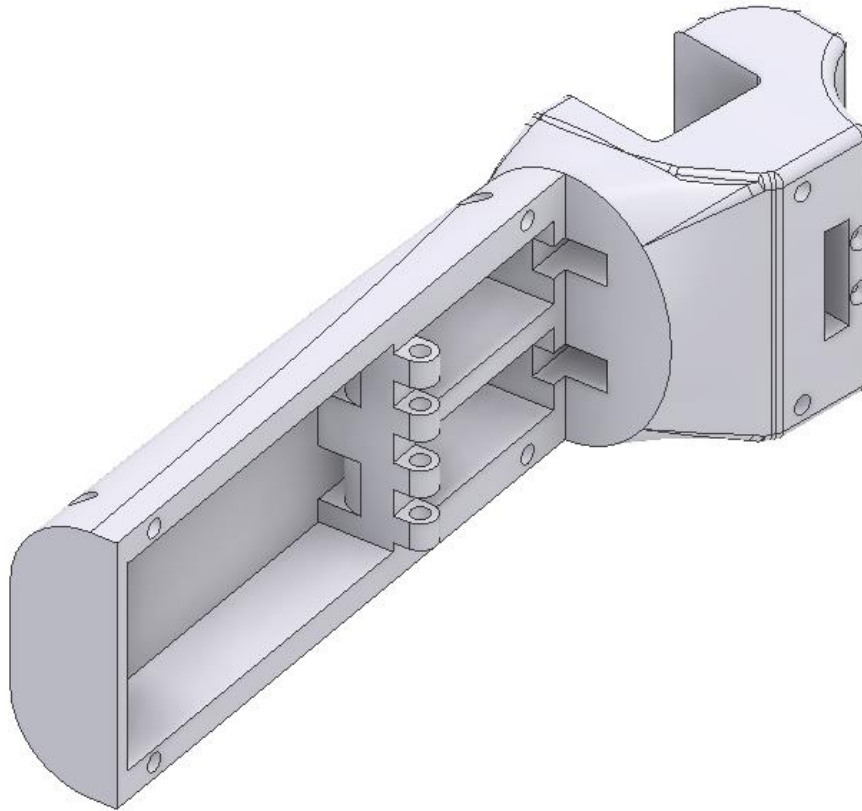
Figure 2.26 Completed Forearm Design

The design underwent numerous prototype interactions with subsequent small changes being made to the design. The most major of which was a redesign of the actuator housing. This prototyping procedure is described in detail in Appendix A2.

2.6.1.2 Forearm Cover

The second component of the arm is the cover. This effectively is the forearm of the device and will keep all the electrical components contained. The design is based on the dimensional requirements of the main body of the arm. This relatively simple component only underwent a single design iteration to accommodate additional internal space for the circuitry. The cover was non load bearing and therefore printed in a vertical direction to minimise the support material usage.
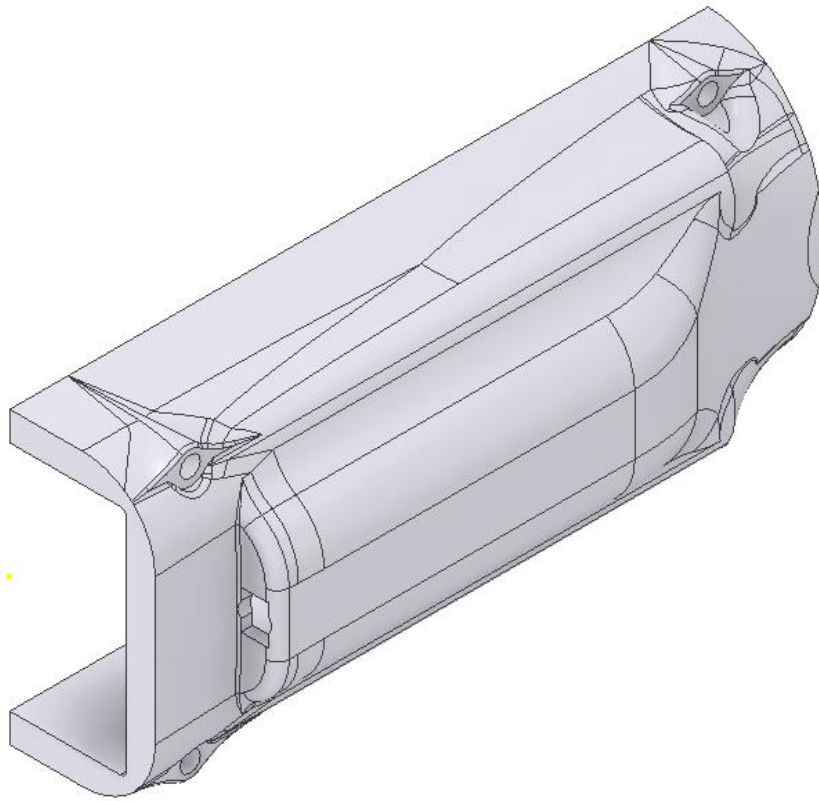
Figure 2.27 CAD Model of Revised Forearm Plate

The sEMG fits firmly in the appropriate socket Figure 2.28. The cover also fits securely on the arm, when attached with the bolts. The soldered electrical circuit fits within the cavity of device, resulting in a fully confined system.

Figure 2.28 sEMG Filter Board Housing

Figure 2.29 Final Printed Forearm Cover

2.6.1.3 Hand Back-plate

This simple component covers the open slot on the back of the hand used for fastening the cables to the linear actuators. The cover contains holes for M3 bolts to attach the plate to the 'hand'. The word "SIMPA" imbedded in the blue of the forward-facing surface, as seen in Figure 2.30. SIMPA, stands for Soft-grasp Infant Myoelectric Prosthetic Arm and is the name given to the device. The final design of the 'arm' and 'hand' is now fully defined, with only the socket remaining.

Figure 2.30 'Hand' Back-plate

2.7   Socket Design

The final part of the design process is to produce a socket for the residual limb stump. The traditional method of preforming this involves using a plaster cast of the residual limb. The process aims to faithfully capture the dimensional data of the stump, so that the fashioned socket fits exactly; failure to do so will result discomfort and slippage, rendering prosthetic unusable. Various studies have shown that socket fit ranks amongst one of the most important factors when rating the performance of a prosthetic device [100]. The casting process relies heavily on the skill of the prosthetist and on the stump being kept stationary during casing. In the case of young children, this lengthy casing process is often traumatic and uncomfortable, this in turn effects the quality of the cast as the child is likely to move around during the lengthy procedure. The high growth-rate too can prove problematic, as the by the time the socket has been produced, the child may have begun to outgrow it.

This project proposes an alternative that utilises 3D-scanning and CAD modelling to design and manufacture the socket [101] without the need for the lengthy casting process. The use of 3D printing for producing prosthetic sockets has been around for some time and in recent years has gained traction as a viable alternative to casting. Devices such as the Prosfit Socket [102] and the UNYQ Socket [103] are ISO 10328[4] certified and are commercially available. Both sockets are for lower limb prosthetics; examples of upper limb sockets include the Hero Arm [65] referred to in section 1.4.2. These sockets all claim to be able to rapidly produce a lightweight yet strong socket. The use of 3D scanning and printing for producing the socket could also benefit low income nations [104], with the rapidity, decentralised design and potential lower cost all having an impact.

2.7.1   3D-Scan Procedure

As part of the project, the 3D-scanning of the residual limb would have ideally been performed in the lab, bringing in a suitable subject on which to preform and validate the stump modelling. Unfortunately, this was not possible in the end, with the stump data instead being sourced externally. The residual limb scan is taken from the left arm of a 4-year-old male, who has undergone near-elbow transradial amputation as a result of dysvascular complications.

The procedure of sourcing the 3D-scan would most likely be performed using a handheld 3D-scanner, such as the Artec Eva [105]. Alternatively, as proposed in [54], a CT-scanner may be utilised to obtain dimensional data of the residual limb. Devices such as this are capable of sub-millimetre accuracy, providing an accurate geometric model of the stump. The accuracy of the socket this now dependent on the skill of the CAD technician to convert this data into a socket and on the 3D-printer to accurately manufacture the designed socket.

---

[4] ISO/CD 10328 Prosthetics — Structural testing of lower-limb prostheses — Requirements and test methods

2.7.2 Socket Modelling

Modelling such complex geometry on CAD has proved challenging prior to 3D-scanning and mesh tools, however with modern CAD packages such as Autodesk's Fusion 360 (Autodesk, Inc.) it is a relatively simple process. Autodesk Design Academy has produced a guide on how to use 3D-scan data taken from a lower limb and design a prosthetic socket based on this geometry [106].

The process detailed in Autodesk's design course is much the same as the one used in this project. The first step is to import the scan data into the CAD environment. This produces the meshed object shown in Figure 2.31. The next step is to enter the 'mesh' modelling environment. This process is broken down in detail in Appendix A3.

Figure 2.31 3D-Scan of a Residual Limb

The designed socket model needs to be joined to the rest of the arm assembly. It was decided that the socket and arm will be printed as a single component to minimise complexity and maximise structural integrity. A sketch was added to the base of the socket that matches the end of the previously designed prosthetic arm. This section here would in practice be adjusted so that the overall length of the limb matches the approximate biological length for the user. In cases of transhumeral amputees, an additional elbow unit would need to be incorporated. This has not been investigated by this project as the reference geometric data and 3D-scan are both from an individual exhibiting high-level-transradial limb reduction. There are already a number of passive elbow options available and the biomechanics of the joint are well understood [107], with manufacturing guides available for body powered devices [108]. There has also been work on active 3D-printed elbows [109], controlled by sEMG. It is therefore

assumed that incorporating an elbow unit into this design should not prove to be a significant challenge, given the large body of work covering this area.

The final socket design model is shown in Figure 2.32. This model was then imported into Autodesk Inventor to be merged with the existing arm model. With the models joined, the CAD design of the prosthetic is completed. The full model, as shown in Figure 2.33, can then be converted into STL format for importing into Cura and eventual 3D-printing.

Figure 2.32 Socket with Attachment Structure
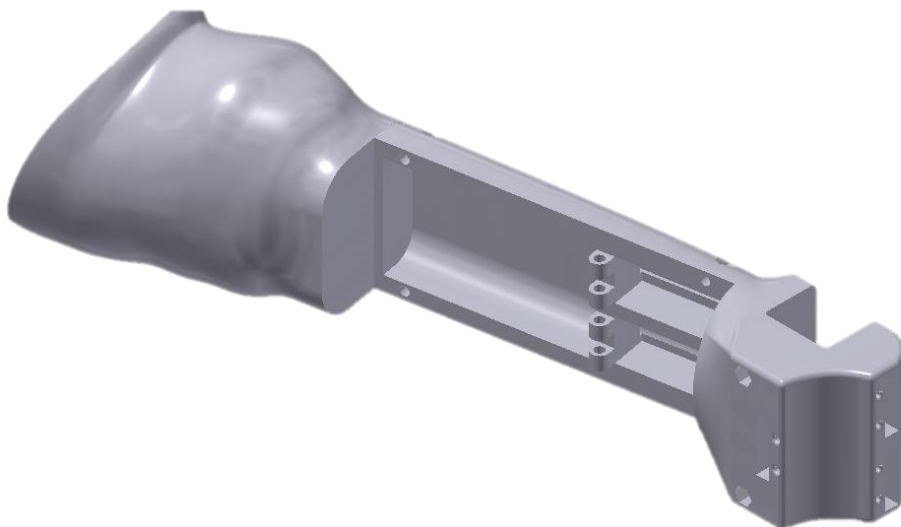
Figure 2.33 Full Arm CAD Model

2.7.3 Full Arm with Socket Manufacturing Process

The manufacturing process for the full arm with the socket was much the same as the previous prints. The STL file was imported into Cura (Figure 2.34), where support blockers for the small holes and cavities were put in place. Due to the complex geometry of this final model, a large support structure is needed to ensure a successful print. As there is no flat surface in the correct orientation, a bed of support material is first printed. The ABS is then printed on this with full support, until no surface overhangs. The relatively large hollow cavity of the socket requires an internal support structure to minimise material sag and thus maximise print quality.
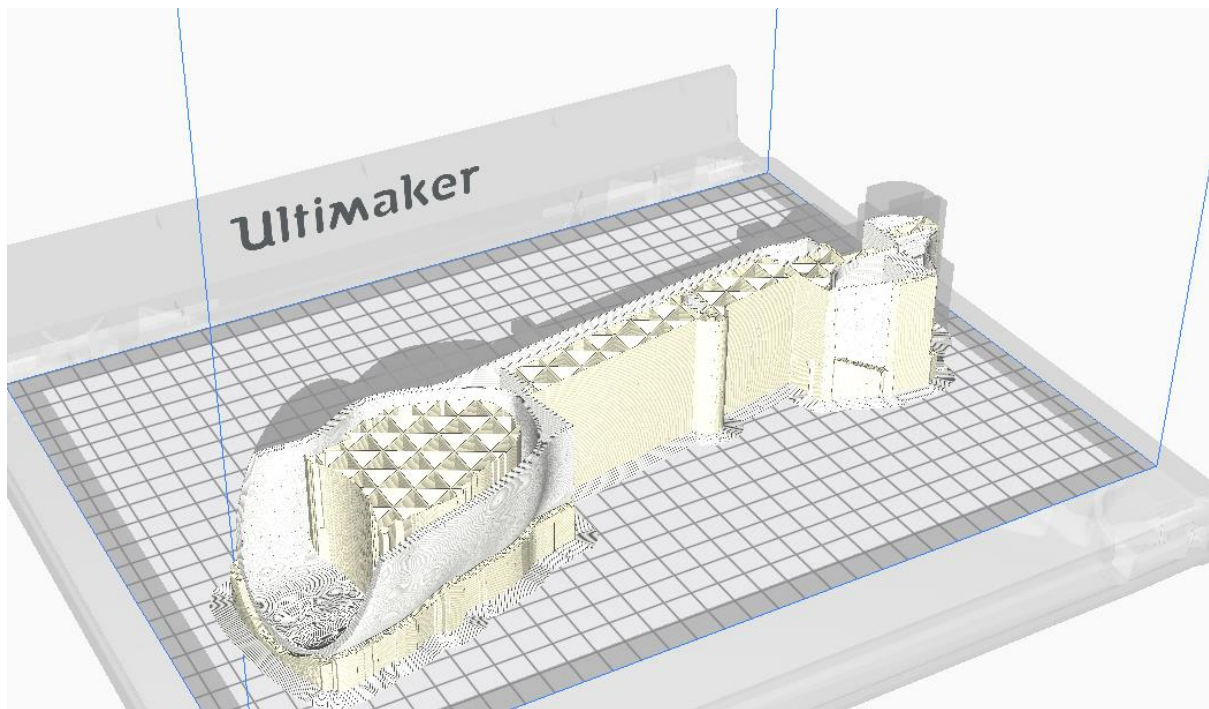
Figure 2.34 Full Arm Cura Setup

The final print has minimal issues with shrinkage, burn marks, or deformities as seen in Figure 2.35. This print will be used in the final working prototype, once assembled.
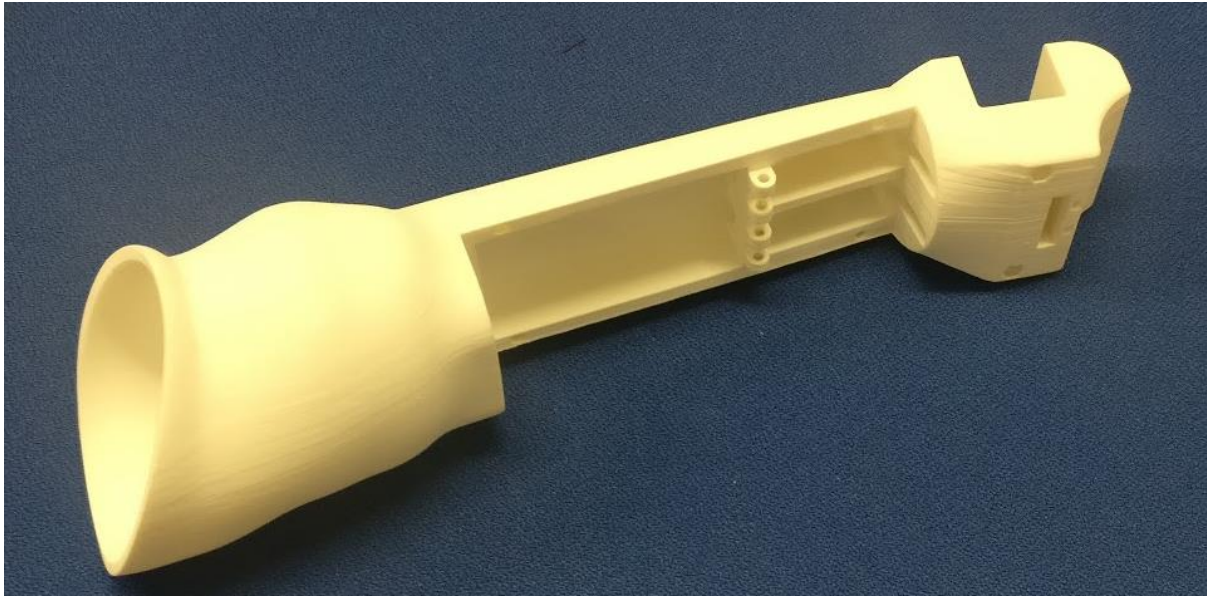
Figure 2.35 Final Printed Arm

2.8   Final Assembly

The arm with socket seen in the previous subsection was assembled with the other components, including the completed electrical circuits, to form the first working prototype of this design. This prototype has been given the name: "*SIMPA – Soft-grasp Infant Myoelectric Prosthetic Arm*".
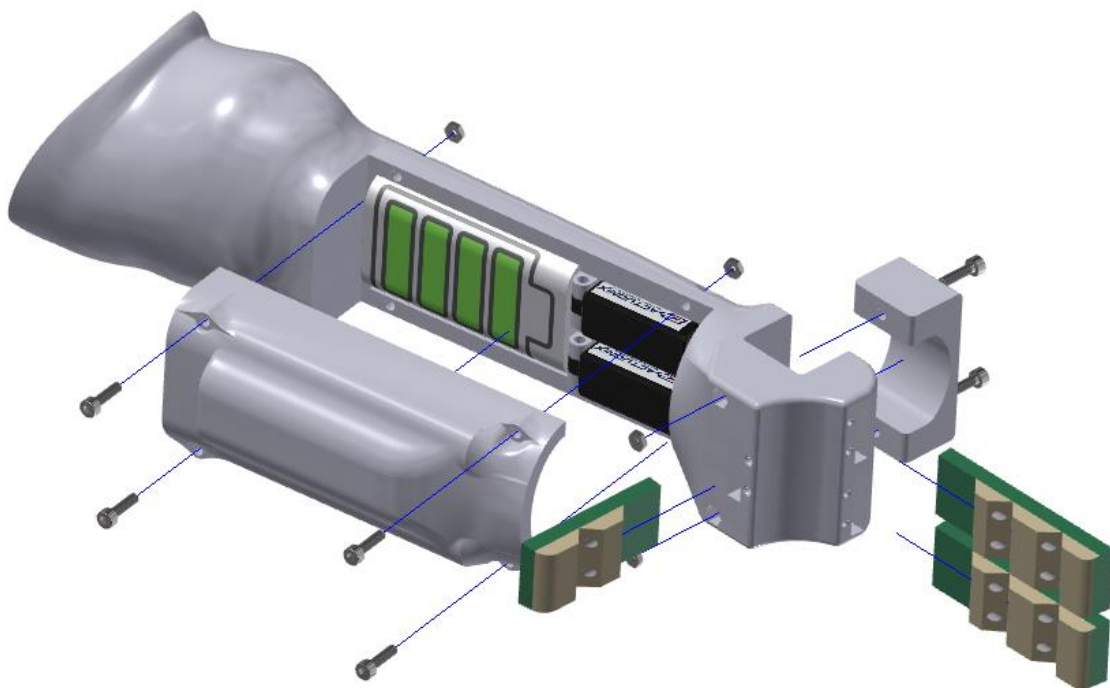
Figure 2.36 CAD Assembly

The assembly was a trouble-free process, with all the printed components and the grippers slotting together securely. The linear actuators, sEMG, and the battery all fit securely in their respective slots. The soldered circuitry (covered in section 3.1), fits within the body of the arm, though due to the tight

space, it is delicate assembly process. A further design point moving on would be a custom build PCB control unit, which would slot cleanly into the body of the arm; this would not however directly affect the functionality of the device.
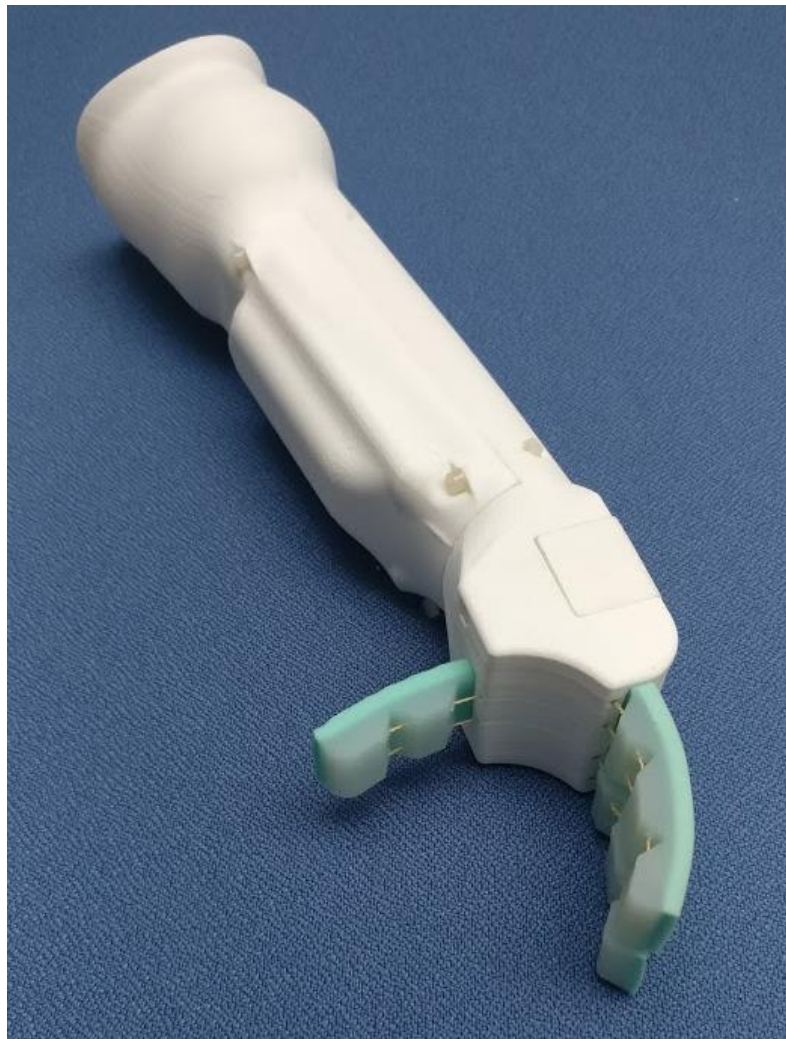
Figure 2.37 Final Assembled Arm (front)

Figure 2.38 Final Assembled Arm (side)

Figure 2.39 Final Assembled Arm (back)

The print of the arm without the socket was chosen for use as a grasp test device. The test arm is connected to an Arduino Uno based prototype breadboard circuit, which utilises buttons, rather than the sEMG to control the opening and closing of the grasp mechanism. It features the same 'hand' geometry as the final prototype; however its simplicity makes isolated testing of the grasp functionality easier.
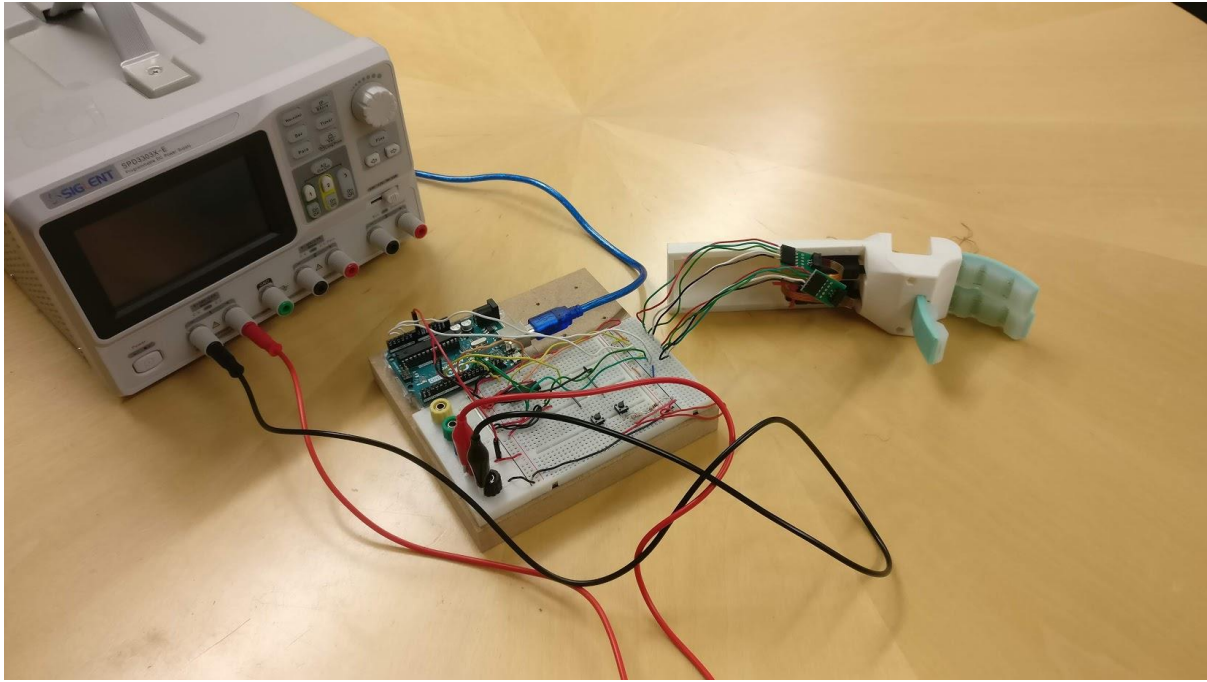
Figure 2.40 Grasp Test Setup

2.9 Chapter Summary

This chapter has covered all the design and manufacturing aspects of the project, from initial design specification to production of a fully assembled prototype prosthetic arm. The presented arm shows that small scale, 3D-printed, myoelectric prosthetic devices are viable from a pure production standpoint. The total cost of producing the component, including prototyping was less than £500, highlighting how cost effective a solution such as this could be.

The proceeding chapter will cover the development and implementation of the control system, as well as the electrical circuitry used.

3   Control System Design

This chapter will focus on the circuit design and the control system that has been integrated into the prosthetic prototype detailed in the previous chapter. The chapter will detail the final control system design in full and make notes regarding the development steps where appropriate.

A voluntary opening control system has been integrated the prosthetic. This system, sometimes referred to as the cookie cutter [76], utilises a single EMG sensor site. The system is Arduino based and programmed via Simulink (The MathWorks, Inc.). A grasp detection system is also to be incorporated. Figure 3.1 shows a finite state machine for the control system. It shows the three non-transit states the system can be in:

- **Closed:** where the 'hand' is in a fully closed position.

- **Open:** where the 'hand' is in a full open position

- **Grasp:** where a grasp has been detected and the 'hand' is held in its current position
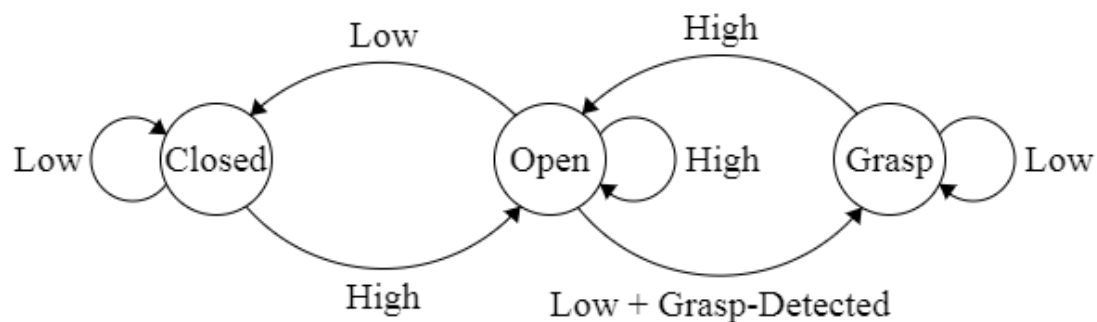
Figure 3.1 Finite State Machine Model of the Control System

3.1   Circuit Design

The basic outline of the circuit design centres on an Arduino board acting as the controller. The primary input into the device comes in the form of the OYMotion Gravity sEMG, detailed in section 2.5. This input will be processed by the controller, so that a recorded muscle flexion sends a positive signal to the actuators, causing the grasp to open. The inverse is true when no flexion is recorded, with the grasp closing. The second input to the controller is from the linear actuators built in potentiometers. These provide a resistance value that correlates to the shaft position, this allows for grasp open and closed limits to be set, as well as the incorporation of a rudimentary grasp detection system.
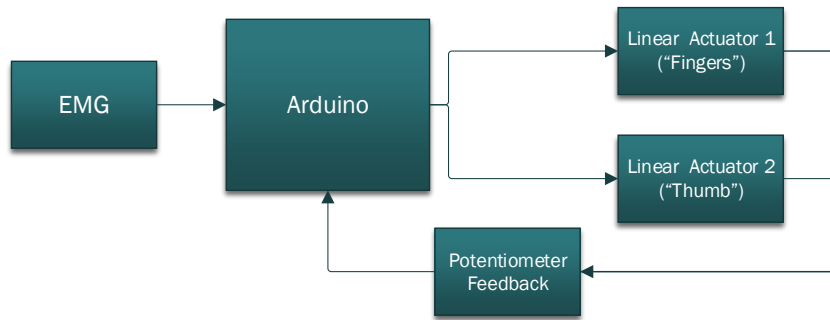
Figure 3.2 Outline for the Control Circuit

The circuit was prototyped on a solderless bread board, using an Arduino Uno as a stand in for the Nano. Three variations of the circuit were created:

1. **Push button controlled**: for developing the motor control and grasp detection system, and for use during the experimental procedures (section 4)

2. **Isolated sEMG**: to develop the grasp detection system

3. **sEMG Controlled System:** a combination of the two circuits, creating the final system that will be incorporated into the prototype prosthetic.

3.1.1   Push Button Controlled Circuit

The push button-controlled circuit uses two push buttons placed on a solderless breadboard to control the actuators, one each for the extend and retract functions. These buttons connect to the Uno's digital input/output pins, with a high signal produced when the button is pressed.

The linear actuators utilise 5 pins. The two power pins activate the motor, with the polarity controlling the direction of the shaft. The voltage and current draw of the motor exceeds the acceptable level for direct drive via the Arduino. For this reason, a motor-driver is constructed using a half-H bridge driver, the L293DNE in this instance. This allows for a separate power supply to drive the motor, whilst still being controlled by the Arduino.

The remaining three pins are for the potentiometer. They consist of a +5V pin, a signal pin, and a ground. The +5V and GND connect to the corresponding pins on the Uno, via the breadboard power rails. The signal pin connects to an analog input pin. The Arduino can take an input voltage of up to 5V, then utilising a built in DAC outputs a 10-bit value of 0 to 1023.

This combination gives us the circuit diagram seen in Figure 3.3. The circuit is hooked up to a power supply unit, which provides the 6V required to drive the motor. The Arduino can either draw its power from the 6V supply or 5V via a USB connection to a PC, the USB also provides a serial connection to monitor the system in real-time.
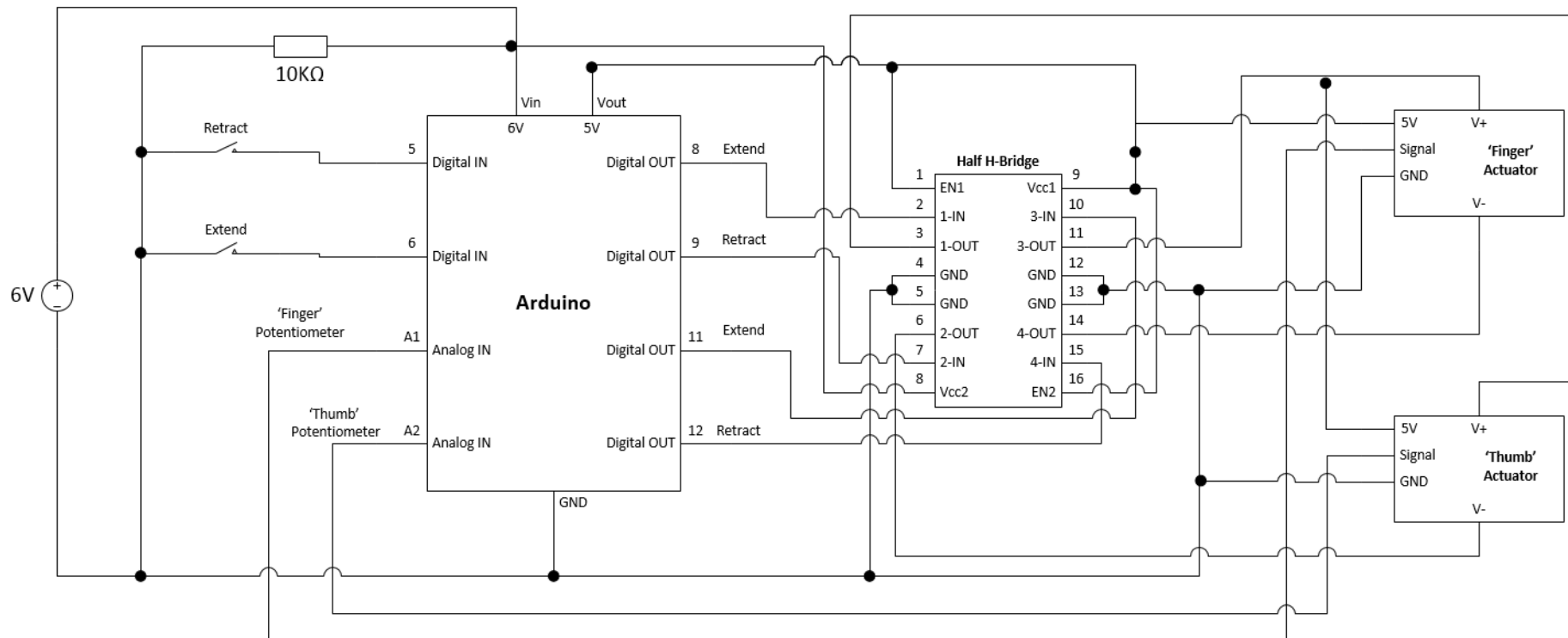
Figure 3.3 Push-Button Circuit Layout

3.1.2 Isolated sEMG System

Developing a system which takes the sEMG recording and converts it into a digital output is one of the main challenges in developing the control system. To simplify the procedure the sEMG system was isolated on a separate Arduino circuit. The OYMotion Gravity (Figure 3.4[5]) is made of two constituent parts, an arm-band and a signal processing board; the armband connects to the board via a 3.5mm jack, the board processes the signal and connects to the Arduino board via three pins:

- **+3.3V:** this provides the power for the sEMG and is taken from the Arduino's built in 3.3V output pin

- **GND:** grounds the sEMG with the rest of the circuit

- **Signal:** this provides a signal voltage that the Arduino can monitor via an analog input pin

The sEMG chosen has been designed specifically to be used with an Arduino board, allowing for a very simple circuit design, shown in Figure 3.5. The signal from the sEMG can be plotted in real-time via a USB serial link, this proved to be of great use when developing the control system.
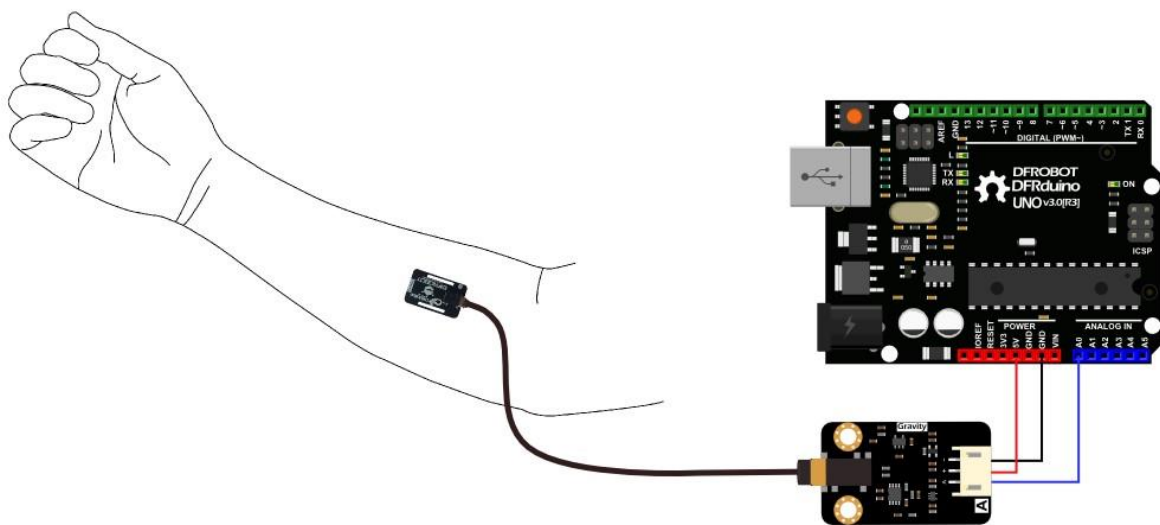
Figure 3.4 Gravity: Analog EMG Sensor by OYMotion [110]

---

[5] Figure 3.4 is sourced from OYMotion and is only indicative, in practice the sensor would be placed on the bicep as previously described
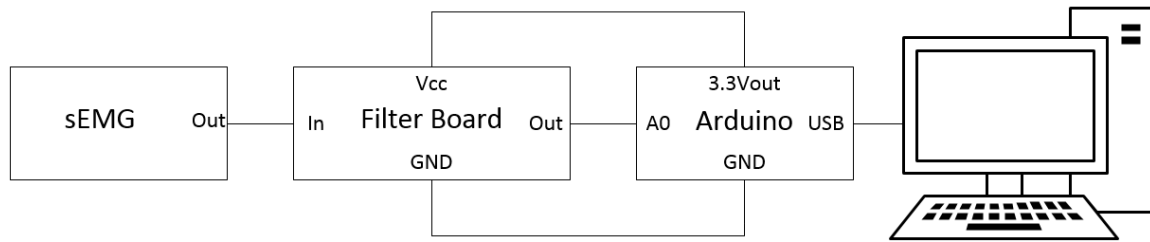
Figure 3.5 Isolated sEMG Circuit

3.1.3   Final sEMG Controlled System

The circuit that was integrated into the final prosthetic is a combination of the previous two (Figure 3.6). The motor control circuitry is identical, however rather than using push buttons, the sEMG is used to control the system. The circuit just as with previous versions was constructed on a solderless breadboard; however, as this is the final circuit design, a soldered version on copper stripboard was also produced for installation in the final prototype prosthetic. This soldered board contains a 6V voltage regulator on the motor circuit, this is required as the battery produces 7.5V. The Arduino has a built-in voltage regulator and can be powered directly from the battery, components such as the sEMG will draw their current from the regulated voltage outputs on the Arduino.
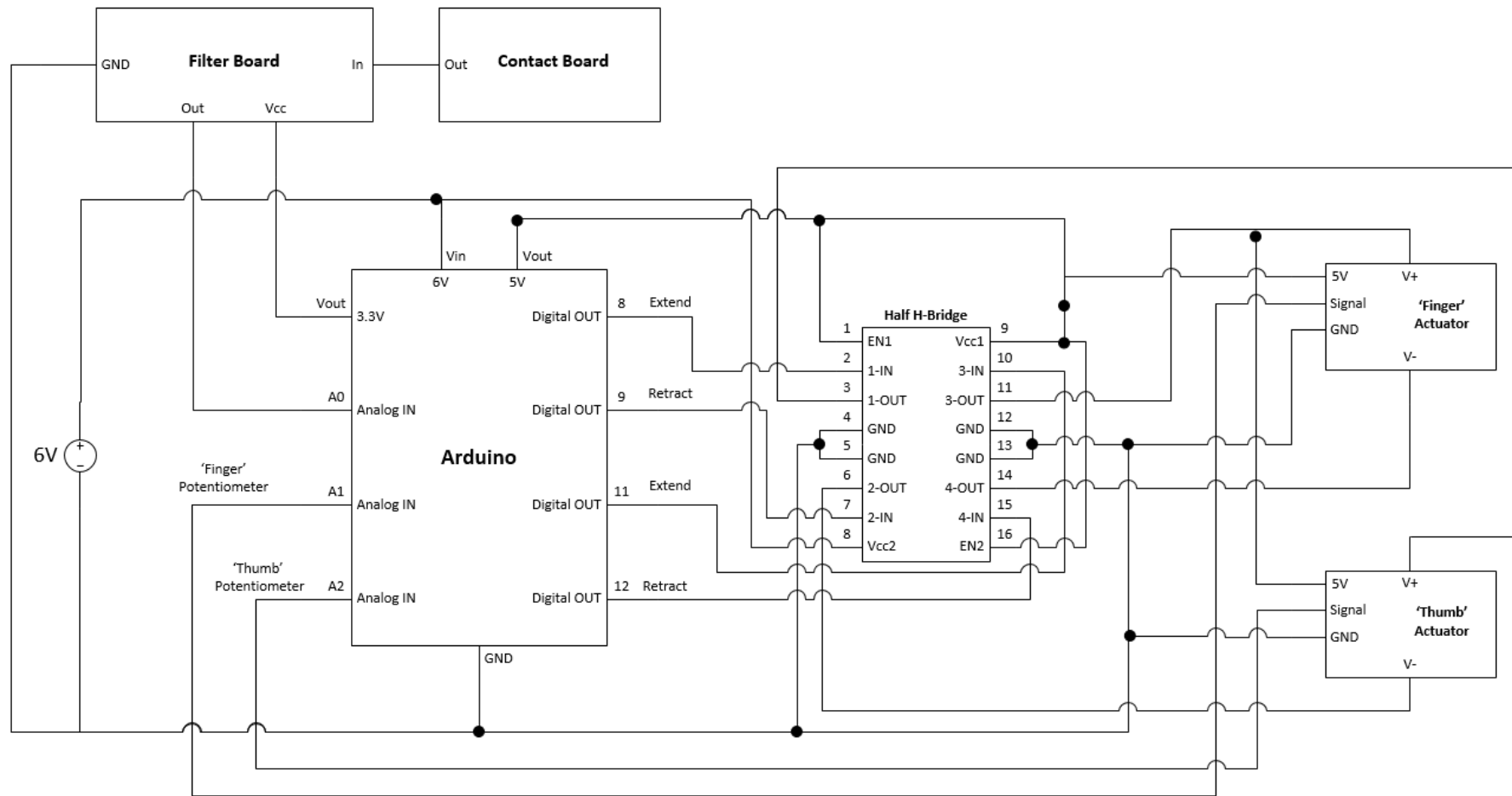
Figure 3.6 Final sEMG Controlled Circuit

3.2   Simulink Model Overview

The programming of the system was performed using the Simulink Support Package for Arduino Hardware. This was chosen over the standard Arduino programming environment as block-based Simulink models provide an intuitive method to develop the system. The use of scopes and serial monitoring also allows for real-time performance analysis far beyond what is capable in the Arduino software. An overview of the entire system can be seen in Appendix B1. This can be broken down into three sections:

    A. The actuator control sections:

        1. The 'finger' actuator

        2. The 'thumb' actuator

    B. The grasp detection system

    C. The sEMG system

The other parts of the model act to support these sections and will be explained where appropriate in the preceding subsections.

3.3   Actuator Control

The Simulink model shown in Figure 3.7 and Figure 3.8 display how the actuators the drive the 'fingers' and 'thumb' respectively are controlled. The first block in the takes the potentiometer input from the actuator, this provides a 10-bit value between 0 and 1023, representing full retraction and full extension (20mm) respectively. The two constant blocks represent the limits for shaft extension and retraction. The unit conversion and if function blocks of the subsystem are detailed in Appendix B2.
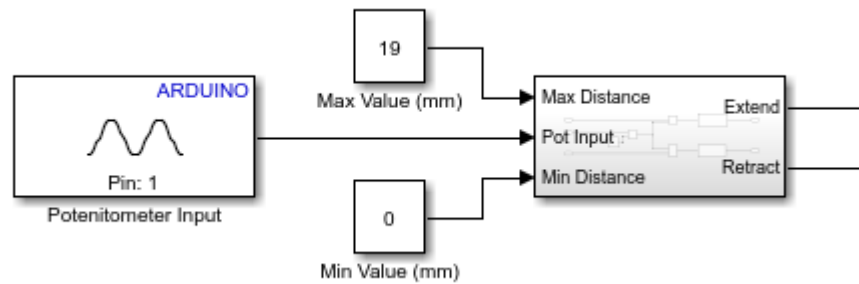
Figure 3.7 'Fingers' Actuator Simulink Model - A1
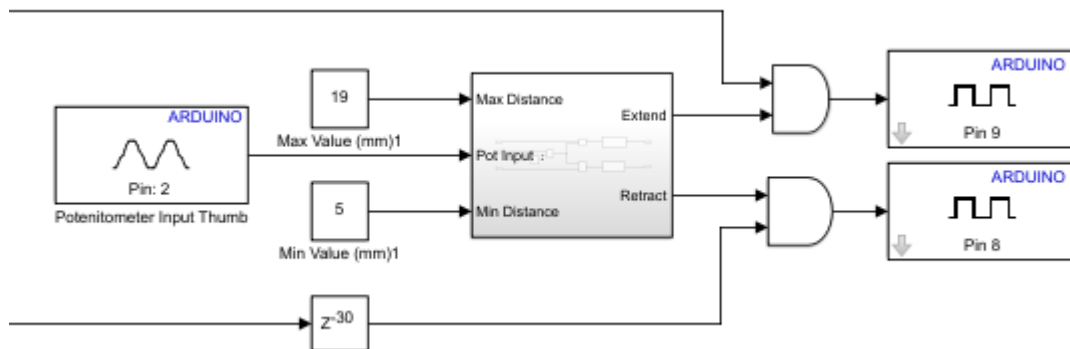
Figure 3.8 'Thumb' Actuator Subsystem – A2

In order to test this system and determine the limits for the actuators, a test-rig which holds a single actuator and gripper was produced via 3D-printing. This rig was implemented as a simple way of isolating the gripper and actuator system, the circuit used was the "Push Button Controlled Circuit" displayed in section 2.8. From this system the limits of 5mm-19mm for the 'thumb' and 0mm-19mm for the 'fingers' were determined.
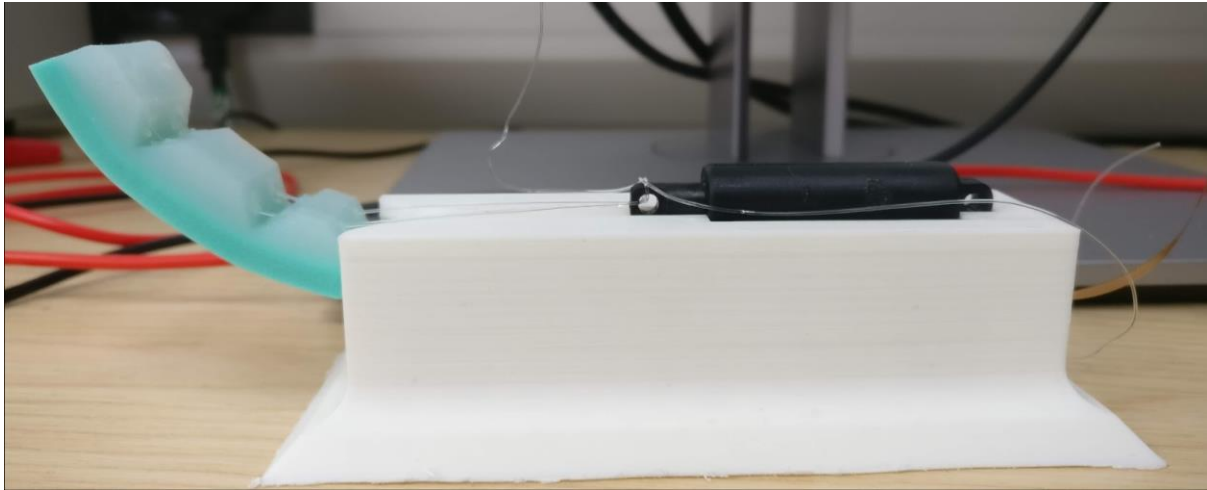
Figure 3.9 Test Rig

3.4   Grasp Detection

The grasp detection system has been implemented to determine if an obstruction has occurred that has caused the actuator to slow to a near stall. This is to prevent the motor from burning out when an object is grasped, as ordinarily under sEMG control, the actuator would continue to be driven, attempting to retract until the limit is reached.

The first step in determining if an obstruction is present is to measure the velocity of the shaft (Figure 3.10). For this the potentiometer signal is processed through a moving average filter, along with a necessary data conversion step. A 10-step delay is introduced on a separate path and subtracted from the real-time signal. This in effect produces a velocity value, as direction is not of importance, it is converted to an absolute value.
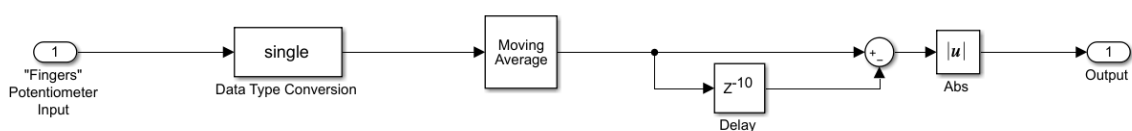
Figure 3.10 Grasp Velocity Subsystem

This velocity value will then pass to the next subsystem, where an interval test will determine if the value has exceeded the set limit. If the value has been exceeded then the actuator is deemed to be moving without obstruction, producing a high output signal; should the value drop below this limit, a low signal is produced (Figure 3.11). The optimal threshold is determined to be 15, this equates to 2.9mm/s or 19% of the motor's published maximum shaft travel speed [111]. The EMG Signal Switch block will only activate the grasp detection once a high signal has been present for 10 steps; this is to allow to actuators to initially travel from a stationary position.
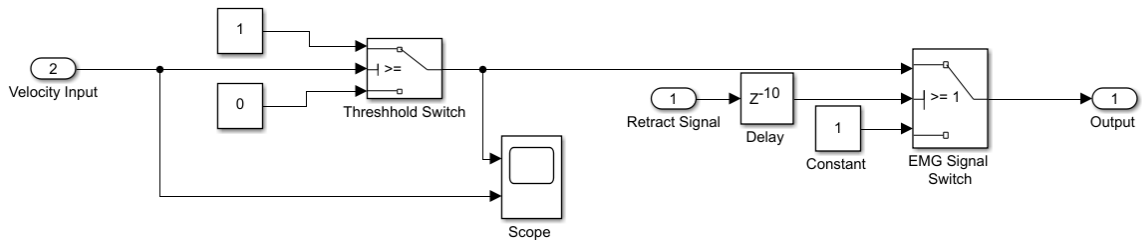
Figure 3.11 Threshold Subsystem

Figure 3.12 shows the plot for binary output and the velocity detected. The two signals correspond with each other, with all significant periods of movement producing a high output. The AND gate links together the activation signal (from a button or sEMG), the shaft limits, and the grasp detection (Figure 3.13). Only when all are high will the grasp retract. There is also a 30-step delay on the 'thumb', this is to allow the 'fingers' to close, with the 'thumb' then wrapping around them. Without this delay, the grippers collide with each other and are unable to form a fully closed grasp.
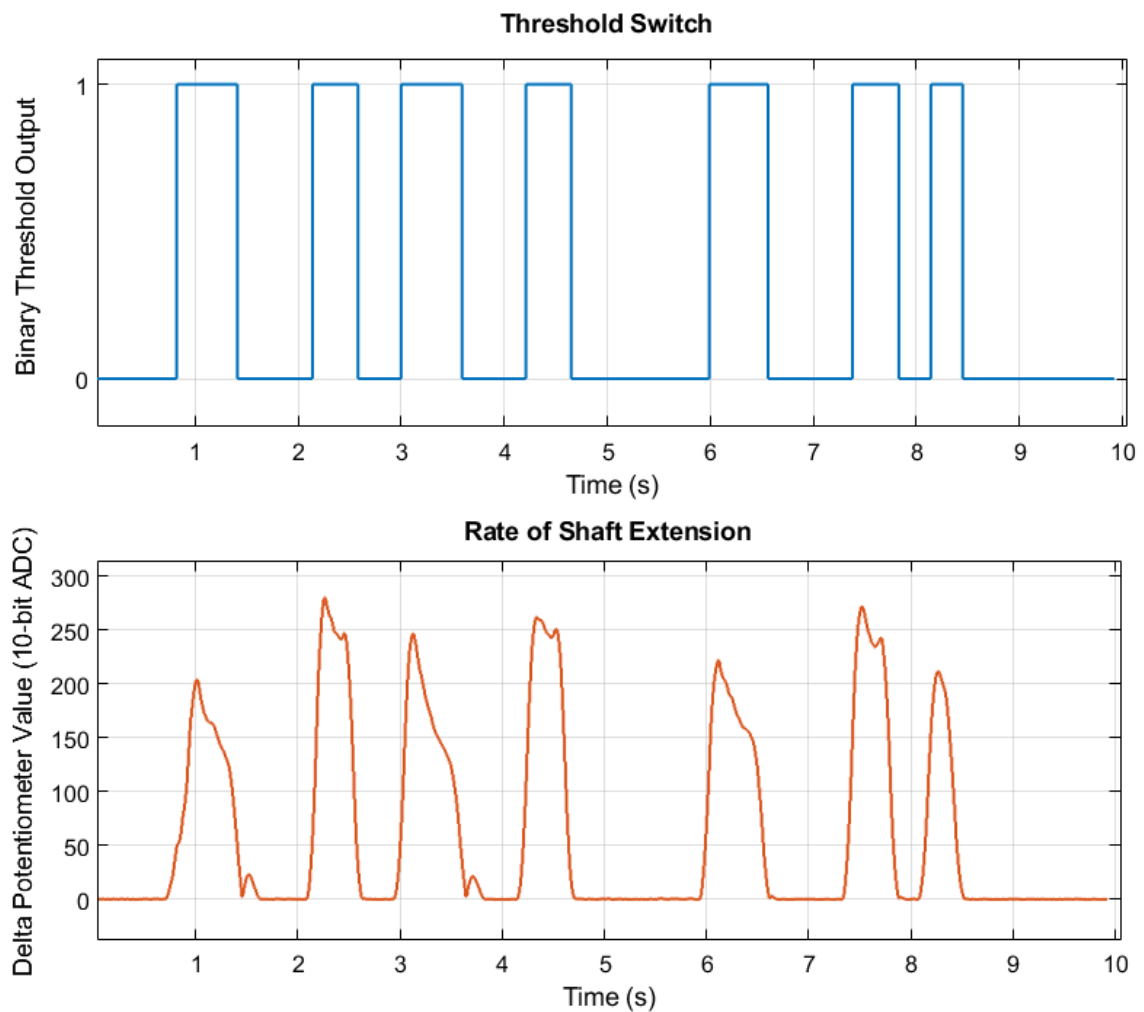
Figure 3.12 Binary Output (top), Grasp Velocity (bottom)
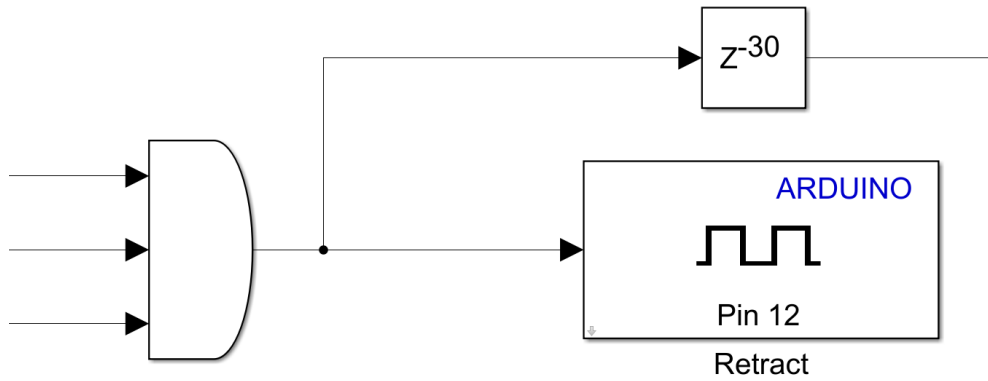
Figure 3.13 AND Gate and Motor Output

3.5   EMG

Electromyography or EMG as described in section 1.6, is the process of recording electrical signals produced by muscles under flexion. As the purpose of the project is to provide a simple system that would be a child's introduction to prosthetic control, the simplest system, 'single-site single-action', will be utilised. The control method can be setup as either voluntary opening or voluntary closing. In a voluntary opening system, the 'hand' opens when a high signal is recorded by the EMG, once the single stops the grasp retracts; in a voluntary closed system the reverse is true, with the 'hand' remaining open until activated. Voluntary opening (often referred to as "cookie-crusher") was chosen in this instance due to its relative prevalence in literature compared to voluntary closing [77]. Should future research or the user indicate a preference for voluntary closing, the system could easily be converted to fall in line with this.

The sEMG system integrated here uses an armband-based device that connects directly to the Arduino's analog input. This is imported into the Simulink model with the "analog input" block. The signal is then processed (Figure 3.14), eventually producing a binary output. Scopes are placed at various points on the subsystem to highlight the process. All of the graphs in the following subsections are taken from Figure 3.14 the same reading, allowing for comparison between the steps.
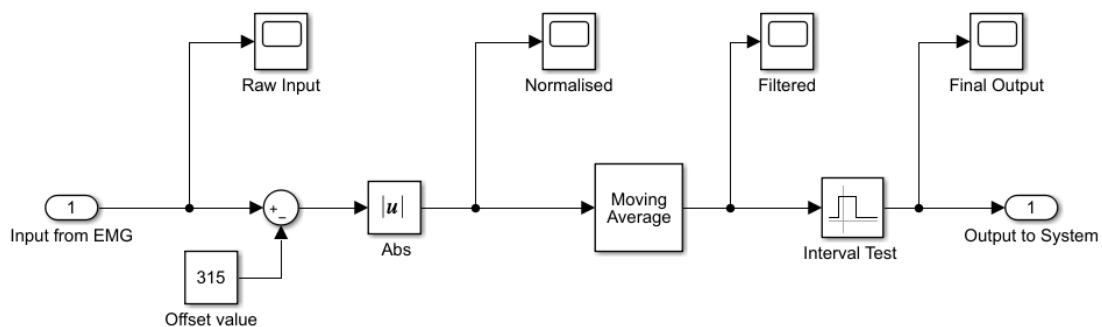
Figure 3.14 sEMG Signal Processing Subsystem

3.5.1 Raw Analog Input

The initial raw signal from the sEMG is shown in Figure 3.15. The units displayed represent the Arduino's built in 10-bit ADC (0-1023); for the purposes of this system the units can remain in this format, as only the amplitude of the signal is required. It is clear from looking at the plotted raw data where the periods of muscle activity are; however, there is a large amount of noise present and the signal oscillates rapidly.
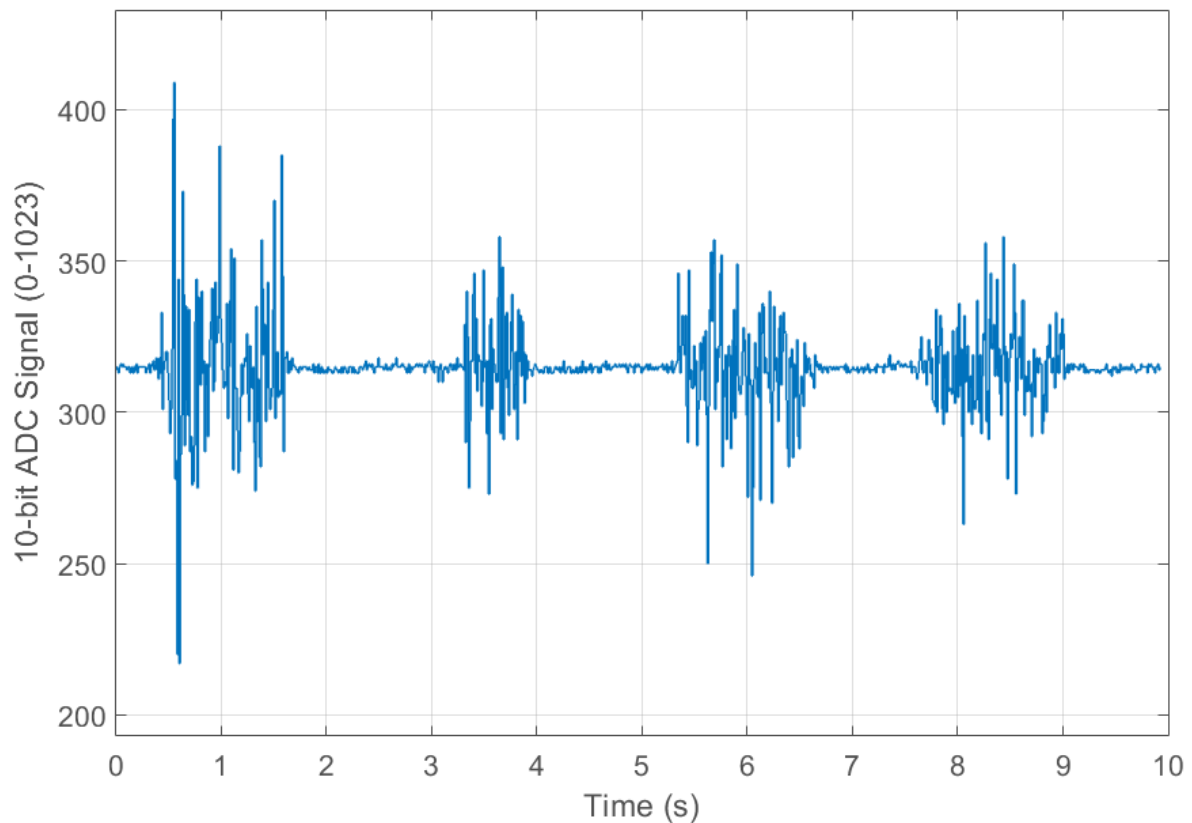
Figure 3.15 Raw sEMG Recording

3.5.2 Normalised

Some work was preformed using peak to peak amplitude, though this achieved unsatisfactory results. Instead it was decided to normalise the signal around 0, as well as converting the signal to an absolute value. This gives us the graph shown in Figure 3.16; here all of the periods of activity are in the positive blocks of activity, with the resting muscle signal hovering around 0.
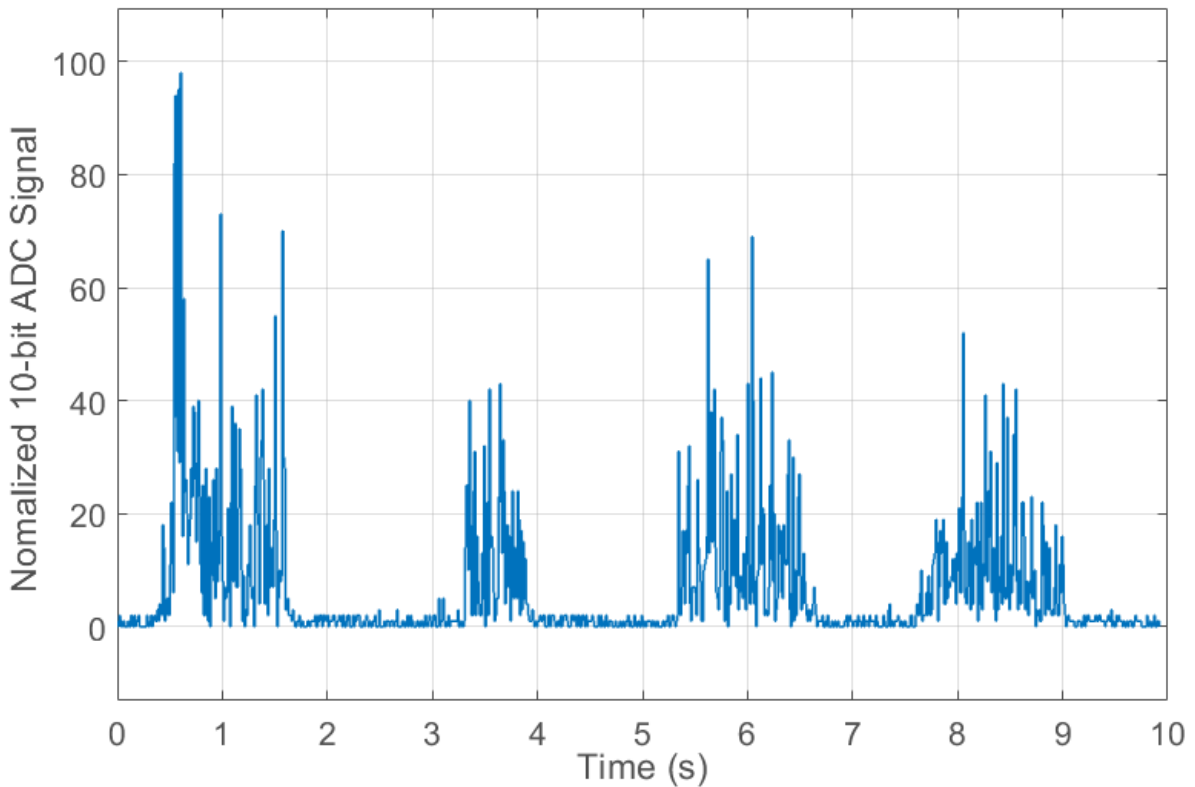
Figure 3.16 Normalized sEMG Recording

For the offset, an average value for the relaxed muscle signal was determined as 315; this value was taken and subtracted from the raw signal. As with all of the signal processing preformed here, the recording is taken from a single individual, a 23-year-old male of average build. Should the device be used on a different subject, the signal may vary due to differing levels of body fat, skin conductivity, muscular strength, etc. This would likely necessitate different offsets and threshold values to be incorporated. The use of Simulink and serial monitoring allows for this to be observed and adjusted easily. Were such a system to be used in a final wearable prosthetic, there would be an initial period of tuning the device to the individuals signal composition.

3.5.3   Filter

The next stage in the process is to filter the signal. There are numerous methods of approaching this, and many were investigated during the initial development stage of the system. Many of the methods tried ended up being too computationally demanding for the Arduino hardware, especially once integrated into the full system. The method eventually chosen utilises a moving average filter, which takes the average value of the signal over a given time window. The filter produces the signal shown in Figure 3.17. It is clear that a significant amount of the noise has been eliminated and critically the active periods of the signal do not intermittently drop to 0. This allows for an 'interval test' block to be used, which determines if the signal is above or below a set threshold.
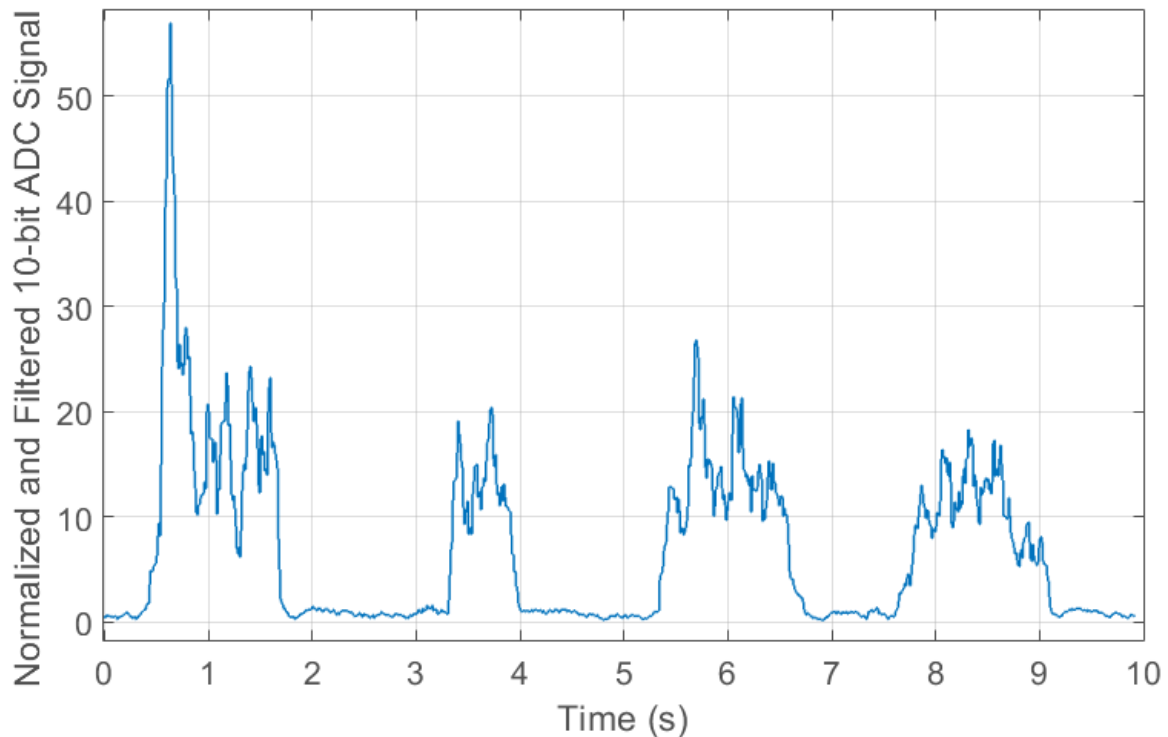
Figure 3.17 Normalized and Filtered sEMG Recording

3.5.4 Final Output

The 'interval test' block produces a binary output; when the signal is above the set threshold, the signal is high, with the inverse being true when the threshold has not been met. This threshold value is easily adjustable within the block parameters. In this instance, a trial and error approach was taken to adjust the threshold value based on the subject's EMG recording. It was eventually determined that 5 was the most effective value, with significantly higher or lower thresholds failing to activate during flexion or activating under non-control-specific motion, such as moving the elbow. Thresholds slightly higher tended to cause jittering on the output signal, due to momentary drops just below the threshold. Optimising this threshold is a major factor in the success of the system, proper initial fitting and tuning would help to ensure it maintains maximum effectiveness. It would also be possible to attach hardware inputs, such as a button or a potentiometer, which would feed a threshold value into a 'dynamic interval test' block. This would allow for the threshold to be adjusted whilst wearing the device. This may prove advantageous in situations where skin conductivity changes, such as when sweating.

Following the parameter turning, the binary output in Figure 3.18 is produced. It accurately matches the periods of recorded muscle activity. The system was tested multiple times and would, with near complete accuracy, produce an output matching the flexion. Very occasionally there would be a jitter, either from an unintentional flexion of the bicep under normal movement, or during an opening when

the signal slightly drops below the threshold; the latter of which would normally only occur when the muscle signal is weakened from rapid repeated flexion.
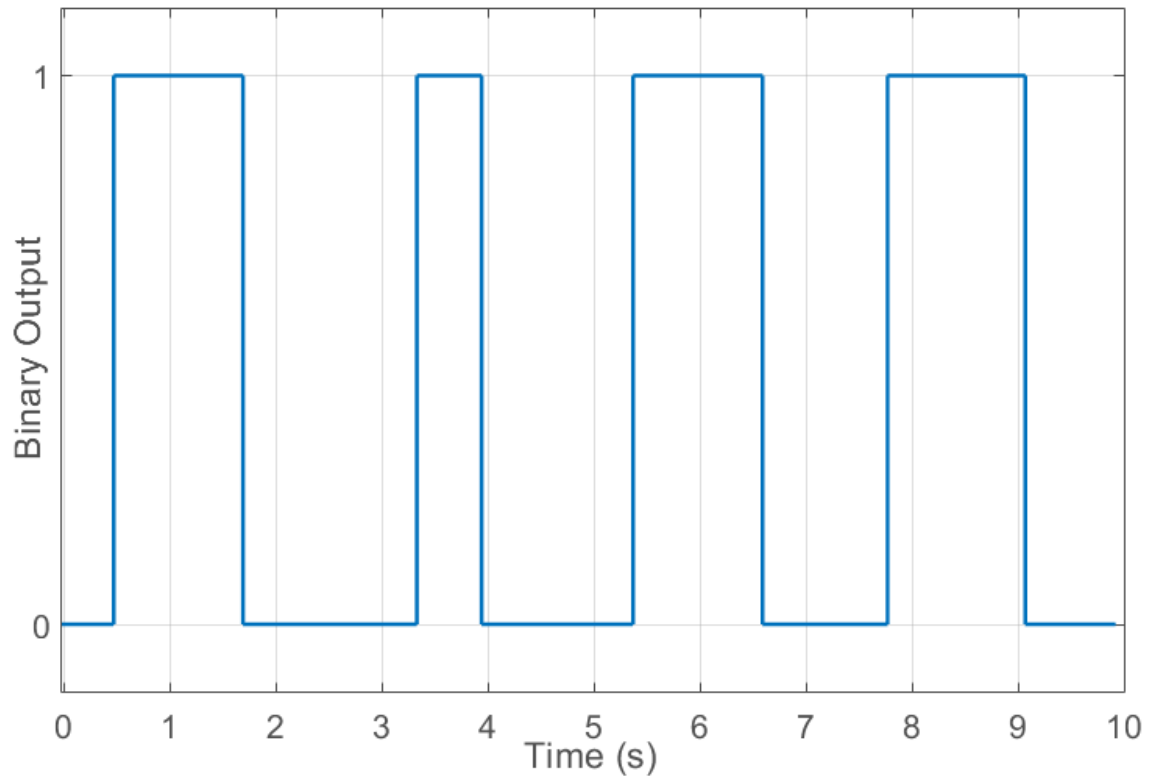
Figure 3.18 Final Binary Output

3.6 Chapter Summary

This chapter has covered the control system used on both the full prosthetic prototype and the grasp testing system. The final Simulink model provides a control system that can easily be adjusted to meet a user's specific requirements based on their sEMG data. Grasp limits and thresholds are also easily customisable, should design changes to the grippers take place.

In the proceeding chapter the push button control system and the grasp test prosthetic will be used to determine the effectiveness of the device, via a series of experimental procedures. Slight variants on the control system are used here, such as the grasp detection being disabled when determining maximum grasping force.

4   Experimental Procedures

The prototyping phase of the project produced the full prosthetic that could be directly used by a patient. Alongside this, a second arm with the same design, absent of the socket and internal controller was produced. This second prototype was used throughout this chapter in order to verify and quantify the performance of the system from a grasp effectiveness perspective. The prototype will be arranged in a configuration where all of the grippers are 3-segmented 'fingers' and in a configuration where the 'thumb' is a 2-segment gripper, offset from the two 3-segment grippers acting as 'fingers'.

Four main tests were conducted using this prototype. The first assesses the grasping ability of the hand in securely grasping objects of various weights and geometric profiles. The next procedure involves attaching weights to various objects to show the maximum grasp capability of the 'hand' with regards to the weight of objects. The third test measured the grasp force of the 'hand' using a specialised device, allowing it to be compared with published results. The final test measures pinch force, again for comparison with published results, in this instance for maximum pinch strength in children and adults, as well as other prosthetic devices.

These tests were chosen as a suitable volunteer was unable to be recruited to perform practical usage tests. This would have been the primary source of validation, using a method similar to the Southampton Hand Assessment Procedure (SHAP) [126], along with user/parental feedback likely in the form of a questionnaire. As this was not possible, the focus has been to conduct tests with a metric which can be compared to other comparable commercial and research devices.

4.1   Object Grasps

In this experimental procedure, a number of objects were grasped using the prosthetic test device, as shown Figure 4.1. Section 5.1 will cover the results and include further images of the various grasps. These objects vary in size, shape, and weight, comprising of geometric shapes and everyday objects. The test procedure was to grasp each object 10 times. The orientation of the grasp is varied and the successfulness of each is noted. The objects are in almost all cases grasped directly from the workbench, in the case of the pen and wooden stick, some manual orientation is performed prior to a grasp. Once grasped, the arm is steadily shaken for a period of 10 seconds, this is to replicate the movement of the user whilst holding an object. If after this 10 second period had elapsed the object is still securely held within the 'hand', then the grasp is deemed to be successful. The experiment is performed with both the 2-segment and 3-segment 'thumb' set-ups; the results for both are noted for later comparison.
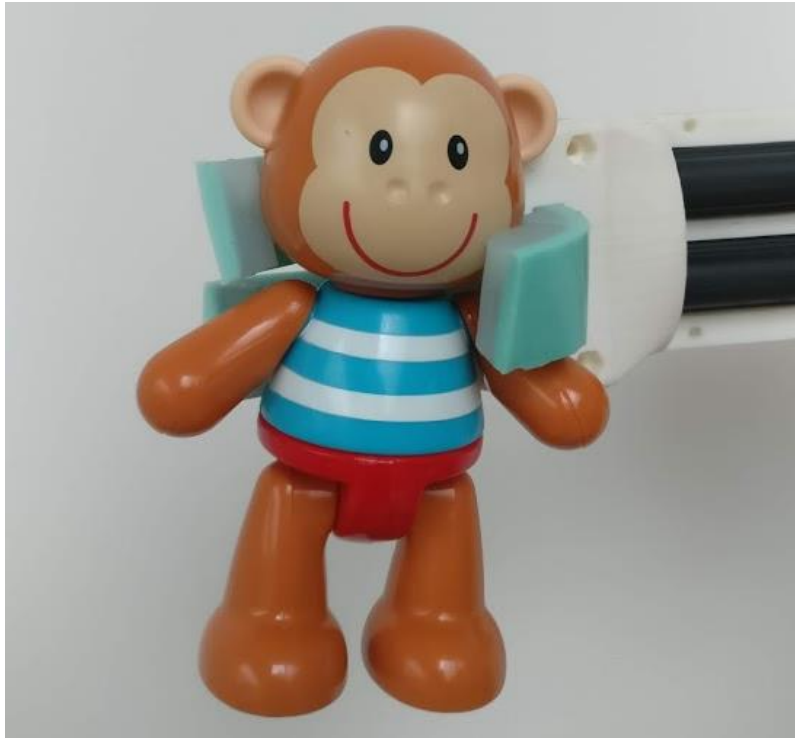
Figure 4.1 Example of Grasp Test Procedure using a Plastic Toy

4.1.1 Geometric Shapes

This first batch of objects comprised of 5 common geometrically defined shapes made up of a cylinder, cone, cube, 4-sided-pyramid, and triangular-prism (Figure 4.2). These objects were 3D-printed using an open source[6] STL file [112]. The parts were printed with a 10% infill and 0.2mm layer height (Figure 4.3), as high structural integrity and a fine surface-finish are not necessary factors in this test.

Figure 4.2 3D-Printed Geometric Shapes – from left to right: Cylinder, Cone, Cube, Pyramid, and Triangular-Prism

---

[6] Licensed under the Creative Commons - Attribution License

Figure 4.3 3D-Printing Process, Highlighting the Internal Structure

The weight of each geometric object is noted in Table 4.1. In this instance the maximum weight of an object is only 20.4g and as such does not have a large impact on how graspable the blocks are.

Table 4.1 Weight of Geometric Objects

Object	Weight (g)
Cube	31
Cone	9
Pyramid	13.2
Tri-Prism	13.2
Cylinder	20.4

4.1.2   Everyday Objects

In this second part of the object grasp experiments, the prosthetic's grasping ability with everyday objects is studied. The objects vary greatly. Most of the items are exemplary of ones that a young child might interact with, some, such as the set of keys, have simply been chosen to display the range of grasps available from the device.
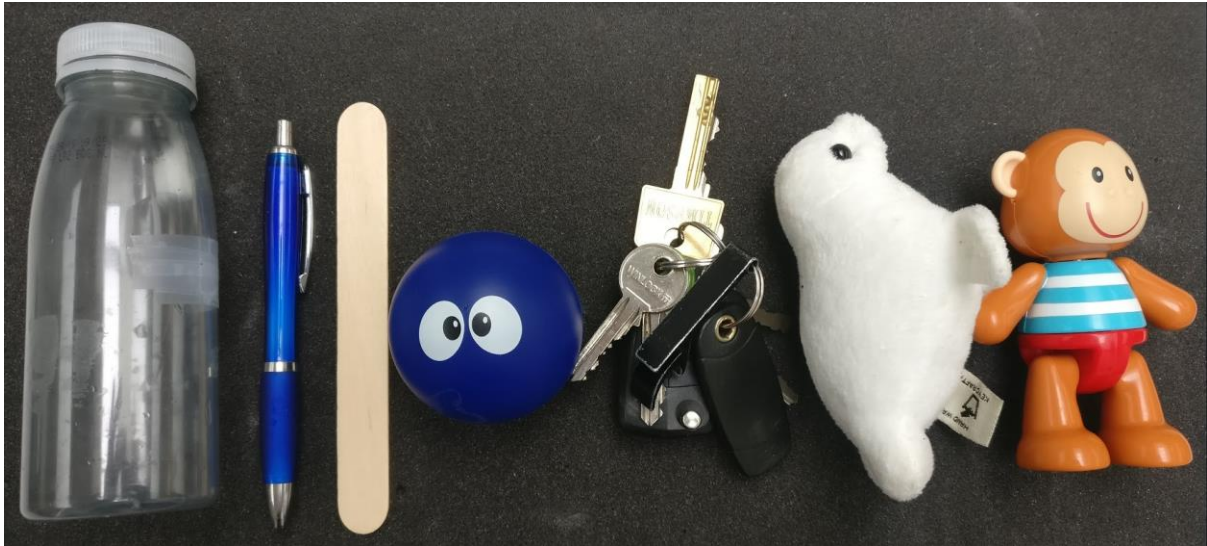
Figure 4.4 "Everyday Objects" – from left to right: Plastic Bottle, Pen, Wooden Stick, Sponge Ball, Keys, Soft Toy, and Hard Plastic Toy

The weight of each object was once again noted (Table 4.2). In this instance the maximum object weight was 270.6g, thought again the weight seemed to have minimal impact in this experiment.

Table 4.2 Weight of 'Everyday Objects'

Object	Weight (g)
Plastic Water Bottle (Empty)	20.6
Plastic Water Bottle (Full)	270.6
Pen	11.5
Wooden Stick	2.7
Sponge Ball	23.7
Set of Keys	94.2
Soft Toy	21.3
Hard Plastic Toy	56

4.2   Weighted Object Test

Although the weight of the objects was noted in the previous experimental procedure, it was not the primary focus. In this second test a series of objects were 3D-printed again, this time with a loop on which weights can be attached (Figure 4.5).

Figure 4.5 3D-Printed Objects for 'Weighted Test'

A hook with attachable weights is used on each object (Figure 4.6). The weights are measured from 0.1N to 5N and can be stacked to adjust the overall weight to the elected value. The experiment aimed to determine three characteristics from yeah of the grasped objects.

1. The load point at which the gripper begins to deform laterally

2. The point at which grasp slippage occurs whilst the prosthetic is steadily shaken

3. The point at which absolute grasp slippage occurs with a stationary device

During each test, the weight was slowly increased until a targeted outcome was met. At this point the total load is noted and the experiment is repeated an additional 9 times. The recorded data was tabulated in Excel (Microsoft Corporation) to determine an average maximum load for each parameter on each object. Just as with the non-weighted objects, the experiment is performed using both the 2-segment and 3-segment 'thumb' configurations, for the purpose of comparison.

Figure 4.6 Example of Weighted Test

4.3 Grasp Force Test

For this test, a numerical value is obtained for the grasp force of the hand. The test is performed on the Takei Physical Fitness Test: Grip-A [113]. This apparatus (Figure 4.7) has been shown to be an accurate method of measuring grip force [114]. The system uses an analog dial to display the grasp force in Kg. The force is applied by pulling the bar connected to the dial towards the base of the frame. This bar is adjustable in order to meet a range of hand sizes.

The grasp test is conduced ordinarily by having the user apply their full strength, with the dial indicating the maximum force recorded. In the case of the prosthetic the same procedure is used, as shown in Figure 4.8. The bar is adjusted to size the prosthetic hand. The test is then performed by closing the grasp of the hand. Two variations of this are preformed, one using the grasp detection system and a second run where the system is temporally deactivated. For each configuration, the test is performed 10 times to gain an average result. The markers of the apparatus, Takei Scientific Instruments, provide a table containing the average grasping force by age; this allows for comparison between the prosthetic and a correspondingly age-appropriate biological limb. The test was performed on both configurations, though there was found to be no discernible difference between the two, as such only the results for the 3-segment 'thumb' have been noted and analysed.
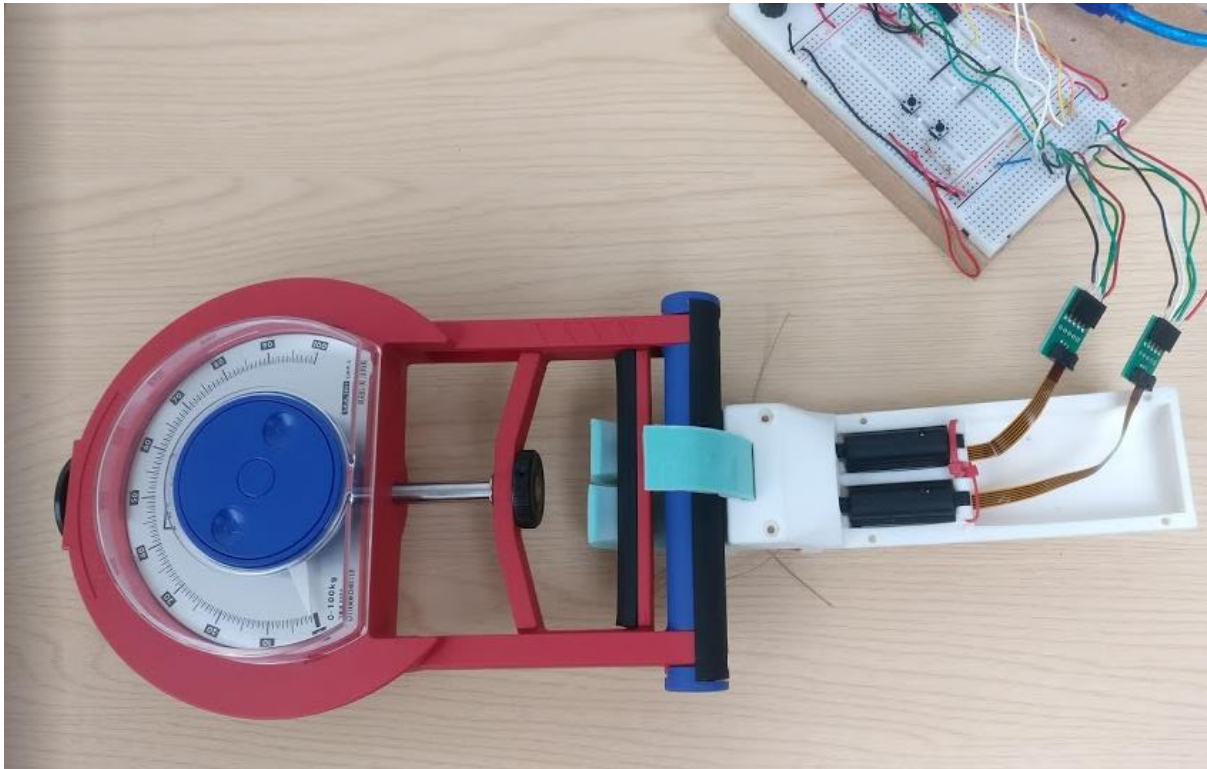
Figure 4.8 Grasp Force Test

4.4　Pinch Force Test

This final experimental procedure determines the "pinch force" of the grippers. The intention is to compare with published results of both biological grasping force and other prosthetic hands. The test utilised a set of high accuracy scales, perched on a stand, which can be pinched by the grippers.

Figure 4.9 Pinch Test Procedure

The pinch test is performed by closing the grasp of the prosthetic, thus applying a force that can be read on the scale. The test is performed under 3 system configurations:

1. **Actuators-on:** under this configuration the motor is continuously powered during the grasp

2. **Actuators-off:** in this instance, the grasp is performed then the actuators are powered down before is reading is taken

3. **Grasp detection system active:** here the grasp detection system is active, automatically powering down the actuators once a grasp has been recorded

The test, just as with previous examples was repeated 10 times for each configuration, with an average result being calculated from these readings. As the scale reading fluctuates slightly during a grasp, the noted reading is approximate to within ±10g. Much like the previous experiment, there was found to be a negligible difference between the 'thumb' variants, as such only the 3-segment configuration was recorded here.

4.5   Activities of Daily Living

Activities of Daily Living (ADL) is a term used to indicate tasks or actions that are commonly conducted or essential in everyday life. These tasks include simple things like feeding and bathing oneself and is a commonly used term in medical assessments. For the purposes of this project, three example ADLs are performed. This is done to highlight the 'real-world' applicability of the device, though it is limited to example tasks as an appropriate test subject to wear and use the arm could not be found, any further trials should aim to incorporate and build upon this ADL procedure.

4.5.1   Writing

The first task looked at is writing. This was performed by placing a common ballpoint pen in the appropriate grasp to be held by the device (Figure 4.10). In order to write correctly, the pen must be place by the user as the prosthetic is unable to manoeuvre the pen if grasping it from a surface. The prosthetic is then held at the forearm in such a way as to allow for the pen to mark the paper. A few simple shapes are then drawn on the paper to highlight the possibly of the arm being used for this ADL.

Figure 4.10 Pen Grasped by the Hand in Writing Position

4.5.2   Pouring Water from a Bottle

The second ADL looked at is pouring water from the plastic bottle used in the object grasp test, into another container. Figure 4.11 shows the bottle and container used in this procedure. This test is designed to show how the arm copes with the shifting weight of the bottle as the water pours out. It is also indicative of ADLs such as drinking.
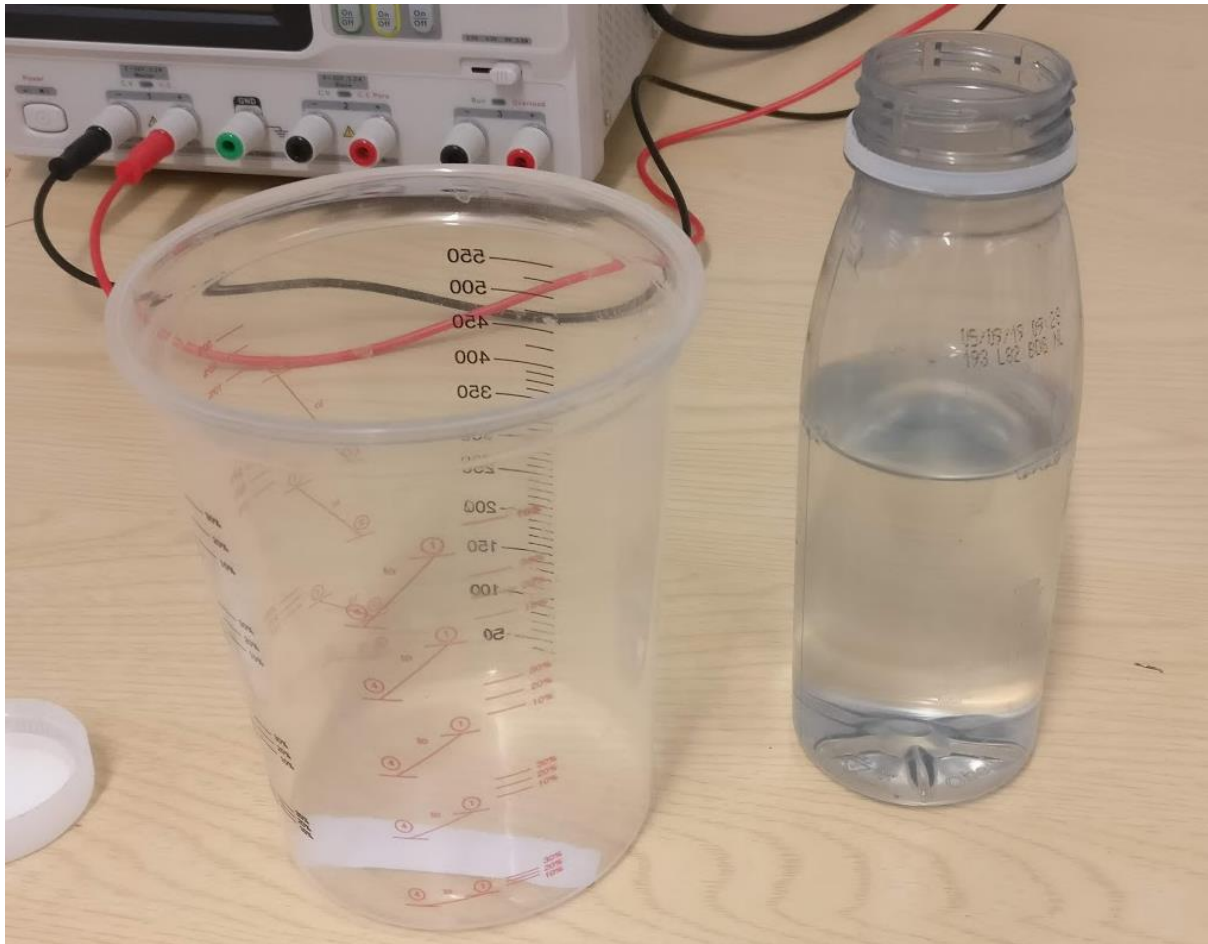
Figure 4.11 Bottle and Container used in ADL Test

4.5.3 Object Placement

This final ADL is used to demonstrate the device's ability to grasp, manoeuvre, and place objects. This has applications in a wide variety of ADLs including feeding oneself and in the case of children, playing with toys. The procedure used matches a common shape pattern block toy, given to children to develop their motor and object placement skills. A block for the shapes was 3D-printed to match the geometric shapes used in a previous experimental procedure (Figure 4.12). The test simply involves grasping objects from the surface to then place then in the appropriate slot. The object could only be grasped and oriented using the prosthetic during this test.
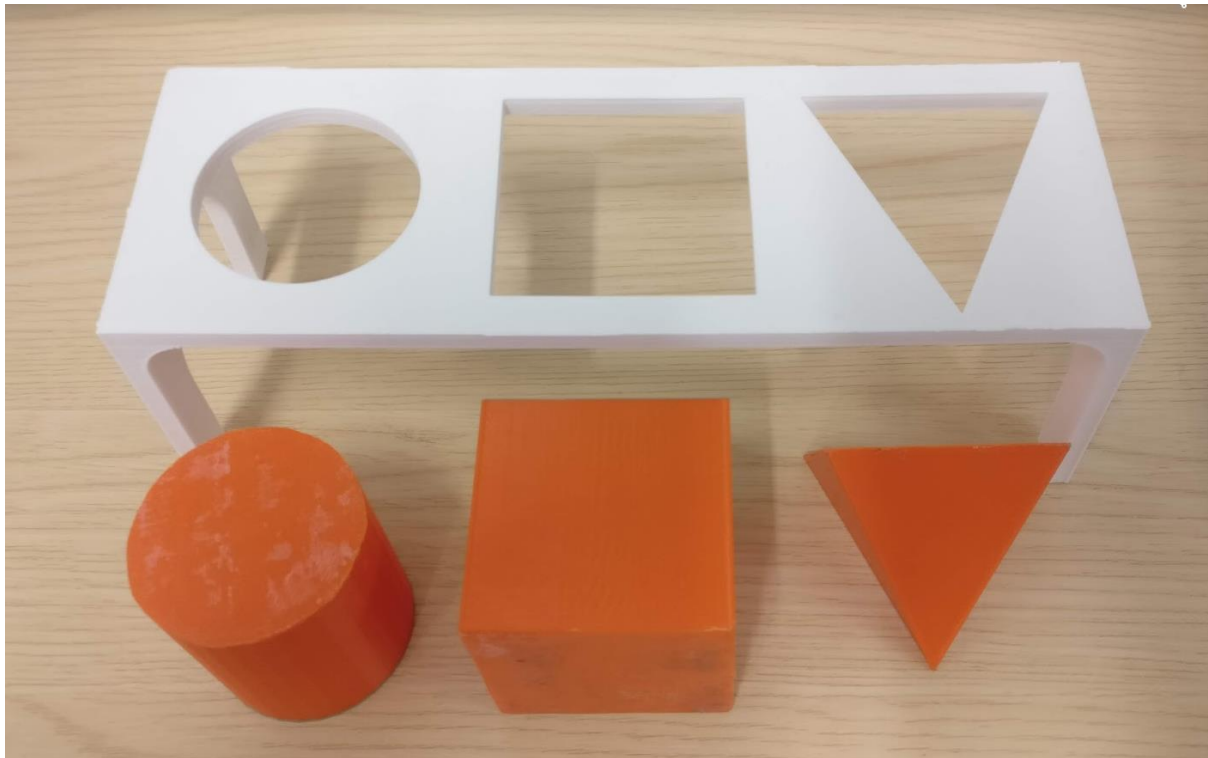
Figure 4.12 Block Placement Test Setup

4.6   Chapter Summary

The experimental procedures documented here are exemplary of kinds of grasp procedures used on prosthetic and biological limbs alike. The objects grasped are varied to show in an attempt to validate the assumption that soft-grippers will provide a highly functional grasp. The other tests to measure the strength of the prosthetics grasp attempt to provided numerical validation that the device performs competitively when compared to current active prosthetics. Due to limitations on lab equipment, the grasp tests are relatively basic in their design, but provide a basis for further validation. The proceeding chapter will examine the results of the aforementioned experimental procedures.

5 Results

This chapter will cover the tabulated results taken from the experiments shown in the previous chapter. The results are to be displayed in tables and graphically where appropriate. There will also be comments on the performance to back up the numerical data and provide a clear picture of the device's effectiveness. There will also be comparison to published results, taken from both biological limbs and other prosthetic devices.

5.1 Object Grasps

There is no singular agreed definition for grasp types, however in general terms grasps can be broken down into two categories, power and precision [115]. Power grasps typically involve the use of the whole hand to surround the object and is used in tasks such as unscrewing a lid on a jar. Precision applications conversely normally only use the fingers to hold a small point on an object, allowing for an exact action to be performed. These broad grasp types can be broken down further still. In the context of the present prosthetic, 4 grasp types that the device is able to perform have been identified (Figure 5.1).
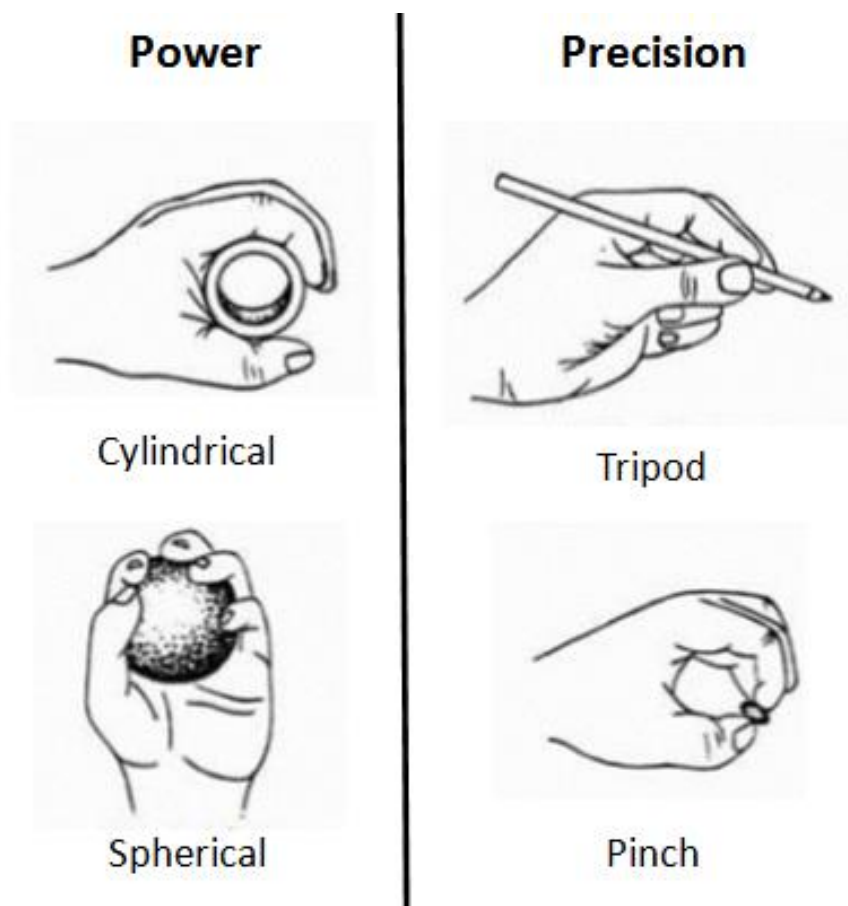
Figure 5.1 Illustration of Grasp Types [116]

- **Cylindrical:** a style of grasp where the fingers are kept in line, offset from the thumb to encompass the object e.g. grasping a bottle

- **Spherical:** a style of grasp where the fingers and thumb are spread to encompass the object e.g. grasping a round door handle

- **Tripod:** this grasp uses three fingers and often the palm to hold an object in a controlled manner e.g. writing with pen

- **Pinch:** a grasp which uses just the fingers, generally the fingertips to grasp an object e.g. holding a key

Figure 5.2 shows these grasps performed using the prosthetic device. In the proceeding subsections, the predominant type of grasp used will be noted. This is determined as the most natural or common way of grasping the object, for instance a bottle would normally be grasped cylindrically from the side, even though different types of grasp could also securely grip the bottle. In cases where the term 'mixed' is used, this donates that various grasp types can be used on the object with no definitive or obvious preference.
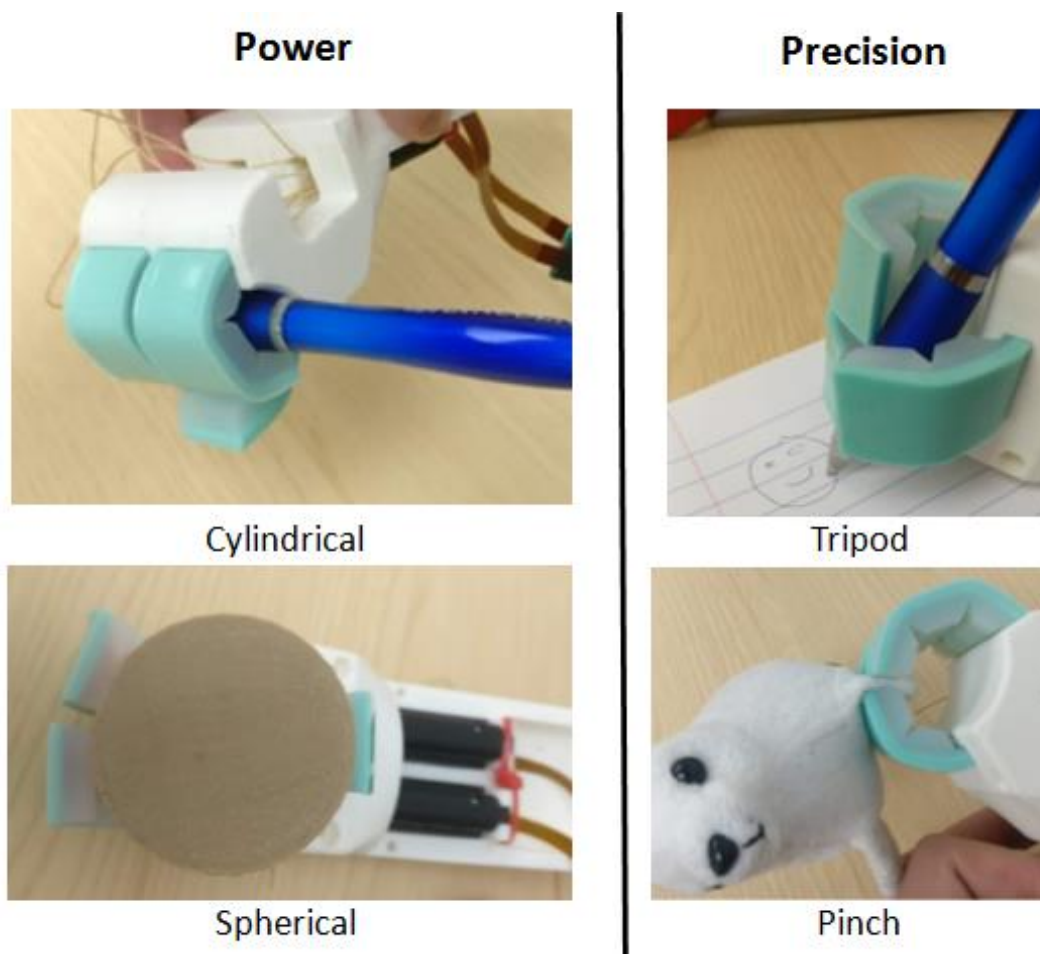
Figure 5.2 Grasp Types as using the Prosthetic

5.1.1 Geometric Shapes

In this procedure, 5 geometric shapes were 3D-printed to be grasped by the prosthetic. Table 5.1 shows the results of the test across all 5 objects:

Table 5.1 Result of Geometric Shapes Test

Test Object	Predominate Grasp Type	Three Segment Thumb	Two Segment Thumb
Cube	Mixed	100%	100%
Cone	Mixed	60%	50%
Pyramid	Mixed	60%	60%
Tri-Prism	Cylindrical & Pinch	80%	80%
Cylinder	Cylindrical	100%	100%
Mean Average		80%	78%

From the results a combined average grasp success rate of 79% is noted. Of the failures, the majority come from grasps attempted on the angled sides of the cone and pyramid. When the slanted sides of these objects are grasped using a pinch approach (Figure 5.3, Figure 5.4), they have a tendency to slide free after a few seconds; other grasp approaches (Figure 5.5, Figure 5.6) provide a secure grasp on the object. The triangular prism also experienced slippage when pinch grasped on the slanted sides.

Figure 5.3 Cone under Failed Pinch Grasp
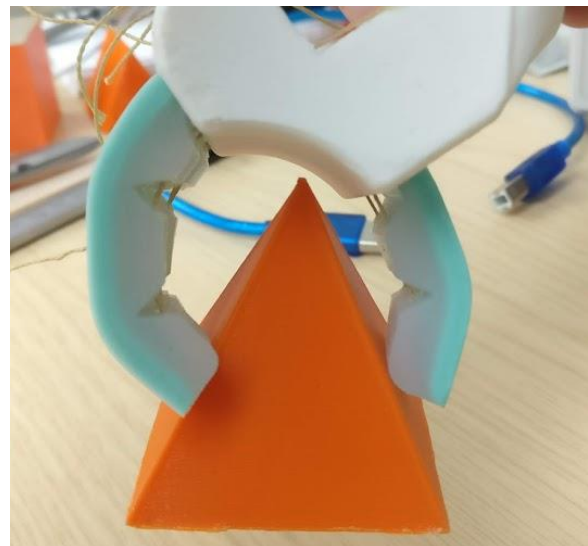
Figure 5.4 Pyramid under Failed Pinch Grasp
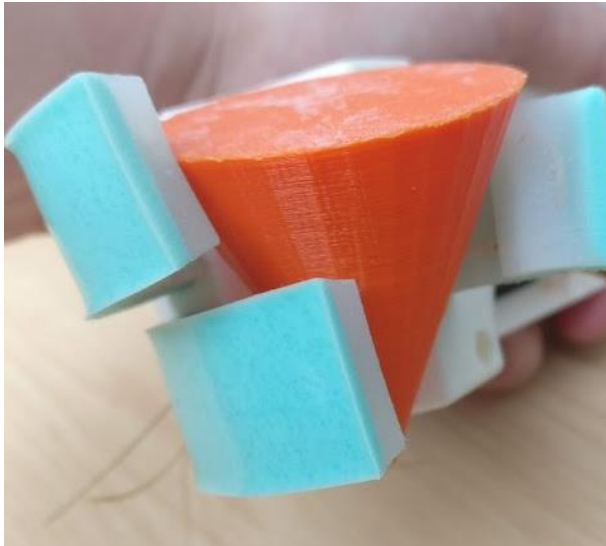
Figure 5.5 Cone under Successful Cylindrical Grasp

Figure 5.6 Pyramid under Successful Pinch Grasp

Figures 5.7-5.11 show the various objects being securely held in a grasp. The figures only display the grasp using the 2-segment thumb as the images are indicative of the performance for both gripper configurations.
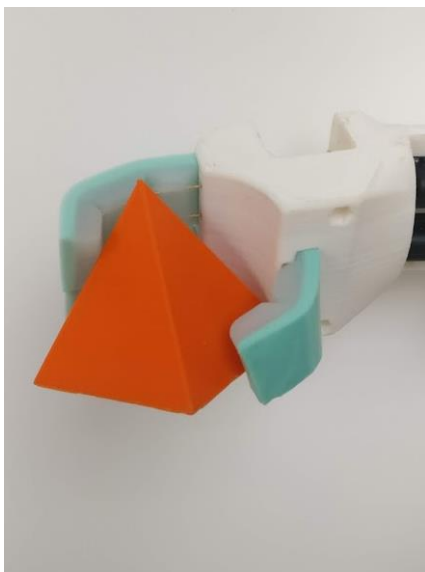
Figure 5.7 Pyramid
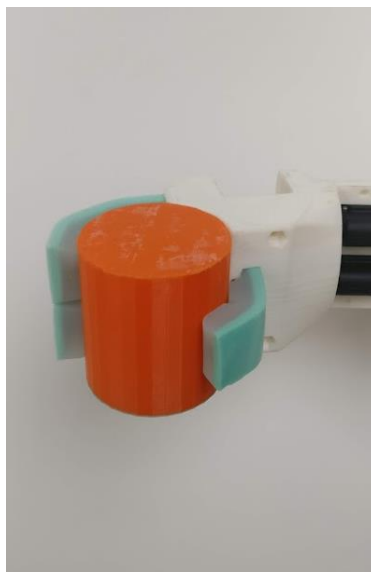
Figure 5.8 Cylinder

Figure 5.9 Cone
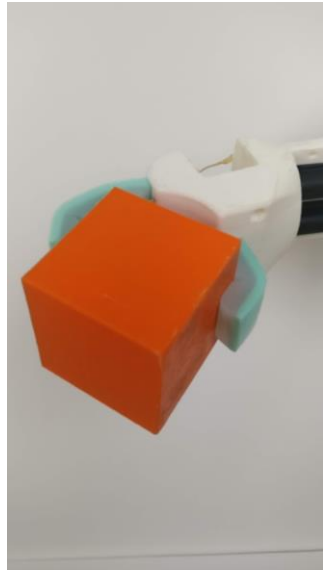
Figure 5.10 Cube
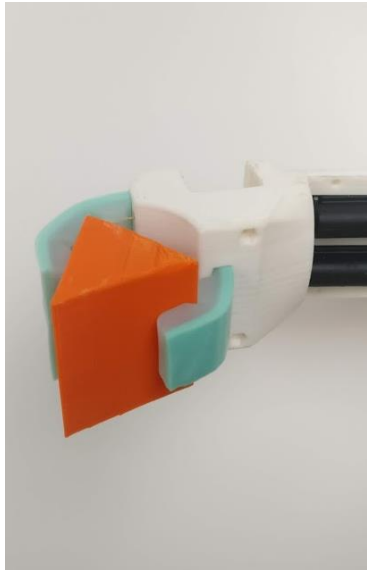
Figure 5.11 Triangular Prism
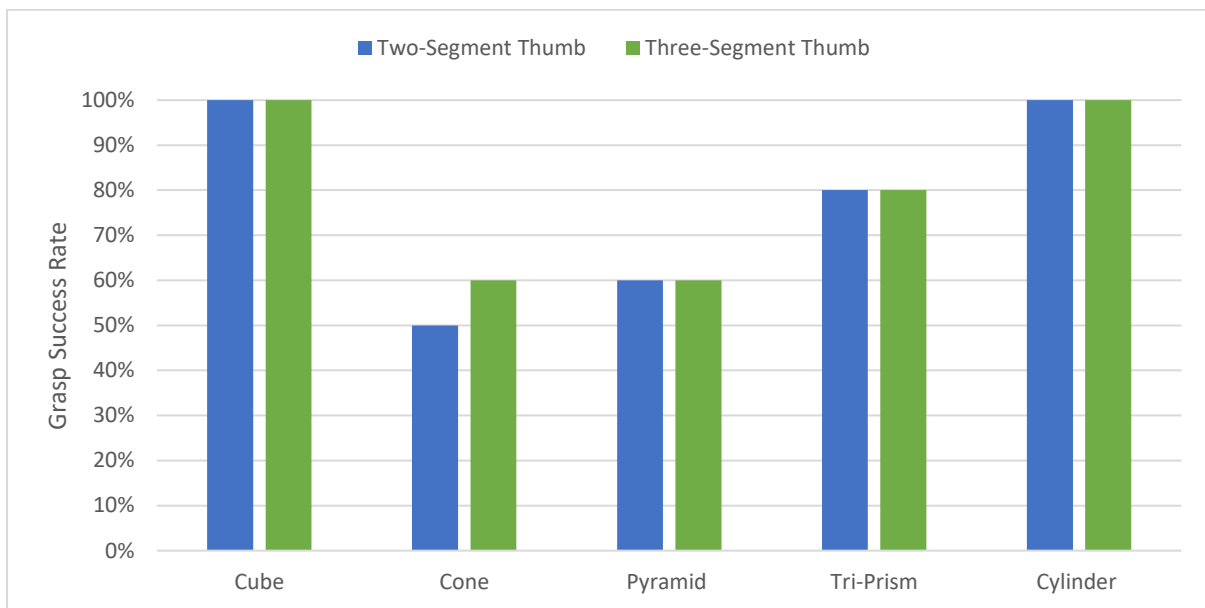
Figure 5.12 Geometric Objects Grasp Success Rate by Item and Gripper Configuration

Figure 5.12 compares the effectiveness of both gripper configurations with regards to each object. The overall difference is just 2%, with the 3-segment and 2-segment 'thumbs' achieving a success rate of 80% and 78% respectively.

5.1.2 Everyday Objects

This experimental procedure examines the devices ability to grasp several everyday objects. Table 5.2 displays the results for the grasp procedure. Just as in the previous section, the table compares the different gripper configurations and notes the type of grasp predominately used.

Table 5.2 Result of "Everyday Objects" Test

Test item	Predominate Grasp Type	Three Segment Thumb	Two Segment Thumb
Plastic water bottle (Empty)	Cylindrical	100%	100%
Plastic water bottle (Full)	Cylindrical	100%	100%
Pen	Tripod	100%	100%
Wooden stick	Pinch	60%	60%
Sponge ball	Spherical	100%	100%
Set of Keys	Cylindrical/ Spherical	80%	50%
Soft Toy	Mixed	100%	90%
Hard Plastic Toy	Cylindrical	90%	80%
Mean Average		91%	82%

The results note that the combined mean grasp effectivness of 86.5%. with the more geometically simple objects, such as the plastic bottle, a 100% grasp effectivenss is observed. The set of keys had issues with slippage in instances where the keys are picked up from a flat surface using only the prosthetic (Figure 5.13), this is esspaically true with the 2-segment 'thumb'. In instances where the keys are bundled and presented to the device, a secure clindrincal grasp is achived.

Figure 5.13 Attempted Grasp of 'Set of Keys' from a Flat Surface

Similar issues with the wooden stick occurred that lead to a low grasp success rate with this object. When the sick is placed flat on a surface (Figure 5.14), the device struggles gain any grip on the stick, resulting in a failed grasp. Presenting the object to the hand conversely results in a successful pinch grasp.
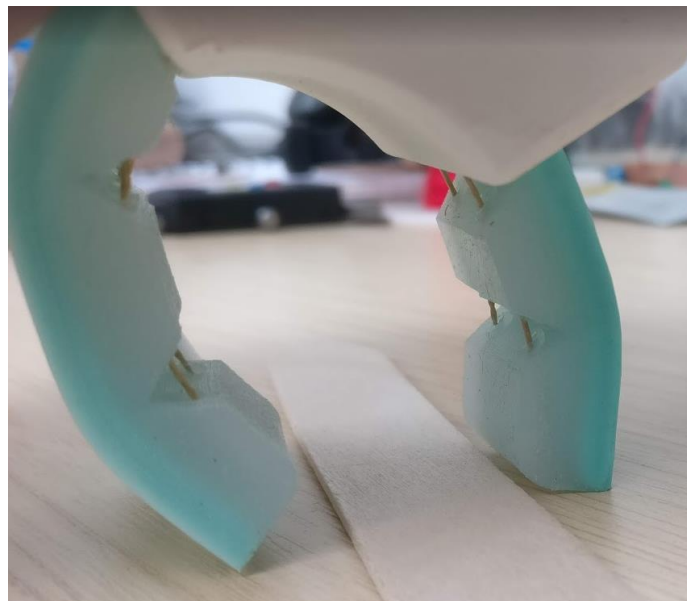
Figure 5.14 Attempted Grasp of 'Wooden Stick' from a Flat Surface

Figures 5.15-5.21 showcase the objects being securely grasped by the prosthetic device. Just as in the previous subsection, the different gripper configurations are not shown, with only the 2-segment 'thumb' being displayed here.
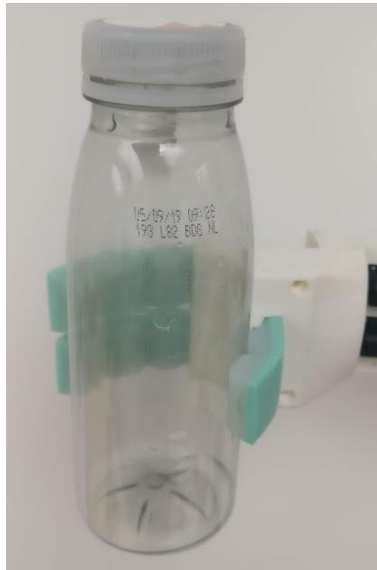
Figure 5.15 Bottle (Empty)

Figure 5.16 Pen
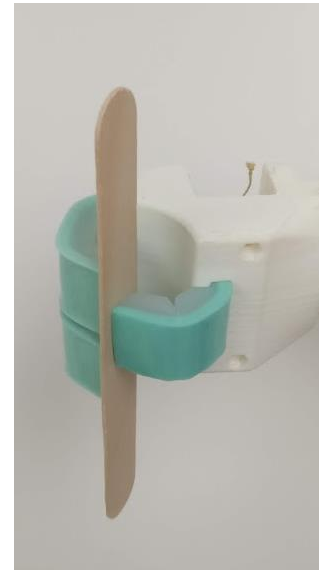
Figure 5.17 Wooden Stick

Figure 5.18 Sponge Ball

Figure 5.19 Set of Keys

Figure 5.20 Soft Toy

Figure 5.21 Hard Plastic Toy
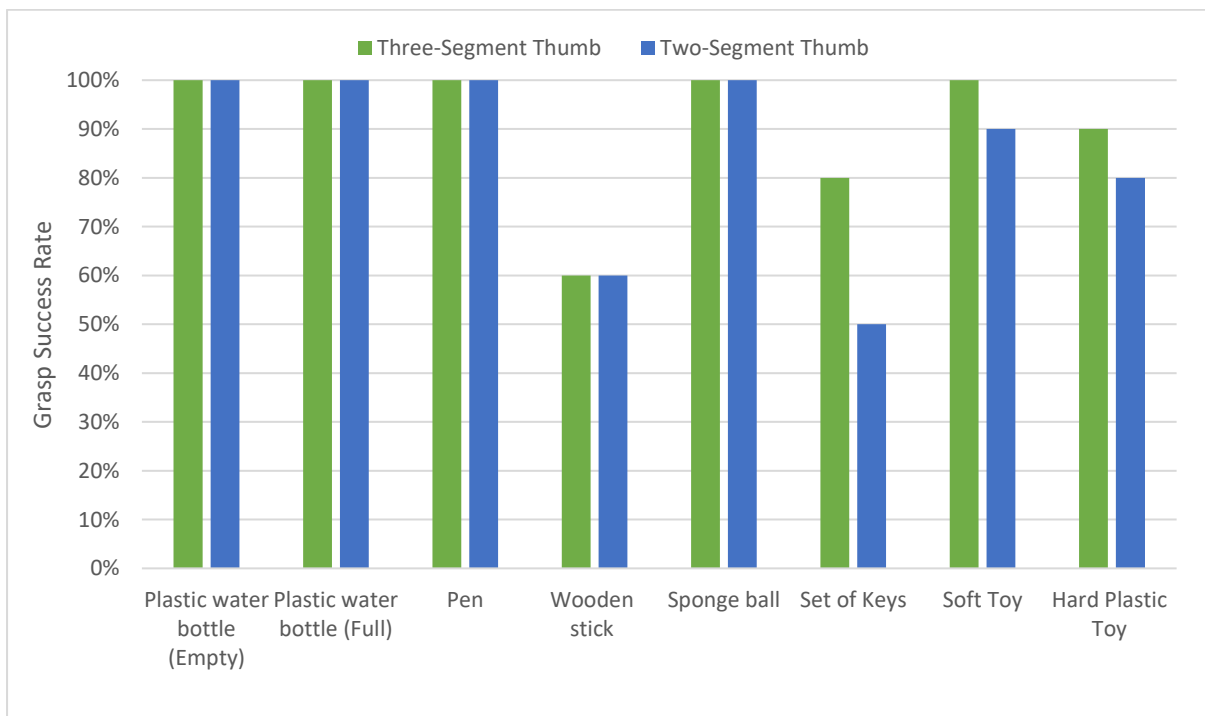
Figure 5.22 'Everyday Objects' Grasp Success Rate by Item and Gripper Configuration

Figure 5.22 compares both gripper configurations with regards to average object grasp effectiveness. The overall difference is larger here than it was in the previous subsection, a difference of 9%, with the 3-segment and 2-segment 'thumbs' achieving a success rate of 91% and 82% respectively. This difference is largely down to the issues picking up the keys from a flat surface using the 2-segment grippers.

5.2 Weighted Object Test

 The experimental procedure presented here used 3D-printed objects with weights attached to them to determine the lifting capacity of the device. The first point of interest is the weight required to deform the grippers laterally.

Figure 5.23 and Figure 5.24 show the gripper deformation when performing the test with the triangular prism and 45mm cylindrical block respectively. The test was performed on all four objects, using both gripper configurations to produce the results in Figure 5.25.

Figure 5.23 Gripper Deformation (Tri-prism)
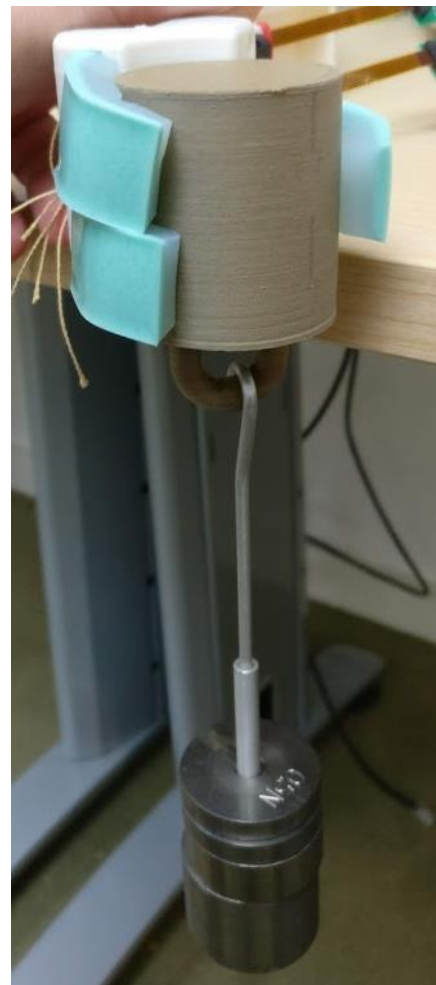
Figure 5.24 Gripper Deformation (Cylinder)
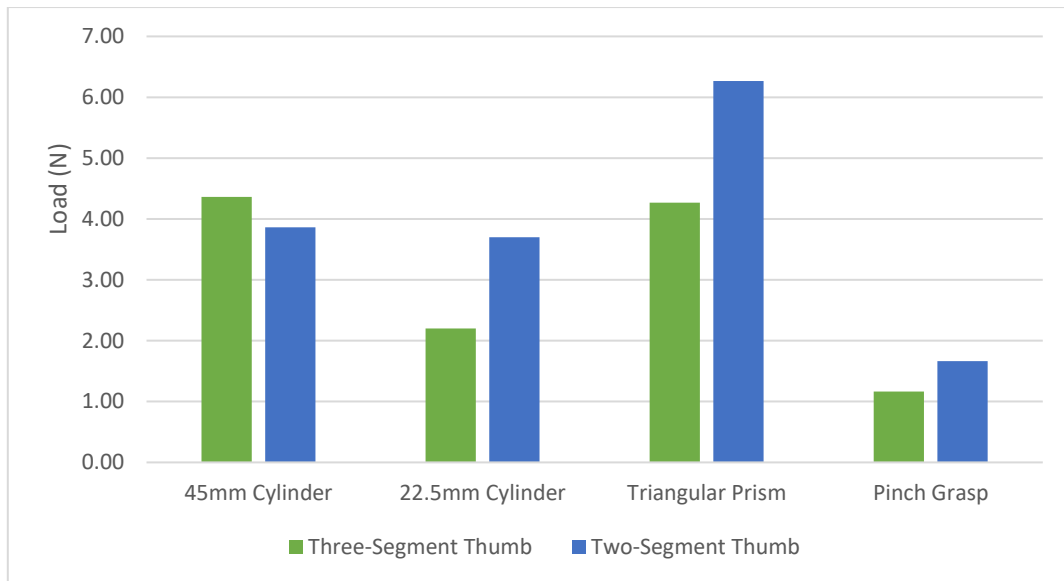
Figure 5.25 Load at Point of Deformation

The results differ from the previous tests, with the 2-segment grippers performing stronger than their 3-segment counterparts. Table 5.3 shows the data for this procedure. The average across all the objects is 3.87N and 3N for the 2-segment and 3-segment configurations respectively, a difference of 0.87N.

Table 5.3 Deformation Test Results

Object	2-Segment Thumb (N)	3-Segment Thumb (N)
45mm Cylinder	3.86	4.36
22.5mm Cylinder	3.7	2.2
Triangular Prism	6.27	4.27
Pinch Grasp	1.66	1.16
Mean Average	3.87	3

The pinch grasp also has by far the lowest threshold, with a combined average of just 1.41N. This is likely due to the impact the moment of force has on the pinch grasp, where the object is supported by only the fingertips, as displayed in Figure 5.26. In other grasps, the object is exposed to more contact area and is often held against the 'palm'.

Figure 5.26 Weighted Test - 'Pinch Grasp'

The next experiment shows the value required to cause the object to slip from the grasp under steady movement. Table 5.4 and the graph in Figure 5.27 display the results of this test. The results again show that the 2-segment thumb-gripper outperforms the 3-segment configuration. The mean difference between the two configurations is 0.83N, fractionally less than in the previous test. Part of the reason for this due to the increased contact area using the 2-segment gripper. This can be seen by comparing Figure 5.28 and Figure 5.29.

Table 5.4 Slippage under Movement Test Results

Object	2-Segment Thumb (N)	3-Segment Thumb (N)
45mm Cylinder	4.86	4.96
22.5mm Cylinder	4.2	3.3
Triangular Prism	7.77	5.27
Pinch Grasp	2.16	2.16
Mean Average	4.75	3.92
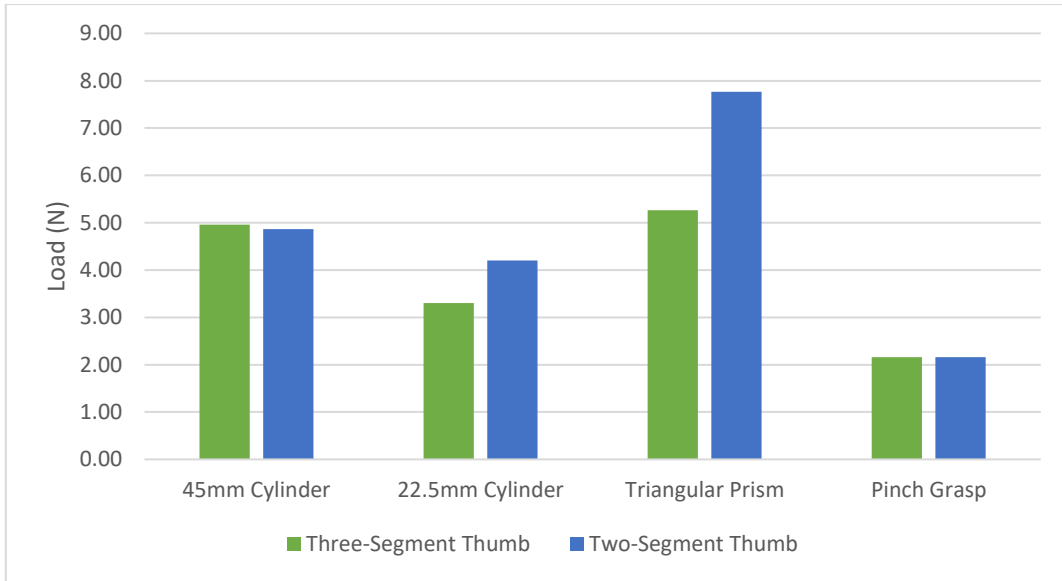
Figure 5.27 Load at Point of Slippage under Movement
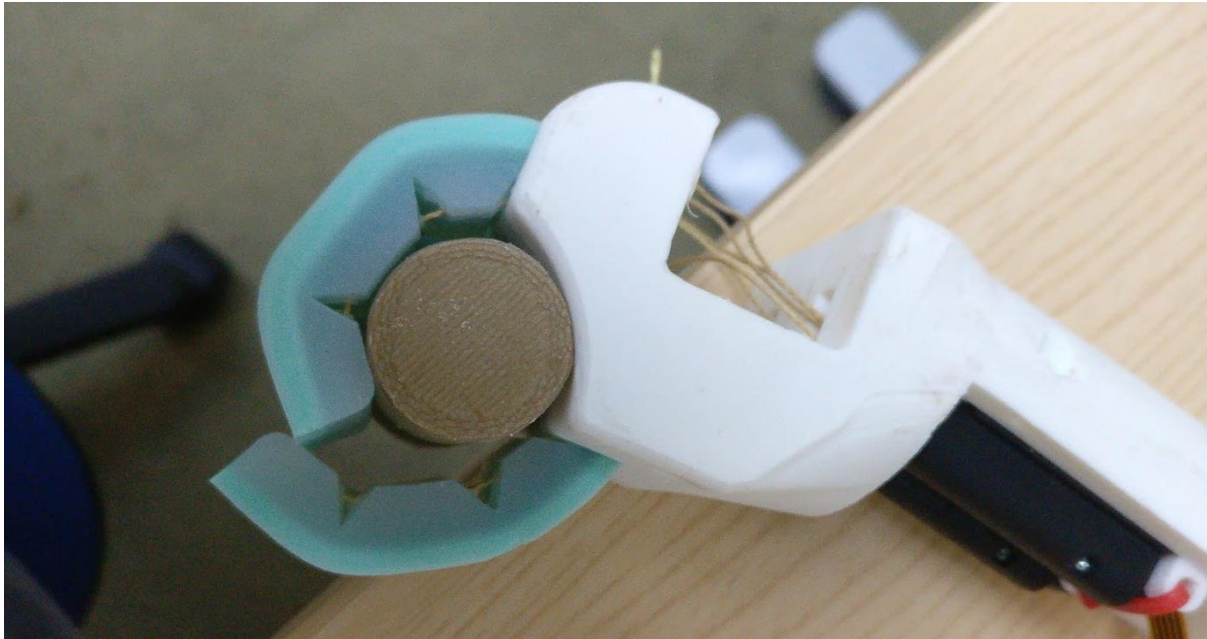
Figure 5.28 Grasp of 22.5mm Cylinder using 3-Segment Thumb

Figure 5.29 Grasp of 22.5mm Cylinder using 2-Segment Thumb

The final test procedure examines the point of absolute slippage that occurs when the arm is kept stationary. Table 5.5 and Figure 5.30 display the results from this experiment. Just as with the previous tests, the 2-segment 'thumb' displayed a heightened performance. The mean difference in this procedure was 1.6N, almost double that seen in the previous two experiments.

Table 5.5 Absolute Slippage Test Results

Object	2-Segment Thumb (N)	3-Segment Thumb (N)
45mm Cylinder	5.36	5.36
22.5mm Cylinder	5.7	3.7
Triangular Prism	9.77	5.77
Pinch Grasp	2.76	2.3
Mean Average	5.9	4.3
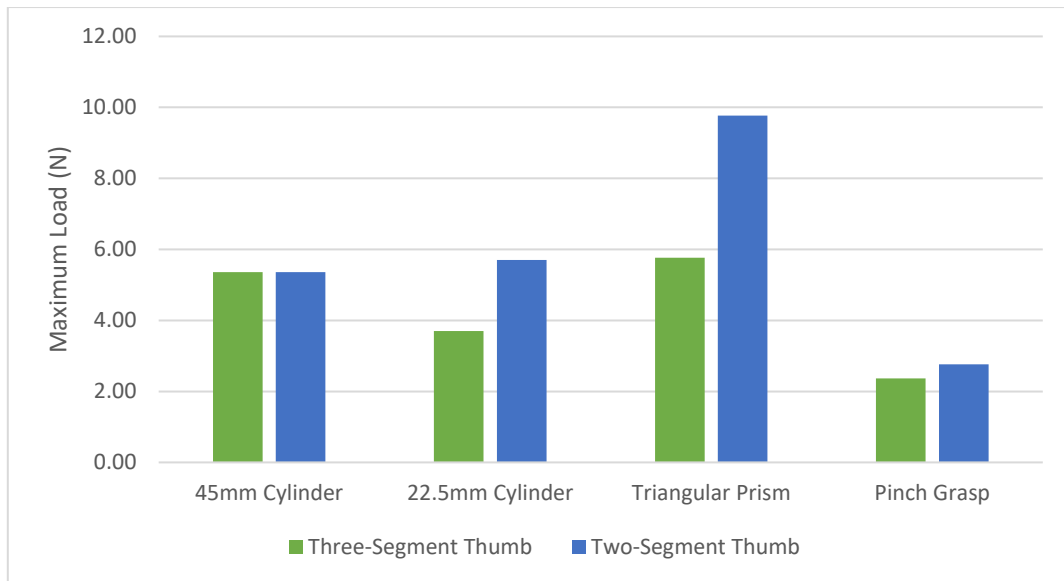
Figure 5.30 Load at Point of Absolute Slippage

5.3   Grasp Force Test

This experimental procedure focuses on the grasp force produced by the device. Figure 5.31 displays the results for the device with actuators continually powered and with the grasp detection system active. It unsurprisingly confirms the assumption that the motor actively being driven will produce a greater grasp force than when the grasp detection system active. The grasp detection is designed to power down the actuators when a grasp occurs as not to burn the motors out and to save power. This does however limit the amount of force that can be applied. Adjustments to the threshold values would allow the maximum force to be increased; though as grasping objects is the devices main purpose, the values remain at those previously determined in section 3.4 to maximise grasp detection effectiveness.
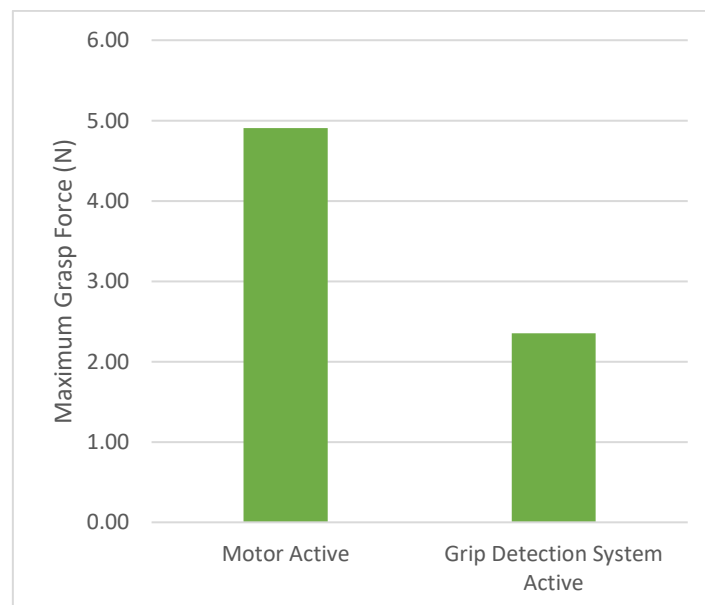
Figure 5.31 Maximum Grasp Force with and without Grasp Detection - Takei Grip Test

Table 5.6 presents the complete results for all 10 runs of the experiment. With the grasp detection system disabled the results remain constant at 4.91N (500g); conversely with the system active the results fluctuate between 1.96N (200g) and 2.94N (300g), giving an average of 2.35N (240g).

Table 5.6 Takei Grip Test Results

Run	Motor Active (N)	Grip Detection System Active (N)
1	4.91	1.96
2	4.91	1.96
3	4.91	2.94
4	4.91	2.94
5	4.91	1.96
6	4.91	2.94
7	4.91	1.96
8	4.91	2.94
9	4.91	1.96
10	4.91	1.96
Mean Average	4.91	2.35

The "Takei Physical Fitness Test: Grip-A" produces a guide with grasp force data sorted by age (Figure 5.32). It states that for a 3-year-old child the grip strength is 6.5kg (63.8N) and 4.4kg (43.2N), for males and females respectively. This represents a difference of 6Kg (58.9N) and 3.9Kg (38.2N) for males and females respectively when compared to the results with the motor active, with the grasp detection system resulting in a difference of 6.26Kg (61.4N) and 4.16Kg (40.8N). The main constraint on grasping force is the motor, with each actuator producing a maximum rated force of 30N. Due to the tight size and weight restrictions in place, the grasping power will be limited. This continues to be an issue, even with larger adult devices.

Average grip values by age (kg)

Age	Male	Female	Age	Male	Female	Age	Male	Female	Age	Male	Female
			10	17.3	15.9	30	49.6	30.8	50	45.4	28.2
			11	20.4	19.1	31	49.8	30.8	51	45.0	28.0
			12	24.6	22.1	32	50.0	30.8	52	44.9	27.6
			13	30.7	24.6	33	50.4	31.0	53	44.2	27.5
			14	36.2	26.1	34	50.0	31.0	54	43.8	27.3
			15	39.8	26.5	35	49.7	30.9	55	43.4	27.3
			16	43.3	27.2	36	49.5	30.9	56	42.7	26.9
			17	44.6	28.0	37	49.5	30.9	57	42.3	26.9
			18	45.2	28.1	38	49.1	30.7	58	42.0	26.4
			19	45.8	28.4	39	48.5	30.7	59	41.5	25.9
			20	46.5	28.6	40	48.5	30.7	60	40.8	25.7
			21	47.1	29.1	41	48.0	30.7	61	39.7	25.5
			22	47.8	29.3	42	48.0	30.6	62	39.2	25.3
3	6.5	4.4	23	48.3	29.3	43	47.3	30.5	63	38.5	24.7
4	7.2	6.0	24	48.8	29.4	44	47.4	30.3	64	37.5	24.7
5	9.3	8.7	25	48.9	29.7	45	47.1	29.8	65	36.8	24.2
6	10.0	9.7	26	49.0	30.0	46	46.9	29.6	66	36.3	24.0
7	11.0	10.3	27	49.3	30.0	47	46.6	29.6	67	36.0	24.0
8	13.0	12.0	28	49.3	30.1	48	45.7	29.0	68	35.8	24.0
9	15.2	14.0	29	49.6	30.1	49	45.6	28.5	69	35.5	23.6
									70	35.0	23.0

Figure 5.32 Average Grip Values by Age [117]

In [118] grip strength with reference to age and sex in also observed. This study uses a different technique where participants grasp a Lode dynamometer. The study shows the average grip maximum strength for children ages 4 to 12 years. Mean strength for boys at 4 is given as 65.9N, this increases to 84N by age 5 and continues to increase yearly. The data for girls aged 4 displays a mean strength of 48.6N, around 30% lower than the male subjects. The data also continues to follow the same trend, increasing to 64.1N at age 5. This is approximately in line with the 63.8N and 43.2N given by the Takei Physical Fitness Test, with a difference between the two results of 2.1N and 5.4N for males and females respectively.

5.4   Pinch Force Test

This final quantitative experimental procedure measures the pinch force of the device. Figure 5.33 displays the results for all three metrics, the actuator powered, unpowered, and grasp detection system active. The results predictably show that the motor when continuously powered produces the highest pinch force. The unpowered test initially uses the full strength of the motor, but then settles to a lower value as the motor shuts off. The lowest value is when the grasp detection system is active, just as in the previous test this value could be increased by adjusting the parameters of the system.
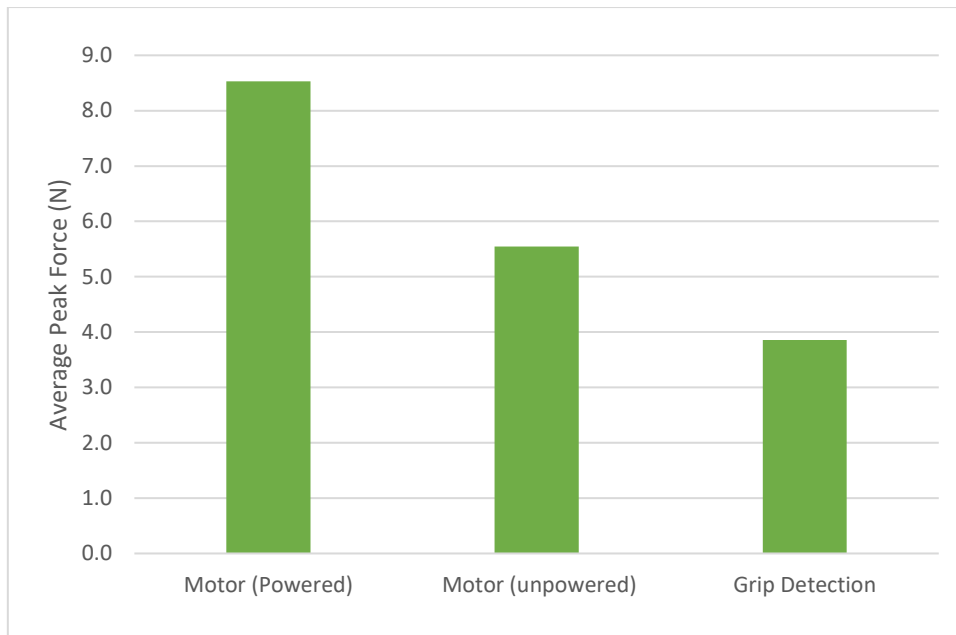
Figure 5.33 Average Pinch Force by Configuration

Table 5.7 breaks down the full results of the experiment. The results here fluctuate more, possibly due to the increased granularity of the measurement device used compared to the "Takei Physical Fitness Test: Grip-A".

Table 5.7 Pinch Force Test Results

Run #	Motor (powered)	Motor (unpowered)	Grip Detection
1	8.63	5.84	3.82
2	8.78	5.64	3.73
3	8.88	5.89	3.94
4	8.49	5.45	3.78
5	8.42	5.49	3.85
6	8.56	5.74	3.93
7	8.29	5.25	3.87
8	8.39	5.40	3.92
9	8.26	5.15	3.76
10	8.63	5.59	3.96
Mean	8.5	5.5	3.9

The results presented can be compared to published results for other prosthetic devices. The presented device performs competitively when compared to published literature on the pinch force of adult prosthetic hands, with the pinch strengths for these devices ranging between 1.71N and 16.11N [50]. Figure 5.34 is taken from the study and notes the speed of the finger movement in degrees per second, as well as a breakdown of the various pinch forces for each device. The average speed across all the devices noted is 89.8°/s. The 3-segment grippers fitted to the prototype have an average retraction time of 2.3s and extension time of 2.1s. As the grippers angular displacement is 180°, the average speed can be given as 81.8°/s; this works out at 8°/s below the referenced average, a difference of 9.34%.

Finger	Avg. Speed (°/s)	Avg. Force (N)
Tact	249.8	4.21
Dextrus	175.4	1.71
i-LIMB Large (middle)	81.8	7.66
i-LIMB Med (index/ring)	95.3	5.39
i-LIMB Small (little)	95.4	5.17
i-LIMB Pulse Med (index)	60.5	4.15
i-LIMB Pulse Large (middle)	60.5	3.09
i-LIMB Pulse Med (ring)	74.3	6.43
i-LIMB Pulse Small (little)	82.2	4.09
Bebionic (index)	45.8	12.47
Bebionic (middle)	45.8	12.25
Bebionic (ring)	45.8	12.53
Bebionic Small (little)	37.8	16.11
Bebionic v2 Large (ring, middle, and index)	96.4	14.5
Vincent Large (ring, middle, and index)	103.3	4.82
Vincent Small (little)	87.9	3.00

Figure 5.34 Data from Current Prosthetics [50].

Looking at published data for pinch forces, there is limited work focused on young children. One study looks at ages 6-19 years [119]. Converting the given forces for age 6-7 years into newtons produces the results shown in Table 5.8. Looking at the overall average of 43.79N compared to 8.5N, the maximum pinch force recorded on the device, a difference of 35.29N.

Table 5.8 Pinch Force for Age 6-7 Years [119]

	Male		Female	
	Non-Dominant Hand	Dominant Hand	Non- Dominant Hand	Dominant Hand
Pinch force (N)	43.25	45.90	41.68	44.33
Average (N)	44.57		43.00	
Combined Average (N)	43.79			

Another earlier work looked at pinch force in children aged 5-12 years [120]. This work gives a lower pinch force value of 26.5N for a 6-year-old male. This results in a difference of 18N when compared to the prosthetic. Interestingly the force given for a 5-year-old male is higher at 28.5N. This is closer to the approximate age of the user and as such may be more value as a reference point. If adult data is looked at, then we can see that currently available prosthetics shown in Figure 5.34 are considerably lower than the right hand average of 463.9N presented in [121]. This highlights how grip strength remains an issue even with adult devices and is unlikely to change without significant advancements in small scale actuator technology.

5.5 Activities of Daily Living

This final procedure does not provide numerical results and mostly acts as a demonstration for how the device may be incorporated into the daily life of the user. The tasks were performed with both 2-semgent and 3-segment 'thumb' gripper configurations, though as there was no notable difference between the performances of the two, only the 2-segment is shown in this section.

5.5.1 Writing

This task requires a secure and stable grasp of the pen. With correct positioning the device is able to do this, with the pen secured strongly enough to apply the pressure required to mark the paper Figure 5.35.
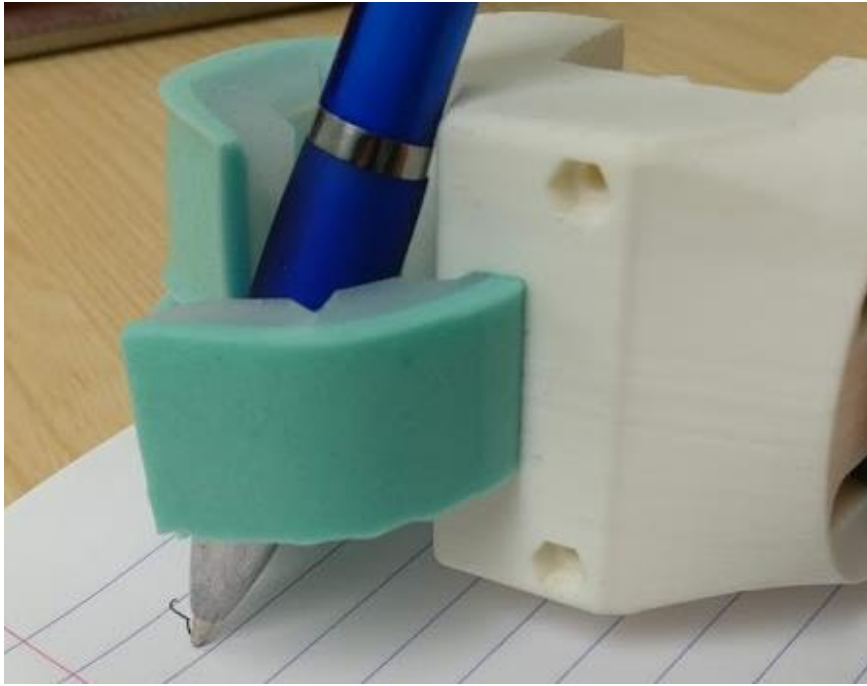
Figure 5.35 Writing Task

As the prosthetic is being gripped at the forearm in order to mark the paper, the accuracy letter 'A' drawn is Figure 5.36 is suboptimal, though this is down to the operator rather than the inadequacies of the device. Overall, the performance in this task is deemed to be highly satisfactory, with the primary task objective met.
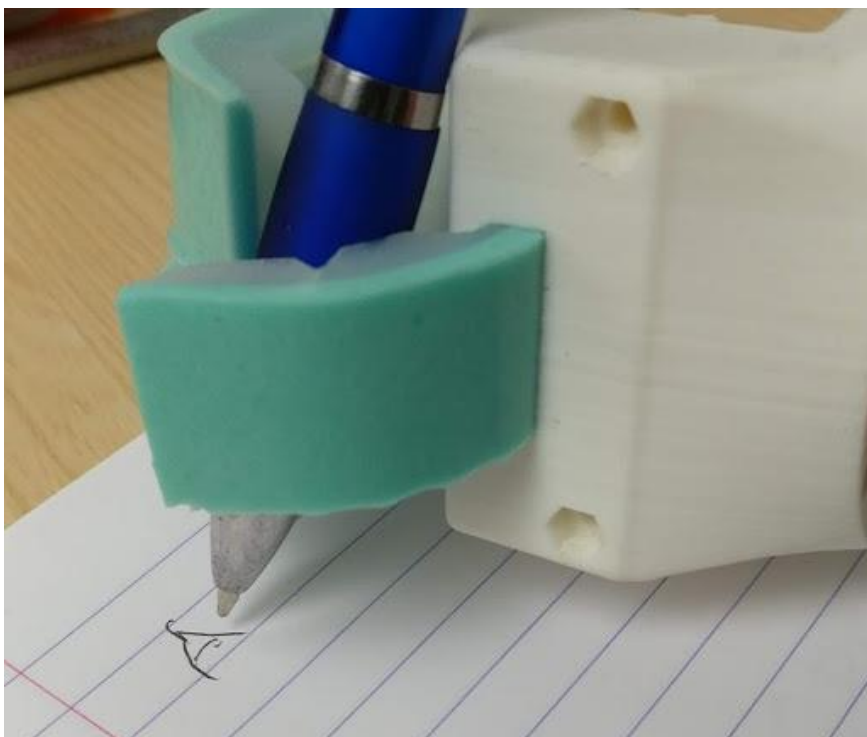
Figure 5.36 Letter "A" Drawn using the Prosthetic

5.5.2 Pouring Water from a Bottle

This next task required a bottle to be grasped using a standard cylindrical grip. The bottle is then tilled over a container and the water is poured in (Figure 5.37). The test requires the hand to have a secure grip of the bottle, especially as the mass and centre of gravity shift during the pour. The prosthetic in both gripper configurations the arm is able to grasp the bottle and pour the liquid without any issues. This performance is likely indicative of the device's ability to perform other ADLs such as drinking from a vessel.
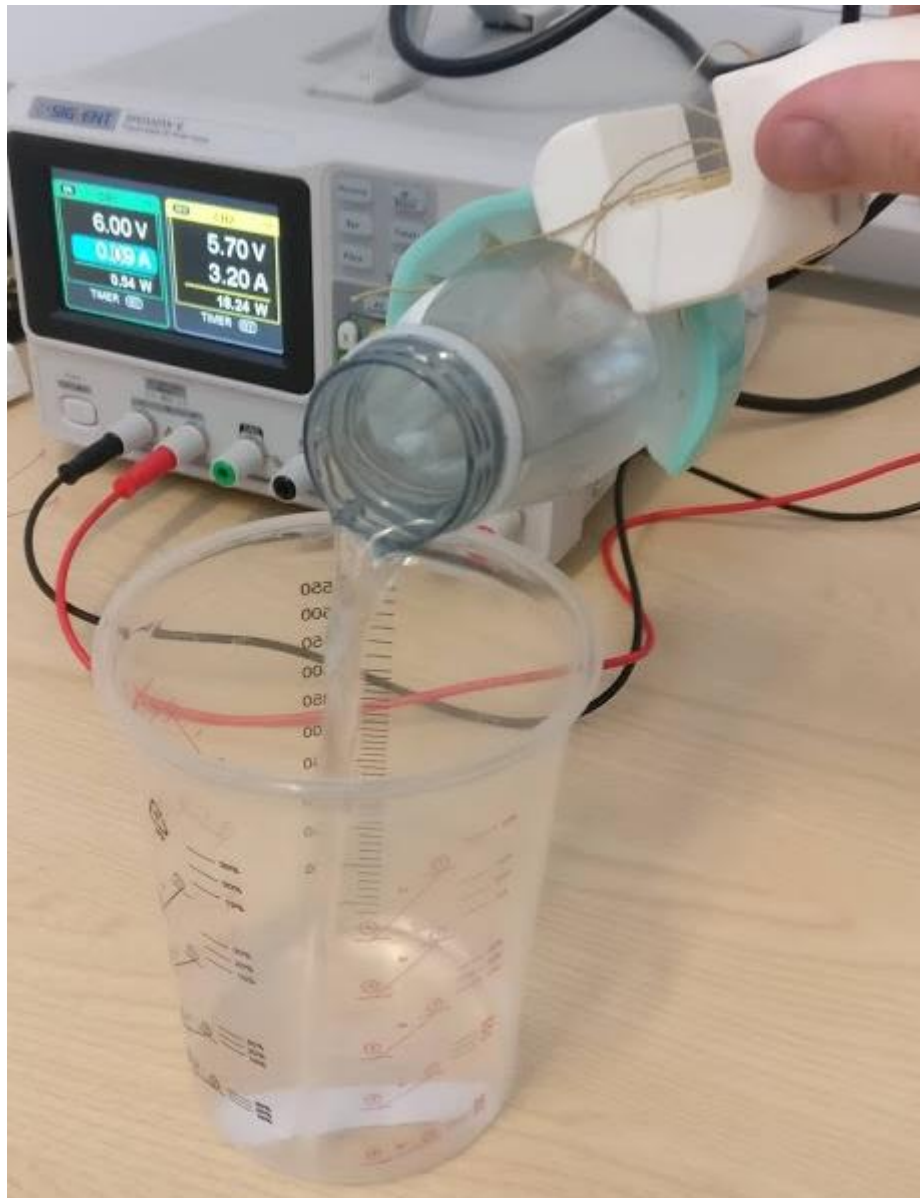
Figure 5.37 Water Pouring ADL

5.5.3 Object Placement

This final procedure shows the prosthetics ability to accurately place objects. Across all of the objects and gripper configurations, the arm is able to perform the task with ease. The device is able to grasp from multiple angles and as such the grasp can be positioned in such a way as to place the objects in their appropriate slot (Figure 5.38-5.40). The procedure highlights how the device might be used in everyday grasping tasks.
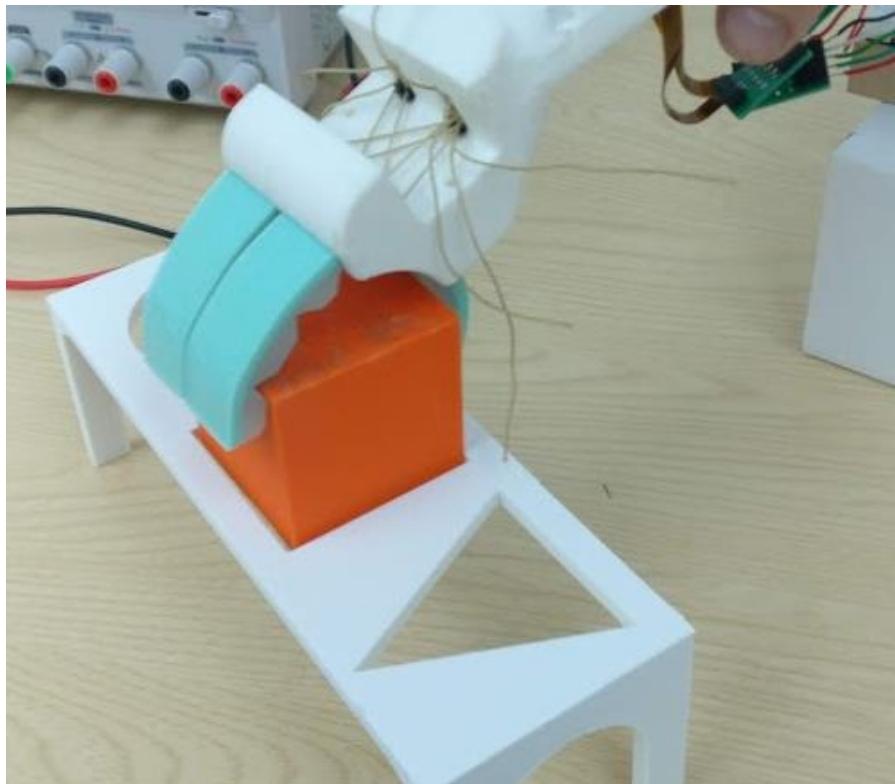
Figure 5.38 Object Placement ADL Test – Cube
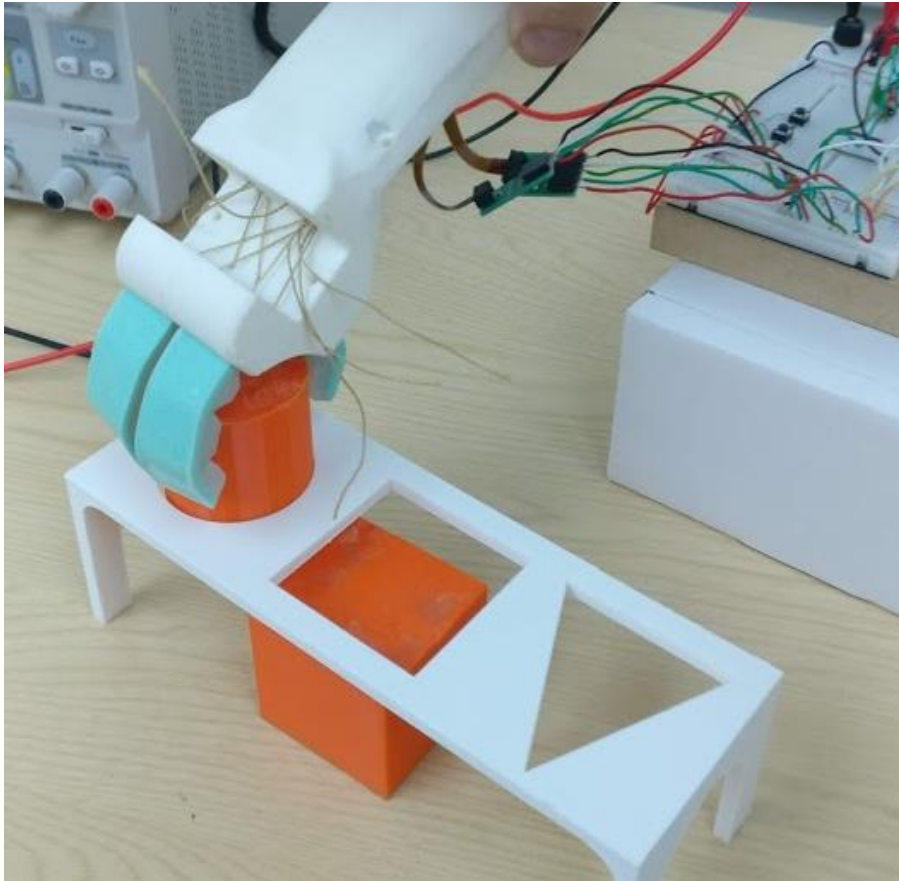
Figure 5.39 Object Placement ADL Test – Cylinder
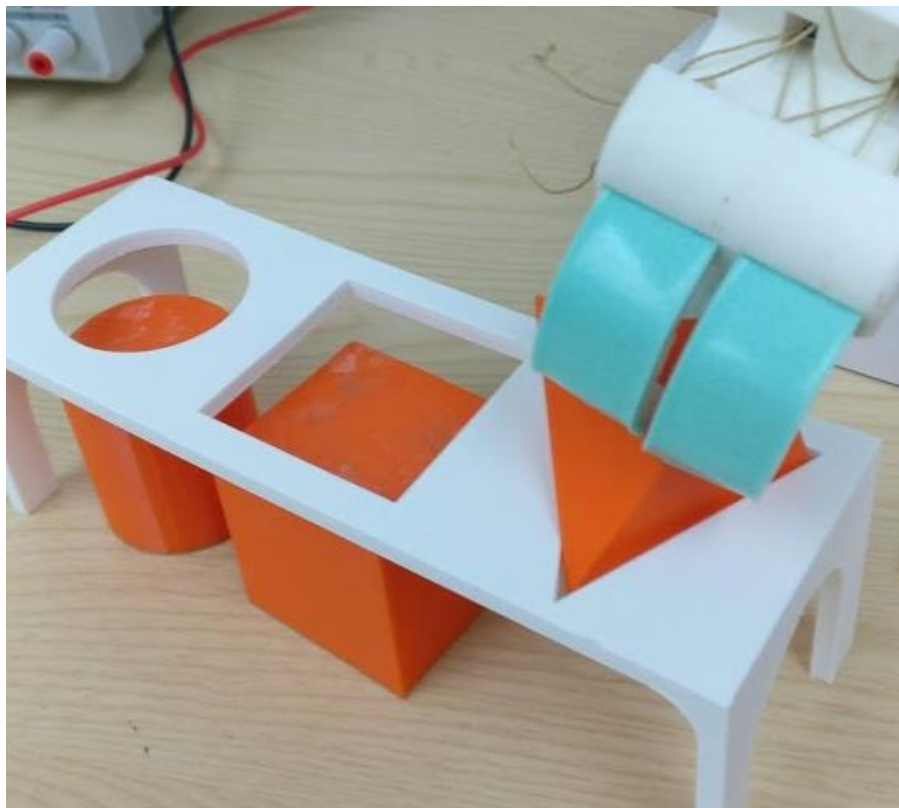
Figure 5.40 Object Placement ADL Test – Pyramid

5.6   Chapter Summary

This chapter covered the tabulated results of the experimental procedures presented in chapter 4. The results highlight the grasp effectiveness of the device, with success rates between 78% and 91% in grasp tests. The force test concurrently show that the device is able to support objects below 400g comfortably when using a power grasp, with up to 995g being possible with certain objects. The grasp force of the prosthetic, which whilst limited by the performance of the actuators, does perform in line with currently available prosthetic devices. The ADLs presented aim to showcase how the device might be used in everyday tasks.

The following chapter will discuss the project in detail, making comments on strengths and weakness, as well as noting areas for future consideration.

6 Discussion

This penultimate chapter will explore the projects successes and shortcomings. The chapter will be broken down into several subsections, with each examining a different aspect of the project.

6.1 Use of Additive Based Manufacturing

The prosthetic was designed with the intention of showcasing the use of advanced manufacturing techniques, such as 3D-printing, in the production and development of paediatric upper limb active prosthetics. In this regard the project has been successful. The prosthetic device produced is predominantly 3D-printed, including crucially the socket. The soft-grippers, whilst not directly 3D-printed, were set using moulds produced via additive manufacturing. Almost of the other components are readily available consumer electronics.

A key reason for the use of 3D-printing in the project is to reduce the cost and lead-times associated with prosthetic devices. This is implemented out of a desire to encourage healthcare providers such as the NHS, to consider the adoption of a policy based around early prosthetic fitting in order to reduce rejection rates. Currently cost ranks among the top reasons for active prosthetics not being fitted as soon as the child has developed enough to use such a device. The material cost of producing the device was around £500 (US$660), including scrappages and prototypes. This may represent a significant reduction in cost compared to the current production myoelectric devices, though it is worth noting that the overheads have not been considered in this instance. The final cost on the device would vary slightly depending on the specific configuration based around the end user and the production scalability of standard parts, such as the grippers. There may also be a labour cost reduction thanks to the speed at which 3D-scan based socket modelling can be performed and the predominantly automated process of 3D-printing. This low production cost however does not factor in the developmental and regulatory expenses that a market device would have to factor in. Currently available additively manufactured prosthetics, as covered in section 1.4.2, are presently offered at a significantly lower price point than other comparable devices. This highlights how this reduction in manufacturing costs may translate to a lower market price for a device such as the one presented in this work. There is also an assumed reduction in lead time for a 3D-printed device, though this a difficult to demonstrate within the scope of this project, outside of the general rapidness of 3D-printing techniques.

The other major reason is the often-poor performance of paediatric devices. With the primary focus, even within scientific literature being on adult devices, their paediatric and in particular toddler sized counterparts are often neglected, with no significant improvements in design over the last few decades. Adult and adolescent scale devices have started to make use advanced technologies such as 3D-printing to improve on past designs. Similarly, the topic of robotics has developed greatly in a number of ways. With regards to this project the adoption of cheap, small scale control units such as Arduino boards and the upcoming field of "soft-robotics" are of particular interest. The present design takes the concept of

3D-printing myoelectric devices, using Arduino based control and soft-grippers, to produce a prosthetic that is highly capable whilst remaining low cost, highly customisable and easy to manufacture.

6.2 Soft-Gripper Performance

The use of soft-grippers as a prosthetic end device is thought to be unexplored within current literature. The use of the grippers in this project was intended to allow for a flexible grasp which also utilises a malleable contact surface. To this end, the grippers have worked as desired. Looking at the results in section 5, it is observed that the grippers are able to grasp all of the objects available. On some of the objects, such as the plastic toy, the grippers can be seen to deform around the object, increasing the contact area and thus improving the grasp. Using a banana as an example, this adaptive grasp can be seen in Figure 6.1. An additional value to the use of the grippers is the safety factor. In more traditional grippers, joints would be used to facilitate the movement. These joints can create pinch points, which would present a hazard to the user, particularly as the target audience is young children. The soft grippers remove the risk posited by pinch points. The grasp detection mechanism, along with the soft material of the grippers, also reduces the risk of injury should the user accidently grasp a part of their body.
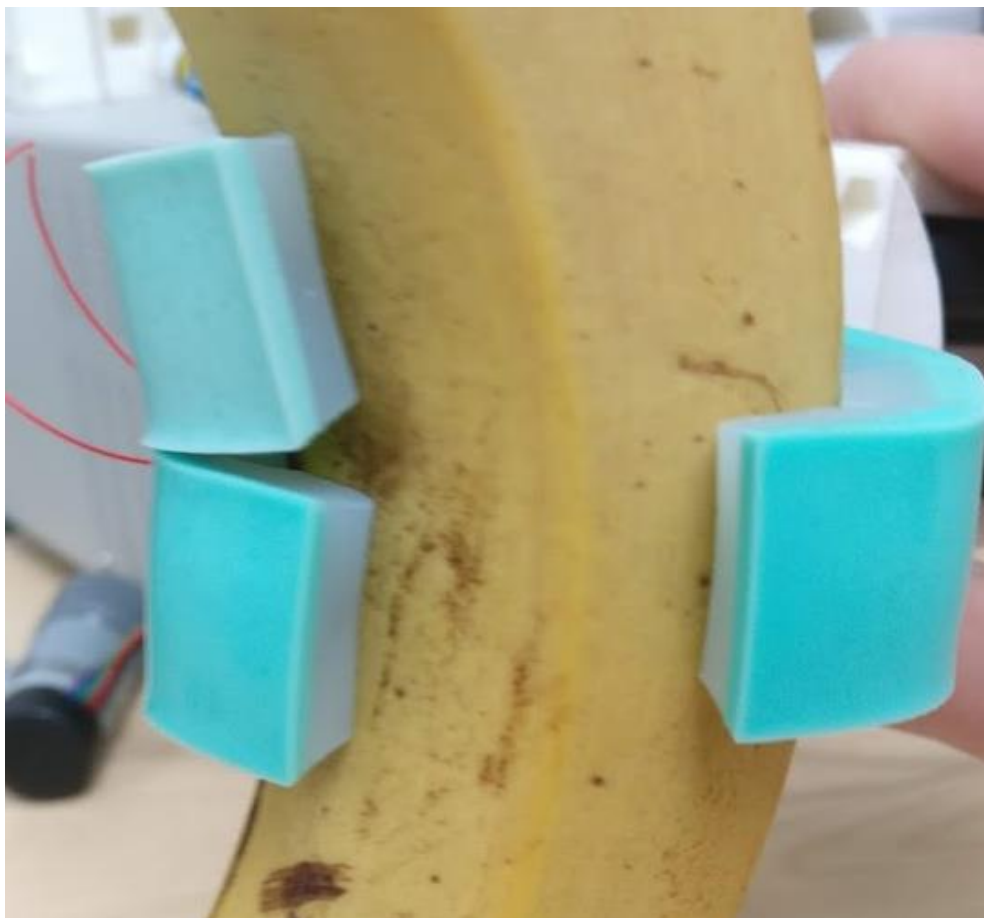
Figure 6.1 Soft-Grippers Adapting to the Shape of a Banana

From experimental data, a mean average grasp effectiveness of 87% and 82% respectively for the three-segment and two-segment thumb has been demonstrated. For the weighted objects the two-segment performed better, with a mean grasped weight of 5.9N, compared to 4.3N with the three-segment variant. In the other grasp force test, the measured difference was negligible. The superior performance in the weighted tests, as well as the close grasp effectiveness in the object tests have formed the conclusion that the more aesthetically pleasing and biologically similar two-segment thumb is the preferred configuration.

The basic ADL tests performed served to highlight the less quantifiable, but arguably more important aspects of prosthetic use. In the tasks the arm performed well, though in order to truly validate the device as one well suited for ADLs, an end user should perform these tasked under monitored conditions. This remains the biggest shortcoming of the project, as a suitable volunteer was not found. And further verification of the grippers should now focus on ADLs and user experience, rather than grasp force metrics or other means of verification.

With regards to the manufacturing process of the grippers, there is the potential for improvement. Currently the process involves inserting 2mm diameter polymer tubes into slots within the mould. This process is very fiddly and if performed even marginally wrong the resulting gripper will be defective. Some work was carried out to improve upon this, though the results were unsatisfactory. As it currently stands several successful grippers have been produced and the process has been shown to be viable. Soft-3D-printable materials are a growing field and it may hold a solution to this issue, as well as allow for a fully 3D-printed device.

6.3   Biomimicry and Kinematics

The design process set out with a desire to mimic the structure of a biological hand. This objective has partly been achieved. However, manufacturing constraints as a result of the small scale of the device necessitated the use of 3 grippers, instead of the true biomimicry of 5 digits. An alternative model to realism would be to stylise the device to the user's or their guardian's taste, for example one 3D-printed prosthetic recipient was given a custom "Iron Man arm" [122] stylised to mimic the superhero character's exoskeletal arm. Some level of decoration was shown on this prototype by having the name of the device, "SIMPA", on the hand back-plate. This could be extended into a fully customisable device in terms of colour and simple decals. As this project is in effect a proof of concept for producing toddler specific devices, appearance customisation has not been explored. If the work continued further, quantified feedback on the appearance from prosthetic users could be gathered for incorporation into revised versions of the prosthetic.

With regards to the kinematics elements of biomimicry, the soft-grippers approximately matches the jointed approximation of the phalanges. The lack of articulation in the palm means that the metacarpal kinematics are not fully exhibited in the device. With respect to

Figure 6.2 and Figure 6.3, the distal interphalangeal joint and the proximal interphalangeal joint are both modelled by the slots present in the soft-gripper. Clearly due to the inherent and desired flexibility of the grippers, the model will not be an exact fit, rather it approximates the joints' movement. The metacarpophalangeal joint (S_1) is not directly modelled in the design of the grippers; however passively defined lateral deformation is possible, effectively adding an additional range of movement to the digit. This limited lateral deformation is approximately ±15°. The thumb gripper is modelled the same as the fingers, with l_2 and θ_2 equalling 0. The thumb gripper does not take into account the range of articulation present in its human counterpart. The complexity required to control a fully articulated thumb is outside of the scope of this device, as it assumed that a young child's first prosthetic should remain as simple to operate as possible, whilst remaining functional. With reference to the results, the performance of the end device is deemed to be effective, despite this divergence from pure biomimicry.
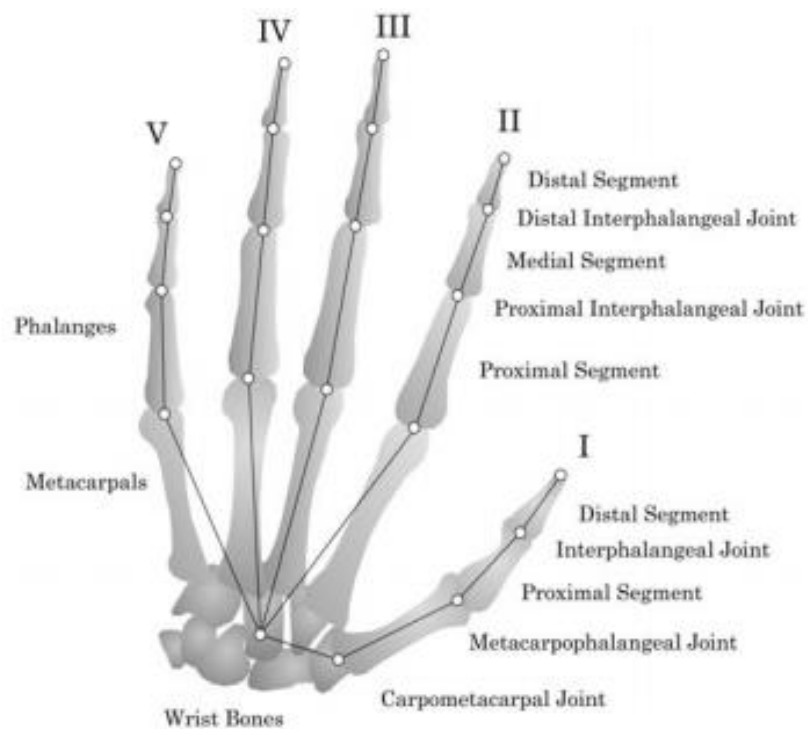
Figure 6.2 Segmentation of the Human Hand
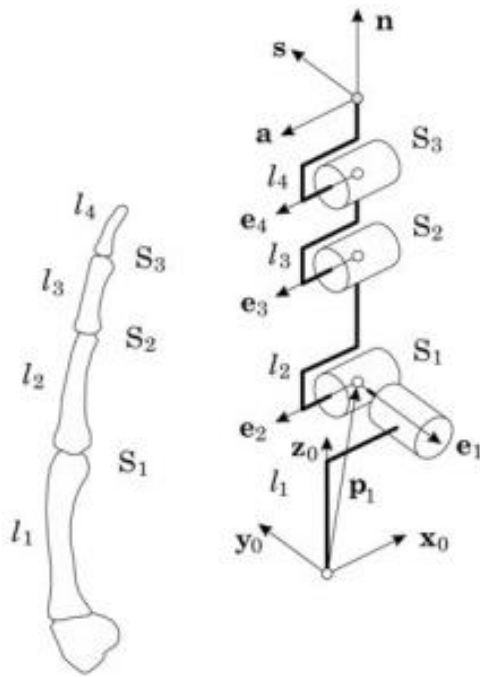
Figure 6.3 DOF of the Human Finger

The following equiations model the kinematics of the gripper as a ridgid body:

$$x = l_{0_x} + l_1 \cos(\theta_1) + l_2 \cos(\theta_2)$$

$$y = l_{0_y} + l_1 \sin(\theta_1) + l_2 \sin(\theta_2)$$
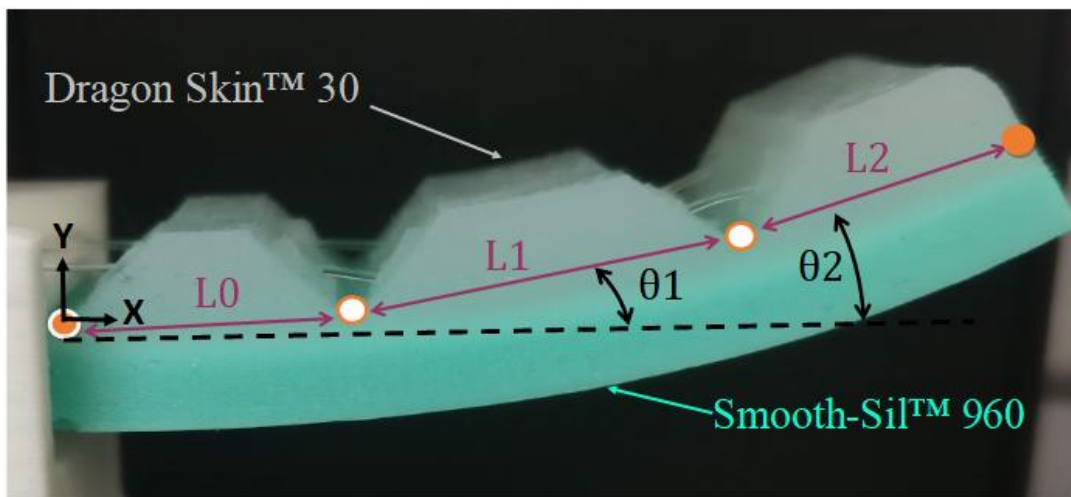
Figure 6.4 Kinematics of the Soft-Gripper

The variables used are shown in Figure 6.4. The kinematic equations are not factoring into account the lateral deformation and serve as a simple approximation of the grippers' range of movement. For the two-segment thumb, the equation can remain the same by having l_2 and θ_2 to equal 0. Figure 6.5 serves to demonstrate the movement of the complete end device in both configurations. The device is shown at approximately 50% open and in a fully closed position.

Figure 6.5 End Device in "Closed" and "Partly Open" Formations

The feel of the device does mimic that of human skin tissue, thanks to the Dragon Skin™ 30. This, whilst difficult to quantify, does appear to serve its intended function in that it provides a supple, textured grasp contact surface.

6.4 Grasp Force

One limitation of the grasp effectiveness is the maximum force produced by the micro-linear actuators. The maximum force recorded during the pinch test was 8.5N with the motor continuously powered. Comparing this to each motors' maximum rated output of 30N demonstrates the losses within the system required to deform the grippers. The contact area deformation too is thought to hinder the application of the force, as some of the energy will be stored as elastic potential, rather than directly acting on the grasped surface. Comparisons to biological grasp strength highlights the stark inadequacy of the actuators, with the study examined in the previous chapter showing a mean average of 43.79N for a 4-year-old child [119]. Examining the "Takei Physical Fitness Test: Grip-A" again shows a large discrepancy between the prosthetic end device and its biological counterpart, with a difference of 6Kg (58.9N) and 3.9Kg (38.2N) for males and females respectively when looking at given data for a 3-year-old child. This discrepancy will only be overcome if small scale actuators develop in such a way as to provide these heightened force outputs. Perhaps a more beneficial comparison is to look at data for current prosthetic devices. In [50] pinch strengths ranging between 1.71N and 16.11N are given for the range of devices examined. This puts the present device at approximately the median average. It is worth factoring in that these devices are all adult size and as such have slightly more flexibility in their approach to actuation; it also would seem appropriate that adult prosthetics should have a higher grasp strength than their paediatric counterparts. As such the grasp strength of this device is deemed to be appropriate, given the hardware limitations. The grasp tests also showed that despite a relatively low grasping force, the grippers perform well.

6.5 Control

The control system integrated, whilst simple, has been shown under lab conditions to be effective. One of the advantages of soft-grippers is the ability to simplify the control structure, allowing the grippers to deform and naturally perform a stable and secure grasp.

6.5.1 EMG

The system presented is a simple single-site single-action voluntary opening setup. This system from reviewing literature, has been shown as an effective simple means of introducing a user to EMG based prosthetic control [30], [76]. The Simulink model could easily be adjusted to incorporate a second detection site. The device itself could also with relative ease, be able to incorporate a multisite system. It is still assumed however that toddlers would still initially use the single-site system, hence this projects approach to control. The approach was not validated on a appropriate subject, again highlighting the projects fundamental weakness of not having a volunteer present during the verification phase.

The Simulink model created for EMG recording and processing allows for the system to be monitored and tuned to the individual user. Under test conditions the EMG performed extremely well once the parameters were optimised for the test subject. One major issue with validating the approach is the lack of an appropriate user on which to test the system. The scale of the project has sadly not allowed for an age-appropriate user, ideally with a limb reduction, to use the system in order to verify its design. Currently only able-bodied adults have tested the system. Young children will evidently have smaller musculature, likely resulting in weaker sEMG recordings. This may be propagated further with a limb reduction present. It is hoped however, since there are other instances of young children using EMG control, that adjustment of the various control parameters would allow for these weaker signals to be recorded and correctly identified.

The use of an EMG armband, rather than incorporating recording site into the socket should allow for a more optimal placement of the sensor. It also allows it to be easily placed/removed unlike sites that require adhesion to the skin. The armband is designed for adults but is small enough in scale that it would still fit comfortably on a child's arm.

6.5.2 Grasp Detection

The grasp detection system demonstrated, whilst simple in its design, has proven to be an effective method of determining when a grasp has occurred. As seen in the grasp force results, there is a reduction ultimate gripping force when the system is activated, though this reduction in grasp force does not seem to have a great impact with regards to objects interaction. The benefits of its incorporation are that the motors do not continuously run whilst grasping, which would undoubtedly decrease the working life of the actuators. The stability of the grasp has also been improved. With continuously closing actuators, objects tend to shift even after being securely grasped. This is especially prevalent in cases where an object has tapered surfaces.

Moving forward, this grasp detection system might be improved upon with the incorporation of strain sensors within the soft-grippers. This may work in conjunction with or replace the current actuator shaft position-based system. Grasp detection using this force measurement approach has yet to be

incorporated into a consumer device. There has been some work on printable soft-sensors [123] and it is assumed that such a system could eventually be used in concurrence with the presented soft-grippers.

6.6 Project Management

At the start of the project, a Gantt chart (Appendix E) was produced detailing the approximate timeline for the project. Overall, the actual timeline of the project deviated slightly, though this was mostly to cover the additional early publication and conference attendance not considered at the project's inception.

6.7 Chapter Summary

This chapter has discussed the findings of the project in detail. In terms of the design and performance of the device, great promise has been shown and initial aims of the project have been met. The subsequent final chapter will conclude this thesis and provide suggestions for further work should the project be continued in the future.

7 Conclusions and Further Work

This work has presented SIMPA: Soft-grasp Infant Myoelectric Prosthetic Arm. The present device is developed specifically with the intention of showcasing the viability of an active prosthetic device suitable for young children. The device is thought to be the first myoelectric prosthetic arm for children under 5 to be 3D-printed. It is also first prosthetic arm found in literature to incorporate soft-grippers, even when adult devices are explored.

The main reasoning for the additive manufacturing approach is to significantly reduce both the cost and lead-times associated with the production of prosthetic devices; both factors that that have a heightened impact when considering the paediatric market. The overall material cost, including prototyping of the device is <£500. Should the device be developed further, this cost may be reduced with the addition of standardised parts, such as the grippers. Overheads and labour costs would need to be factored in to provide an accurate production cost. Additionally, the development and regulatory expenditure of bringing a product such as this to market would increase the price, though it is hoped that like other current 3D-printed devices, this would still translate to a reduction in the final cost.

The results from the experimental procedures presented provide early validation that this novel approach to prosthetic design is plausible and may be advantageous, particularly in the case of small-scale paediatric devices. Due to limitations on the project, the design validation process was not optimally comprehensive. This the primary issue upon the completion of this project. Moving forward, appropriate user validation across all facets of the device would be essential to further its development and to justify the approach taken.

In conclusion, the project achieved its aim of showcasing an active prosthetic arm for toddlers by presenting a low cost and rapidly produced 3D-printed alternative to traditionally produced myoelectric prosthetics, almost exclusively aimed at adults and older children. In doing so it is hoped that the topic of paediatric prosthetic arms is re-evaluated in line with the advanced manufacturing techniques highlighted in this work.

7.1 Recommendations for Future Work

7.1.1 Design

The largest limitation on the project was a lack of an appropriate volunteer to on which to base the design and verification process on. Future design revisions should start and end with an appropriately aged subject presenting an upper limb reduction as the focus. This approach, using the design and manufacturing techniques highlighted in this project should deliver a prosthetic device that can be operated by a young child, who in turn would be able to assist in the verification and refinement of the design. This concept of involving the user and other key stakeholders in the design phase is known as co-creation [124], [125]. The aim of this is to merge the knowledge of multiple stakeholders, with

research data to address the research-practice gap. This concept has gained traction in recent years, with the World Health Organisation (WHO) [126] and NHS England [127] both advocating the adoption of co-creation/co-design techniques in the implementation of new health care models. Implementing this co-creation concept in practice is non-trivial, but its implantation can prevent the large research-practice gap that exists in medical devices. Any continuation of this project should follow these principals of co-design/co-creation, bringing together stakeholders including the end user, parents/guardians, and relevant medical professionals to ensure that the project does not further contribute to this research-practice gap.

The methodology whilst designing the device was predominantly based around the use of 3D-printing to prototype and refine. This approached worked well for this initial proof of concept, however further refinement should factor in simulation and analysis techniques such as finite element analysis (FEA). Some early work has been carried out in this area (Figure 7.1), though due to the complexity of accurately modelling the composite silicon grippers and the 3D-printed arm with its intricate internal structure, the work provides little value to the project, hence its exclusion in this work. FEA in further research would be key in validating the structural integrity of the design, with a focus on user safety.
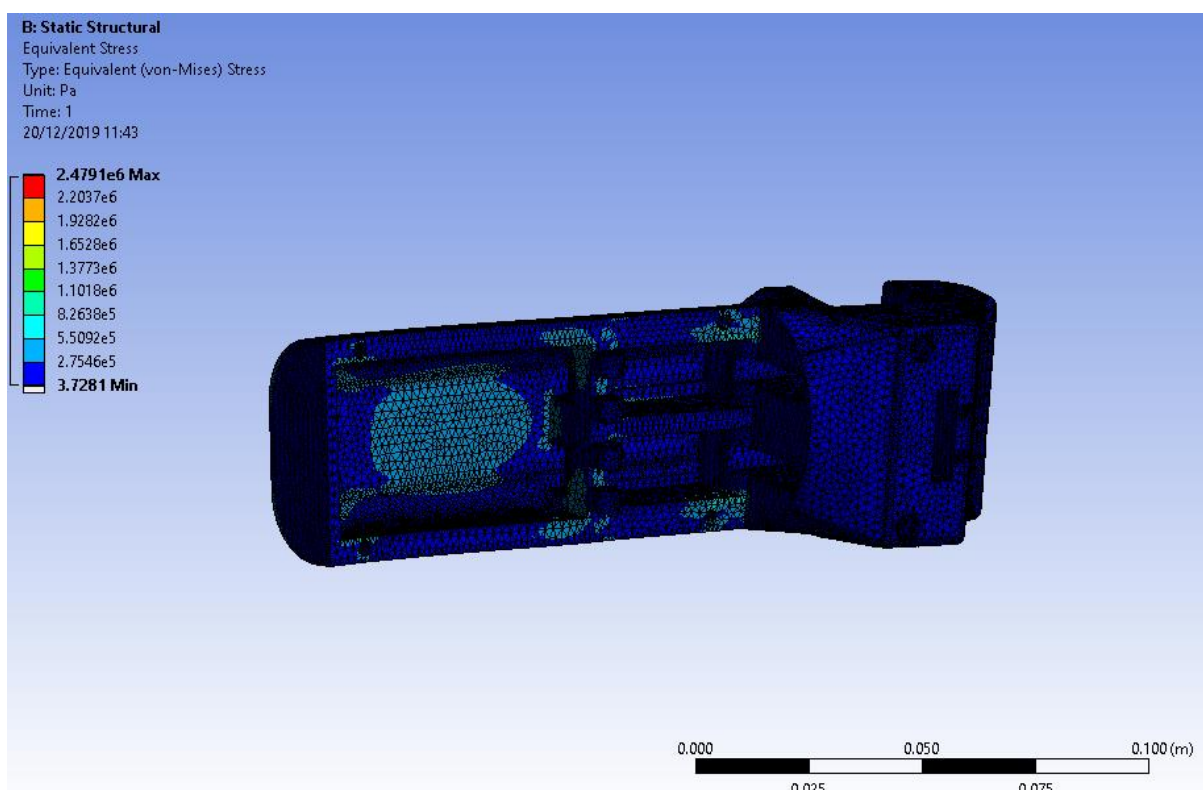
Figure 7.1 Basic FEA Stress Analysis Performed on the Prosthetic Arm CAD Model

7.1.2 Manufacture

During the course of this project, the capability of the lab's available 3D-printers has improved significantly. It is now feasible to print materials with a Shore Hardness of 60A. Such flexible, near silicon soft materials open the possibility directly printing the grippers. This would not only simplify the manufacturing process, but also enhance the flexibly of the gripper design, as moulding would not need to be considered. There is a plan in place for a short publication to explore this concept.

The assembly of the device could be improved, with an increased focus on modularity and interchangeable parts. At present, the main 3D-printed components are all held together with visible screws, ideally these should be either hidden or a different fastening technique be used.

The socket in its current design does not have a lining, meaning that the residual-limb sock would be in direct contact with the hard ABS plastic. The use of a softer material such as TPU or TPE, could add a cushioned layer to the socket, whilst maintaining a good fit. This could be done as a single print if a dual-extrusion printer is used or as a separate sleeve that slots into the hard outer-socket.

The current control system is based around an Arduino Nano, with the rest of the components simply being soldered to a stripboard. In future designs, a custom PCB, incorporating these parts would simplify the internal wiring and make for a more robust prototype.

7.1.3 Control

Just as with the mechanical design, the control system now requires an appropriate subject in order to verify the approach taken and likely improve upon it. The effectiveness of the sEMG system has not been proven on age and limb reduction appropriate subjects. This remains the biggest risk in the project's approach to control and it is critical that the effectiveness of the approach taken can be verified in order to determine whether the sEMG system should be developed further or abandoned in favour of an alternative technique. It is assumed that the user, with an appropriate training period, would be able to operate the device with relative ease providing an adequate EMG signal is recorded. There would also be an ambition to incorporate video games in the training period, such as those devised in [81] & [59]. This would also allow for a refinement of the sEMG system, based on the device's performance with the numerous users.

The possibility of incorporating a strain gauge into the grippers was not explored in this project. This topic could be explored as an improvement on the current grasp detection system. There is the possibility to 3D-print flexible sensors [123] which may be an avenue of interest, though the implementation of feedback loops in soft grippers remains a challenging topic and should perhaps not be the primary focus of any further work.

7.1.4 Verification

Further revision to the mechanical design should incorporate the use of simulation, particularly FEA, in verifying the load baring capabilities of the devices and assessing the issues of safety prior to user based testing. The device would also have to be validated to meet ISO and other standards.

The approach that should be taken for further performance verification would centre on the user performing ADLs that a toddler would normally be able to accomplish with an able limb. The framework for these test should follow the example of the Southampton Hand Assessment Procedure (SHAP) [128], with clearly defined tasks featuring various recordable metrics. A preliminary study confirmed that the SHAP approach is suitable for children, if scaled appropriately [129]. This approach, rather than further grasp force or other dynamic analysis, should verify that the prosthetic is fit for the purpose of replicating the function and capability of a biological limb as best possible.

Should the project be developed to a sufficient level, there is a desire to incorporate a method of logging the daily usage. This approach to usage data-collection, should in conjunction with questionnaires, provide a detailed account of how the device is being used and where areas for improvement might be.

7.1.5 Clinical Transition

With the limited scope of this project, there was not a plan in place for clinical transition. A continuation and expansion of this project would look at gathering clinical evidence in order to translate the engineering knowledge generated into clinical benefit. This continuation would look to use SIMPA and the knowledge generated during the design process as a foundation on which to co-design a refined prototype with input from end users and other key stakeholders. With a refined and lab tested prototype, research would shift towards the to develop a general design framework on which to produce a bespoke prosthetic for a given patient, ensuring appropriate ISO and other standards are met. A clinical study with a healthcare provider, like the collaboration with NHS England described in [35], would provide the clinical validation needed for the device to translate from a research project to something which has real clinical benefit.

Bibliography

[1] E. Vasluian *et al.*, "Birth prevalence for congenital limb defects in the northern Netherlands: A 30-year population-based study," in *BMC Musculoskeletal Disorders*, 2013, vol. 14, doi: 10.1186/1471-2474-14-323.

[2] T. Bedard, R. B. Lowry, B. Sibbald, G. N. Kiefer, and A. Metcalfe, "Congenital limb deficiencies in Alberta-A review of 33 years (1980-2012) from the Alberta Congenital Anomalies Surveillance System (ACASS)," *Am. J. Med. Genet. Part A*, vol. 167, no. 11, pp. 2599–2609, 2015, doi: 10.1002/ajmg.a.37240.

[3] T. R. Dillingham, L. E. Pezzin, and E. J. MacKenzie, "Limb amputation and limb deficiency: Epidemiology and recent trends in the United States," *South. Med. J.*, vol. 95, no. 8, pp. 875–883, 2002, doi: 10.1097/00007611-200208000-00018.

[4] "Rehabilitation and Prosthetic Restoration in Upper Limb Amputation," 2016. https://clinicalgate.com/rehabilitation-and-prosthetic-restoration-in-upper-limb-amputation/.

[5] B. Maat, G. Smit, D. Plettenburg, and P. Breedveld, "Passive prosthetic hands and tools: A literature review," *Prosthet. Orthot. Int.*, vol. 42, no. 1, pp. 66–74, 2018, doi: 10.1177/0309364617691622.

[6] A. Tiele *et al.*, "Design and Development of a Novel Upper-Limb Cycling Prosthesis," *Bioengineering*, vol. 4, no. 4, p. 89, 2017, doi: 10.3390/bioengineering4040089.

[7] Ottobock, "Passive arm prostheses," 2017. https://www.ottobockus.com/prosthetics/upper-limb-prosthetics/solution-overview/passive-arm-prostheses/.

[8] A. M. Jette, C. M. Spicer, and J. L. Flaubert, *The Promise of Assistive Technology to Enhance Activity and Work Participation*. Washington (DC): The National Academies Press (US), 2017.

[9] L. F. Engels and C. Cipriani, "Nature's Masterpiece: How Scientists Struggle to Replace the Human Hand," *Frontiers for Young Minds*, Jun. 2019. https://kids.frontiersin.org/article/10.3389/frym.2019.00083.

[10] D. K. Kumar, "Robotics to the Rescue: Prosthetic hands help amputees in developing countries," 2013. [Online]. Available: https://lifesciences.ieee.org/lifesciences-newsletter/2013/march-2013/robotics-to-the-rescue-prosthetic-hands-help-amputees-in-developing-countries/.

[11] H. Mano, S. Fujiwara, and N. Haga, "Adaptive behaviour and motor skills in children with upper limb deficiency," *Prosthet. Orthot. Int.*, vol. 42, no. 2, pp. 236–240, 2018, doi: 10.1177/0309364617718411.

[12] T. Schmalz, S. Blumentritt, and C. D. Reimers, "Selective thigh muscle atrophy in trans-tibial

amputees: An ultrasonographic study," *Arch. Orthop. Trauma Surg.*, vol. 121, no. 6, pp. 307–312, 2001, doi: 10.1007/s004020000227.

[13]   J. Treby and E. Main, "A survey of physiotherapists involved in paediatric lower limb amputee rehabilitation in the British Isles," *Physiotherapy*, vol. 93, no. 3, pp. 212–217, 2007, doi: 10.1016/j.physio.2006.08.007.

[14]   M. Allami *et al.*, "A comprehensive musculoskeletal and peripheral nervous system assessment of war-related bilateral upper extremity amputees," *Mil. Med. Res.*, vol. 3, no. 1, pp. 1–8, 2016, doi: 10.1186/s40779-016-0102-5.

[15]   S. Postema, "Upper limb absence: Effects on body functions and structures, musculoskeletal complaints, and functional capacity," Rijksuniversiteit Groningen, Groningen, 2017.

[16]   K. Solonen, H. J. Rinne, M. Viikeri, and E. Karvinen, "Late Sequelae of Amputation, a Summary," *Ann. Chir. Gynaecol. Fenn.*, vol. 54, pp. 316–327, 1965.

[17]   B. Greitemann, V. Güth, and R. Baumgartner, "Asymmetry of posture and trunk musculature following unilateral upper limb amputation: A clinical, electromyographic, posture-analytical and photogrammetric study [Asymmetrie der Haltung und der Rumpfmuskulatur nach einseitiger Armamputation - Eine klinis," *Z. Orthop. Ihre Grenzgeb.*, vol. 134, no. 6, pp. 498–510, 1996.

[18]   R. Melzack, R. Israel, R. Lacroix, and G. Schultz, "Phantom limbs in people with congenital limb deficiency or amputation in early childhood," *Brain*, vol. 120, no. 9, pp. 1603–1620, 1997, doi: 10.1093/brain/120.9.1603.

[19]   M. V. Johnston, "Plasticity in the developing brain: implications for rehabilitation," *Dev. Disabil. Res. Rev.*, vol. 15, no. 2, pp. 94–101, 2009, doi: 10.1002/ddrr.64.

[20]   M. A. James, A. M. Bagley, K. Brasington, C. Lutz, S. McConnell, and F. Molitor, "Impact of prostheses on function and quality of life for children with unilateral congenital below-the-elbow deficiency.," *J. Bone Joint Surg. Am.*, vol. 88, no. 11, pp. 2356–2365, Nov. 2006, doi: 10.2106/JBJS.E.01146.

[21]   M. K. Glynn, H. R. Galway, G. Hunter, and W. F. Sauter, "Management of the upper-limb-deficient child with a powered prosthetic device.," *Clin. Orthop. Relat. Res.*, no. 209, pp. 202–205, Aug. 1986.

[22]   R. W. Beasley and G. M. de Bese, "Upper limb amputations and prostheses.," *Orthop. Clin. North Am.*, vol. 17, no. 3, pp. 395–405, Jul. 1986.

[23]   D. Melendez and M. LeBlanc, "Survey of arm amputees not wearing prostheses: implications

for research and service," *J Assoc Child Prosthet Orthot Clin*, vol. 23, no. 3, pp. 62–69, 1988.

[24]   E. Biddiss and T. Chau, "Upper limb prosthesis use and abandonment: A survey of the last 25 years," *Prosthet. Orthot. Int.*, vol. 31, pp. 236–257, Oct. 2007, doi: 10.1080/03093640600994581.

[25]   E. Biddiss and T. Chau, "Upper-limb prosthetics: critical factors in device abandonment.," *Am. J. Phys. Med. Rehabil.*, vol. 86, no. 12, pp. 977–987, Dec. 2007, doi: 10.1097/PHM.0b013e3181587f6c.

[26]   M. Meurs, C. G. B. Maathuis, C. Lucas, M. Hadders-Algra, and C. K. van der Sluis, "Prescription of the first prosthesis and later use in children with congenital unilateral upper limb deficiency: A systematic review," *Prosthet. Orthot. Int.*, vol. 30, no. 2, pp. 165–173, 2006, doi: 10.1080/03093640600731710.

[27]   K. Postema, V. Van Der Donk, J. Van Limbeek, R. A. J. Rijken, and M. J. Poelma, "Prosthesis rejection in children with a unilateral congenital arm defect," *Clin. Rehabil.*, vol. 13, no. 3, pp. 243–249, 1999, doi: 10.1191/026921599668801945.

[28]   M. Toda, T. Chin, Y. Shibata, and F. Mizobe, "Use of powered prosthesis for children with upper limb deficiency at Hyogo Rehabilitation Center," *PLoS One*, vol. 10, no. 6, pp. 1–7, 2015, doi: 10.1371/journal.pone.0131746.

[29]   T. Scotland and H. Galway, "A long-term review of children with congenital and acquired upper limb deficiency," *J. Bone Joint Surg. Br.*, vol. 65-B, no. 3, pp. 346–349, 1983, doi: 10.1302/0301-620X.65B3.6841409.

[30]   M. Egermann, P. Kasten, and M. Thomsen, "Myoelectric hand prostheses in very young children," *Int. Orthop.*, vol. 33, no. 4, pp. 1101–1105, 2009, doi: 10.1007/s00264-008-0615-y.

[31]   J. Shaperman, S. Landsberger, and Y. Setoguchi, "Early Upper Limb Prosthesis Fitting: When and What Do We Fit," *JPO J. Prosthetics Orthot.*, vol. 15, pp. 11–17, Jan. 2003, doi: 10.1097/00008526-200301000-00004.

[32]   R. C. Crandall and W. Tomhave, "Pediatric unilateral below-elbow amputees: retrospective analysis of 34 patients given multiple prosthetic options.," *J. Pediatr. Orthop.*, vol. 22, no. 3, pp. 380–383, 2002.

[33]   D. Andreini and C. Bettinelli, "Differences in myoelectric and body-powered upper-limb prostheses: Systematic literature review Differences in myoelectric and body-powered upper-limb prostheses: Systematic literature review," *Bus. Model Innov.*, vol. 52, no. 3, pp. 1–23, 2017.

[34]   L. Wagner, A. Bagley, and M. James, "Reasons for Prosthetic Rejection by Children With

Unilateral Congenital Transverse Forearm Total Deficiency," *JPO J. Prosthetics Orthot.*, vol. 19, pp. 51–54, Apr. 2007, doi: 10.1097/JPO.0b013e3180421539.

[35]   A. Tabor, "Delivering affordable, functional prostheses in the NHS: a trial across two clinical sites to compare existing care with an affordable, multigrip prosthesis to increase function and choice for children and adolescents with upper limb difference." 2018, doi: 10.1186/ISRCTN11950127.

[36]   NHS England Specialised Services Clinical Reference Group, "Clinical Commissioning Policy: Provision of multi-grip upper limb prosthetics," 2014. [Online]. Available: https://www.engage.england.nhs.uk/consultation/specialised-services-consultation/user_uploads/upper-limb-policy.pdf.

[37]   BUPA, "Prosthetist and Orthotist Network." https://www.bupa.co.uk/healthcare-professionals/for-your-role/therapists/prost-ortho-network.

[38]   NHS England, "Prosthetic review." [Online]. Available: https://www.england.nhs.uk/commissioning/spec-services/npc-crg/group-d/d01/prosthetics-review/.

[39]   M. Wheatley, B. Maddox, and T. Kidney Bishop, "The 2019 Spending Review How to run it well," 2018. [Online]. Available: https://www.instituteforgovernment.org.uk/summary-2019-spending-review-how-run-it-well.

[40]   BBC News, "How easy is it for the limbless to get a bionic arm or leg?" https://www.bbc.co.uk/news/blogs-ouch-33236672.

[41]   Eastern Academic Health Science Network, "OPEN BIONICS RECEIVES FURTHER FUNDING FROM SBRI HEALTHCARE." https://www.eahsn.org/funding/2017/11/open-bionics-receives-funding-sbri-healthcare/.

[42]   The Independent, "NHS launches world's first trial of 3D printed bionic hands for children." https://www.independent.co.uk/news/health/nhs-3d-printed-bionic-hands-children-world-first-bristol-tilly-lockey-a7787156.html.

[43]   The Telegraph, "Funding for NHS running blades for child amputees could become permanent, says health minister." https://www.telegraph.co.uk/politics/2018/04/11/funding-nhs-running-blades-child-amputees-could-become-permanent/.

[44]   D. Farina and S. Amsüss, "Reflections on the present and future of upper limb prostheses," *Expert Rev. Med. Devices*, vol. 13, no. 4, pp. 321–324, 2016, doi: 10.1586/17434440.2016.1159511.

[45] G. McGimpsey and T. Bradford, "Limb Prosthetics Services and Devices: Critical Unmet Need: Market Analysis," *Bioeng. Inst. Cent. Neuroprosthetics*, pp. 1–35, 2017, [Online]. Available: http://www.nist.gov/tip/wp/pswp/upload/239_limb_prosthetics_services_devices.pdf.

[46] Nicolas E. Walsh and Wendy S. Walsh, "Developing, war-torn countries-with damaged infrastruc-tures at government and community levels-lack systems for rehabilitation," vol. 81, no. 03, pp. 665–670, 2003, [Online]. Available: https://www.who.int/bulletin/volumes/81/9/Walsh.pdf.

[47] A. Kannenberg, "Active Upper-Limb Prostheses," *J. Prosthetics Orthot.*, vol. 29, no. 4S, pp. P57–P62, Oct. 2017, doi: 10.1097/JPO.0000000000000158.

[48] J. ten Kate, G. Smit, and P. Breedveld, "3D-printed upper limb prostheses: a review," *Disabil. Rehabil. Assist. Technol.*, vol. 12, no. 3, pp. 300–314, 2017, doi: 10.1080/17483107.2016.1253117.

[49] D. Van Der Riet, R. Stopforth, and G. Bright, "The Low Cost Design of a 3D Printed Multi-Fingered Myoelectric Prosthetic Hand," in *Mechatronics: Principles and Applications*, 2015, pp. 85–117.

[50] P. Slade, A. Akhtar, M. Nguyen, and T. Bretl, "Tact: Design and performance of an open-source, affordable, myoelectric prosthetic hand," *Proc. - IEEE Int. Conf. Robot. Autom.*, vol. 2015-June, no. June, pp. 6451–6456, 2015, doi: 10.1109/ICRA.2015.7140105.

[51] U. Jeethesh Pai, N. P. Sarath, R. Sidharth, A. P. Kumar, S. Pramod, and G. Udupa, "Design and manufacture of 3D printed myoelectric multi-fingered hand for prosthetic application," *Int. Conf. Robot. Autom. Humanit. Appl. RAHA 2016 - Conf. Proc.*, vol. 7, pp. 5–10, 2017, doi: 10.1109/RAHA.2016.7931904.

[52] K. F. Gretsch, H. D. Lather, K. V. Peddada, C. R. Deeken, L. B. Wall, and C. A. Goldfarb, "Development of novel 3D-printed robotic prosthetic for transradial amputees," *Prosthet. Orthot. Int.*, vol. 40, no. 3, pp. 400–403, 2016, doi: 10.1177/0309364615579317.

[53] S. J. Day and S. P. Riley, "Utilising three-dimensional printing techniques when providing unique assistive devices: A case report," *Prosthet. Orthot. Int.*, vol. 42, no. 1, pp. 45–49, 2018, doi: 10.1177/0309364617741776.

[54] J. J. Cabibihan, M. K. Abubasha, and N. Thakor, "A Method for 3-D Printing Patient-Specific Prosthetic Arms with High Accuracy Shape and Size," *IEEE Access*, vol. 6, pp. 25029–25039, 2018, doi: 10.1109/ACCESS.2018.2825224.

[55] M. Yoshikawa, R. Sato, T. Higashihara, T. Ogasawara, and N. Kawashima, "Rehand: Realistic

electric prosthetic hand created with a 3D printer," *Proc. Annu. Int. Conf. IEEE Eng. Med. Biol. Soc. EMBS*, vol. 2015-Novem, pp. 2470–2473, 2015, doi: 10.1109/EMBC.2015.7318894.

[56]   M. B. Burn, A. Ta, and G. R. Gogola, "Three-dimensional printing of prosthetic hands for children," *J. Hand Surg. Am.*, vol. 41, no. 5, pp. e103–e109, 2016, doi: 10.1016/j.jhsa.2016.02.008.

[57]   J. M. Zuniga, A. M. Carson, J. M. Peck, T. Kalina, R. M. Srivastava, and K. Peck, "The development of a low-cost three-dimensional printed shoulder, arm, and hand prostheses for children," *Prosthet. Orthot. Int.*, vol. 41, no. 2, pp. 205–209, 2017, doi: 10.1177/0309364616640947.

[58]   L. Diment, M. Thompson, and J. Bergmann, "Three-dimensional printed upper-limb prostheses lack randomised controlled trials: A systematic review," *Prosthet. Orthot. Int.*, vol. 42, p. 030936461704803, Jun. 2017, doi: 10.1177/0309364617704803.

[59]   A. Manero *et al.*, "Implementation of 3D printing technology in the field of prosthetics: Past, present, and future," *Int. J. Environ. Res. Public Health*, vol. 16, no. 9, 2019, doi: 10.3390/ijerph16091641.

[60]   K. S. Tanaka and N. Lightdale-Miric, "Advances in 3D-printed pediatric prostheses for upper extremity differences," *J. Bone Jt. Surg. - Am. Vol.*, vol. 98, no. 15, pp. 1320–1326, 2016, doi: 10.2106/JBJS.15.01212.

[61]   J. M. Beck and M. D. Jacobson, "3D Printing: What Could Happen to Products Liability When Users (and Everyone Else in Between) Become Manufacturers," *Minnesota J. Law, Sci. Technol.*, vol. 18, no. 1, pp. 144–205, 2017, [Online]. Available: http://scholarship.law.umn.edu/mjlst%0Ahttp://scholarship.law.umn.edu/mjlst/vol18/iss1/3.

[62]   Ottobock, "Electric Hand 2000." https://professionals.ottobockus.com/Prosthetics/Upper-Limb-Prosthetics/Myo-Hands-and-Components/Myo-Terminal-Devices/Electric-Hand-2000/p/8E51~5L5.

[63]   T. UnLimbited, "Team Unlimbited Arm," 2016. http://enablingthefuture.org/team-unlimbited-arm/.

[64]   Limbitless Solutions, "Bionic Arms," 2016. http://limbitless-solutions.org/.

[65]   Open Bionics, "Hero Arm," *Hero arm*, 2016. https://openbionics.com/hero-arm/.

[66]   L. PULI, "Opinion Piece: The Pretend Health Professional – The Risks," *The Australian Orthotic Prosthetic Association*, 2018. https://www.aopa.org.au/news/opinion-piece-the-pretend-health-professional.

[67] L. Resnik *et al.*, "Advanced Upper Limb Prosthetic Devices: Implications for Upper Limb Prosthetic Rehabilitation," *Arch. Phys. Med. Rehabil.*, vol. 93, pp. 710–717, Apr. 2012, doi: 10.1016/j.apmr.2011.11.010.

[68] D. van der Riet, R. Stopforth, G. Bright, and O. Diegel, "An overview and comparison of upper limb prosthetics," in *2013 Africon*, Sep. 2013, pp. 1–8, doi: 10.1109/AFRCON.2013.6757590.

[69] V. Slesarenko, S. Engelkemier, P. I. Galich, D. Vladimirsky, G. Klein, and S. Rudykh, "Strategies to control performance of 3D-printed, cable-driven soft polymer actuators: From simple architectures to gripper prototype," *Polymers (Basel).*, vol. 10, no. 8, 2018, doi: 10.3390/polym10080846.

[70] M. Manti, T. Hassan, G. Passetti, N. D'Elia, C. Laschi, and M. Cianchetti, "A Bioinspired Soft Robotic Gripper for Adaptable and Effective Grasping," *Soft Robot.*, vol. 2, no. 3, pp. 107–116, 2015, doi: 10.1089/soro.2015.0009.

[71] J. H. Low, M. H. Ang, and C. H. Yeow, "Customizable soft pneumatic finger actuators for hand orthotic and prosthetic applications," *IEEE Int. Conf. Rehabil. Robot.*, vol. 2015-Septe, pp. 380–385, 2015, doi: 10.1109/ICORR.2015.7281229.

[72] P. Polygerinos, Z. Wang, K. C. Galloway, R. J. Wood, and C. J. Walsh, "Soft robotic glove for combined assistance and at-home rehabilitation," *Rob. Auton. Syst.*, vol. 73, pp. 135–143, 2015, doi: 10.1016/j.robot.2014.08.014.

[73] M. B. I. Reaz, M. S. Hussain, and F. Mohd-Yasin, "Techniques of EMG signal analysis: Detection, processing, classification and applications," *Biol. Proced. Online*, vol. 8, no. 1, pp. 11–35, 2006, doi: 10.1251/bpo115.

[74] P. Geethanjali, "Myoelectric control of prosthetic hands: state-of-the-art review," *Med. Devices (Auckl).*, vol. 9, pp. 247–255, Jul. 2016, doi: 10.2147/MDER.S91102.

[75] L. Smith and L. Hargrove, "Comparison of surface and intramuscular EMG pattern recognition for simultaneous wrist/hand motion classification," *Conf. Proc. IEEE Eng. Med. Biol. Soc.*, vol. 2013, pp. 4223–4226, Jul. 2013, doi: 10.1109/EMBC.2013.6610477.

[76] A. Muzumdar, *Powered Upper Limb Prostheses: Control, Implementation and Clinical Application*. Berlin, 2004.

[77] M. W. Chapman and M. A. James, *Chapman's Comprehensive Orthopaedic Surgery: Four Volume Set*, 4th ed. Jaypee Brothers Medical Publishers, 2017.

[78] S. Engdahl, B. Christie, B. Kelly, A. Davis, C. Chestek, and D. Gates, "Surveying the interest of individuals with upper limb loss in novel prosthetic control techniques," *J. Neuroeng.*

Rehabil., vol. 12, p. 53, Jun. 2015, doi: 10.1186/s12984-015-0044-2.

[79]   B. Peerdeman *et al.*, "Myoelectric forearm prostheses: State of the art from a user-centered perspective," *J. Rehabil. Res. Dev.*, vol. 48, pp. 719–737, Jul. 2011, doi: 10.1682/JRRD.2010.08.0161.

[80]   A. Chadwell, L. Kenney, S. Thies, A. Galpin, and J. Head, "The Reality of Myoelectric Prostheses: Understanding What Makes These Devices Difficult for Some Users to Control ," *Frontiers in Neurorobotics* , vol. 10. p. 7, 2016, [Online]. Available: https://www.frontiersin.org/article/10.3389/fnbot.2016.00007.

[81]   P. A. Smith, M. Dombrowski, R. Buyssens, and P. Barclay, "Usability testing games for prosthetic training," *2018 IEEE 6th Int. Conf. Serious Games Appl. Heal. SeGAH 2018*, pp. 1–7, 2018, doi: 10.1109/SeGAH.2018.8401376.

[82]   M. Dombrowski, P. Smith, and R. Buyssens, "Advances in Affective and Pleasurable Design," vol. 774, pp. 647–655, 2019, doi: 10.1007/978-3-319-94944-4.

[83]   P. A. Smith, M. Dombrowski, R. Buyssens, and P. Barclay, "The Impact of a Custom Electromyograph (EMG) Controller on Player Enjoyment of Games Designed to Teach the Use of Prosthetic Arms," *Comput. Games J.*, vol. 7, no. 2, pp. 131–147, 2018, doi: 10.1007/s40869-018-0060-0.

[84]   Y. Hiyoshi *et al.*, "Development of a Parent Wireless Assistive Interface for Myoelectric Prosthetic Hands for Children ," *Frontiers in Neurorobotics* , vol. 12. p. 48, 2018, [Online]. Available: https://www.frontiersin.org/article/10.3389/fnbot.2018.00048.

[85]   J. Dearden, C. Grames, B. D. Jensen, S. P. Magleby, and L. L. Howell, "Inverted L-arm gripper compliant mechanism," *J. Med. Devices, Trans. ASME*, vol. 11, no. 3, pp. 1–6, 2017, doi: 10.1115/1.4036336.

[86]   R. F. Shepherd *et al.*, "Multigait soft robot," *Proc. Natl. Acad. Sci. U. S. A.*, vol. 108, no. 51, pp. 20400–20403, 2011, doi: 10.1073/pnas.1116564108.

[87]   P. Polygerinos *et al.*, "Towards a soft pneumatic glove for hand rehabilitation," *IEEE Int. Conf. Intell. Robot. Syst.*, pp. 1512–1517, 2013, doi: 10.1109/IROS.2013.6696549.

[88]   E. Nathalia Gama Melo, O. Fernando Avilés Sánchez, and D. Amaya Hurtado, "Anthropomorphic robotic hands: a review Manos robóticas antropomórficas: una revisión," vol. 32, pp. 279–313, 2014.

[89]   J. Lenarčič, T. Bajd, and M. M. Stanišić, "Robot Grasp," in *Robot Mechanisms*, 2013, pp. 291–311.

[90] A. Primer, "Drawing the Human Body," *Craftsy*. 2014, [Online]. Available: https://shop.mybluprint.com/drawing/guides/drawing-the-human-body/453235.

[91] D. A. Winter, *Biomechanics and Motor Control of Human Movement*, 4th ed. 2009.

[92] M. Bonthuis *et al.*, "Use of national and international growth charts for studying height in european children: Development of up-to-date european height-for-age charts," *PLoS One*, vol. 7, no. 8, pp. 1–11, 2012, doi: 10.1371/journal.pone.0042506.

[93] Youbionic, "Youbionic Hand," 2019. https://www.youbionic.com/youbionic-hand-2019.

[94] Actuonix Motion Devices Inc., "PQ12-P Linear Actuator with Feedback," 2019. https://www.actuonix.com/Actuonix-PQ-12-P-Linear-Actuator-p/pq12-p.htm.

[95] Arduino, "Arduino Nano," 2019. https://www.arduino.cc/.

[96] Digi-Key, "Gravity: Analog EMG Sensor by OYMotion," 2019. https://www.digikey.com/catalog/en/partgroup/gravity-analog-emg-sensor-by-oymotion/78252.

[97] RS Components Ltd., "ENIX Energies 7.5V Wire Lead Terminal Lithium Rechargeable Battery, 2.2Ah 2," 2018. https://uk.rs-online.com/web/p/lithium-rechargeable-batteries/5306331/.

[98] Ottobock, "MyolinoWrist 2000," 2019. https://shop.ottobock.us/Prosthetics/Upper-Limb-Prosthetics/Myo-Hands-and-Components/Myo-Wrist-Units-and-Rotation/MyolinoWrist-2000/p/10V51~51.

[99] P. J. Kyberd *et al.*, "Two-degree-of-freedom powered prosthetic wrist," *J. Rehabil. Res. Dev.*, vol. 48, no. 6, pp. 609–618, 2011, doi: 10.1682/JRRD.2010.07.0137.

[100] M. W. Legro *et al.*, "Issues of importance reported by persons with lower limb amputations and prostheses," *J. Rehabil. Res. Dev.*, vol. 36, no. 3, pp. 155–163, 1999.

[101] F. Speers, "Designing an adjustable prosthetic socket using ReMake and Fusion 360," *Autodesk Design Academy*, 2016. https://academy.autodesk.com/inspiration/blog/designing-adjustable-prosthetic-socket-using-remake-and-fusion-360.

[102] "Prosfit Optimal Sockets," *Prosfit*, 2020. https://prosfit.com/.

[103] "The UNYQ Socket," *UNYQ*, 2019. http://unyq.com/the-unyq-socket/.

[104] R. Ismail *et al.*, "Affordable and Faster Transradial Prosthetic Socket Production Using Photogrammetry and 3D Printing," *Electronics*, vol. 9, no. 9, p. 1456, Sep. 2020, doi: 10.3390/electronics9091456.

[105] Artec 3D, "Creating Optimal Orthotics and Prosthetics with Artec Eva and Spider." https://www.artec3d.com/cases/creating-optimal-orthotics-and-prosthetics-artec-eva-and-spider.

[106] J. Billing, "Product Design: Prosthetic Design," *Autodesk Design Academy*. https://academy.autodesk.com/course/119049/product-design-prosthetic-design.

[107] N. A. Abd Razak, N. A. Abu Osman, H. Gholizadeh, and S. Ali, "Biomechanics principle of elbow joint for transhumeral prostheses: comparison of normal hand, body-powered, myoelectric & air splint prostheses," *Biomed. Eng. Online*, vol. 13, p. 134, Sep. 2014, doi: 10.1186/1475-925X-13-134.

[108] International Committee of the Red Cross, "Physical Rehabilitation Programme trans-humeral Prosthesis Manufacturing guidelines," [Online]. Available: https://www.icrc.org/eng/assets/files/other/eng-trans-humeral.pdf.

[109] T. Sittiwanchai, I. Nakayama, S. Inoue, and J. Kobayashi, "Transhumeral prosthesis prototype with 3D printing and sEMG-based elbow joint control method," *Int. Conf. Adv. Mechatron. Syst. ICAMechS*, pp. 227–231, 2014, doi: 10.1109/ICAMechS.2014.6911655.

[110] DFRobot, "Gravity: Analog EMG Sensor by OYMotion," 2019. https://www.dfrobot.com/product-1661.html.

[111] Actuonix Motion Devices Inc., "Miniature Linear Motion Series · PQ12." 2019.

[112] Simakrima, "Geometrical shapes." Thingiverse, 2017.

[113] L. Takei Scientific Instruments CO., "Psychological & Physiological Apparatus." Takei Scientific Instruments CO., LTD, [Online]. Available: http://www.takei-si.co.jp/pdf/TakeiCatalog_En100.pdf.

[114] J. A. Balogun and A. T. Onigbinde, "Intra-tester Reliability and Validity of the Takei Kiki Kogyo Hand Grip Dynamometer," *J. Phys. Ther. Sci.*, vol. 3, no. February 2015, pp. 55–60, 1991.

[115] Y. Yang, C. Fermüller, Y. Li, and Y. Aloimonos, "Grasp type revisited: A modern perspective on a classical feature for vision," *Proc. IEEE Comput. Soc. Conf. Comput. Vis. Pattern Recognit.*, vol. 07-12-June, no. June, pp. 400–408, 2015, doi: 10.1109/CVPR.2015.7298637.

[116] Western University Canada, "Critiques Page Carpal Tunnel Syndrome (CTS) & Prehension," *Neck & Upperback Pain - MSc Occupational Therapy*. https://ayahia3.wixsite.com/team7case/blank-1.

[117] L. Takei Scientific Instruments CO., "Takei Physical Fitness Test: Grip A - Instruction Manual."

2015.

[118]   H. M. Molenaar, R. W. Selles, J. M. Zuidam, S. P. Willemsen, H. J. Stam, and S. E. R. Hovius, "Growth Diagrams for Grip Strength in Children," *Clin. Orthop. Relat. Res.*, vol. 468, no. 1, pp. 217–223, 2010, doi: 10.1007/s11999-009-0881-z.

[119]   A. C. de C. Ferreira, A. C. Shimano, N. Mazzer, C. H. Barbieri, V. M. C. Elui, and M. de C. R. Fonseca, "Grip and pinch strength in healthy children and adolescents," *Acta Ortop. Bras.*, vol. 19, no. 2, pp. 92–97, 2011, doi: 10.1590/S1413-78522011000200006.

[120]   C. L. Ager, B. L. Olivett, and C. L. Johnson, "Grasp and pinch strength in children 5 to 12 years old.," *Am. J. Occup. Ther. Off. Publ. Am. Occup. Ther. Assoc.*, vol. 38, no. 2, pp. 107–113, 1984, doi: 10.5014/ajot.38.2.107.

[121]   R. P. Mullerpatan, G. Karnik, and R. John, "Grip and pinch strength: Normative data for healthy Indian adults," *Hand Ther.*, vol. 18, no. 1, pp. 11–16, 2013, doi: 10.1177/1758998313479874.

[122]   S. Galo, "Real-life Iron Man: Robert Downey Jr gives boy bionic arm," *The Guardian*, 2015. https://www.theguardian.com/film/2015/mar/12/iron-man-robert-downey-jr-gives-child-bionic-arm (accessed Dec. 01, 2019).

[123]   K. Elgeneidy, G. Neumann, M. Jackson, and N. Lohse, "Directly Printable Flexible Strain Sensors for Bending and Contact Feedback of Soft Actuators," *Front. Robot. AI*, vol. 5, no. February, pp. 1–14, 2018, doi: 10.3389/frobt.2018.00002.

[124]   M. Farr, "Power dynamics and collaborative mechanisms in co-production and co-design processes," *Crit. Soc. Policy*, vol. 38, no. 4, pp. 623–644, Dec. 2017, doi: 10.1177/0261018317747444.

[125]   J. Langley, D. Wolstenholme, and J. Cooke, "'Collective making' as knowledge mobilisation: the contribution of participatory design in the co-creation of knowledge in healthcare," *BMC Health Serv. Res.*, vol. 18, no. 1, p. 585, 2018, doi: 10.1186/s12913-018-3397-y.

[126]   WHO, "WHO global strategy on people-centred and integrated health services," 2015, Accessed: Dec. 08, 2020. [Online]. Available: https://www.who.int/servicedeliverysafety/areas/people-centred-care/global-strategy/en/#.X8-r_u2E6Qo.mendeley.

[127]   NHS England, "NHS Five Year Forward View," 2014. [Online]. Available: https://www.england.nhs.uk/five-year-forward-view/.

[128]   C. M. Light, P. H. Chappell, and P. J. Kyberd, "Establishing a standardized clinical assessment tool of pathologic and prosthetic hand function: Normative data, reliability, and validity," *Arch.*

Phys. Med. Rehabil., vol. 83, no. 6, pp. 776–783, 2002, doi: 10.1053/apmr.2002.32737.

[129] E. Vasluian, R. M. Bongers, H. A. Reinders-Messelink, P. U. Dijkstra, and C. K. van der Sluis, "Preliminary study of the Southampton Hand Assessment Procedure for Children and its reliability," *BMC Musculoskelet. Disord.*, vol. 15, no. 1, p. 199, 2014, doi: 10.1186/1471-2474-15-199.

[130] C. M. Lewandowski, "the Effect of Build Orientation on the Mechanical Properties in Inkjet 3D Printing," *Eff. Br. mindfulness Interv. acute pain Exp. An Exam. Individ. Differ.*, vol. 1, no. August 2015, pp. 983–992, 2015, doi: 10.1017/CBO9781107415324.004.

[131] 3D Hubs, "How to design parts for FDM 3D Printing," 2019. https://www.3dhubs.com/knowledge-base/how-design-parts-fdm-3d-printing.

Appendices

Appendix A

Appendix A1

Version 1

The first print of the gripper mould was unsuccessful due to warping. This was likely the result of a lack of adhesion to the print bed, the cause of which is unknown. For the next print, the print bed was cleaned and a layer of PVA glue was applied to help with adhesion. The second attempt at printing the mould was a success. There was minimal warping present and the overall print quality was deemed to be enough for moulding.

Figure 0.1 First Mould Print Displaying Warping

Figure 0.2 Mould, Soft Gripper, and 5mm LED for Scale
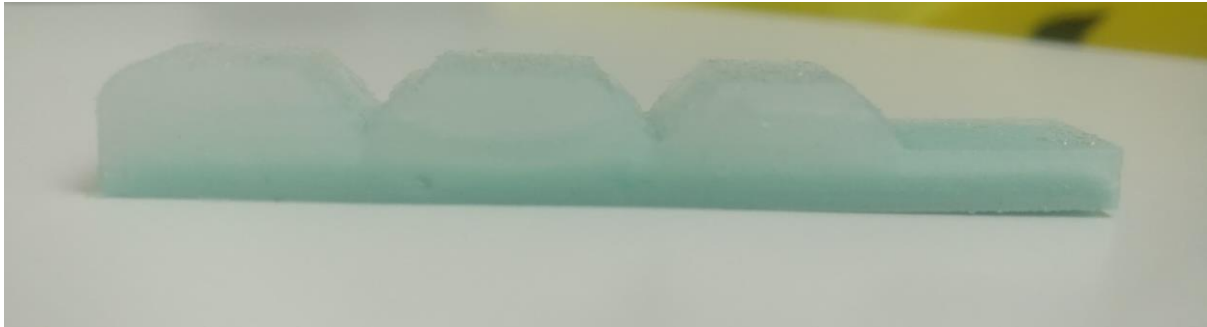
Figure 0.3 Side-view of the Soft-Gripper

This first prototype showed promise, however the kink in the end loop needed to be resolved in the next iteration.

Version 2

This second attempt at producing a gripper uses the same design as the previous attempt, with a slight modification to remove the kink in the tubing. As part of the moulding process, plastic tubes are placed in the mould. The end of the tube forms a loop, which due to the tight radius kinked when the silicon rubber was poured into the mould. To counteract this, a segment of wire was inserted into the tube, to act as a reinforcement preventing the loop from developing a kink.

Figure 0.4 Gripper with Threaded End-Loop
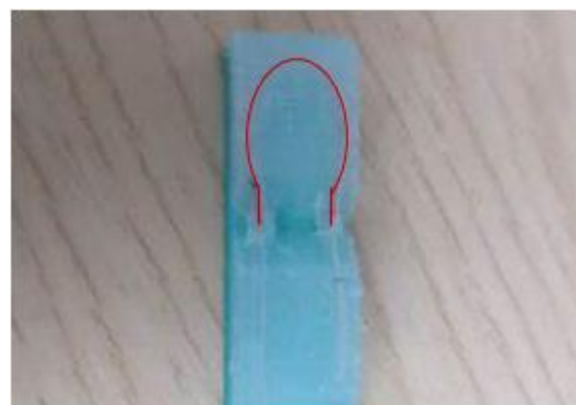
Figure 0.5 Gripper with End-Loop Highlighted

The gripper was moulded in the same method as before, again requiring finishing techniques to remove excess material. The first attempted moulding however was unsuccessful, due to one of the tubes coming loose when the silicon rubber was poured. A second attempt was successful and produced a gripper without a kink in the end loop, however the same issue with the thread not passing though the loop occurred. The reason seems to be that the radius is simply too tight to be threaded. A range of threads were attempted ranging from flexible Kevlar string to stiffer plastic-coated wire. None of these were able to pass through the loop. This second version of the gripper must also be deemed a failure due to this threading issue.

Version 3

A revised 20mm wide version of the grippers was able to be threaded. The production process still had some failures, mostly due to the tubes slipping from the holes in the mould during the process (Figure 0.6). Some experimentation with 3D-printed flexible insets (Figure 0.7) was unsuccessful, as the material was still too rigid to be used in conjunction with the grippers. Ultimately the malleable plastic tubing is still the best method found for producing the grippers, though this area is a weak spot in the production process, particularly with the long set-time of the silicon rubbers. Should further work be carried out, this aspect of the project should be refined. One possible option would be to directly 3D-print the grippers using an ultra-soft filament.

Figure 0.6 Soft-Gripper with Extruding Internal Tubes
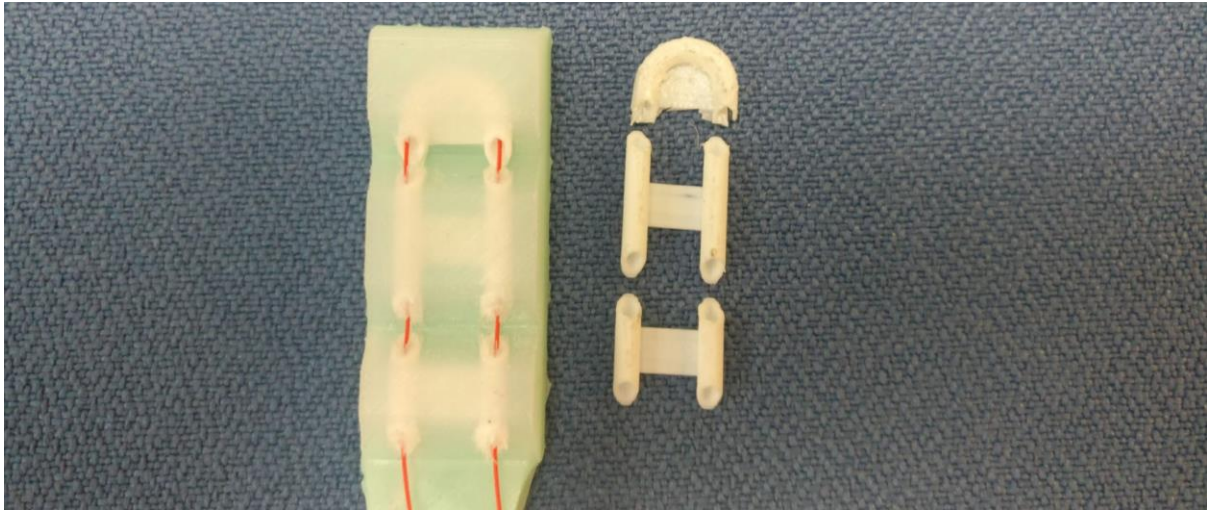
Figure 0.7 Gripper with 3D-Printed Inserts

Appendix A2

Hand Prototyping

This CAD model was imported into Cura to be manufactured on the Ultimaker S5 (Figure 0.8). The material used was white acrylonitrile butadiene styrene (ABS), a material commonly used to create functional 3D-printed components. The material is quite rigid and relatively durable, a full breakdown of the material specification can be found in Appendix C1. The other material considered was polylactic acid (PLA) due to its comparable properties, however as the material is made from biomass, it will degrade when exposed to sunlight. As the prosthetic may be used in a range of environments, including outdoors under direct sunlight, the decision was made to manufacture using ABS. The print did not require support material and took approximately 5h to complete, with a layer height of 0.15mm and default Cura print parameters for ABS.
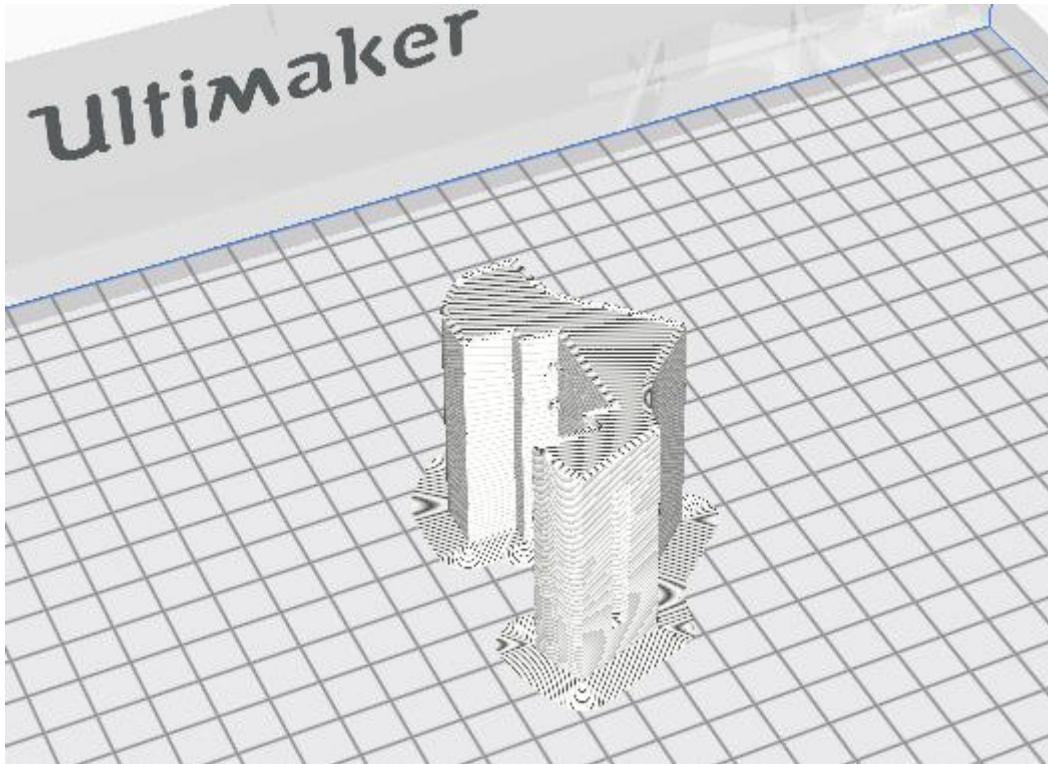
Figure 0.8 'Hand' Prototype Sliced using Cura

The print was successful, requiring a minimal finishing. There was some shrinkage present and this prevented the grippers from being slotted into the 'hand'. By removing some material from the sides of the gripper insert, the grippers were able to fit. Future prints were scaled by +2.5% to accommodate this shrinkage. The tubes for feeding the cables through printed successfully, there was a slight worry due to the small diameter that a blockage may occur, though this proved unfruitful.

Figure 0.9 Successful Print of Initial 'Hand' Prototype
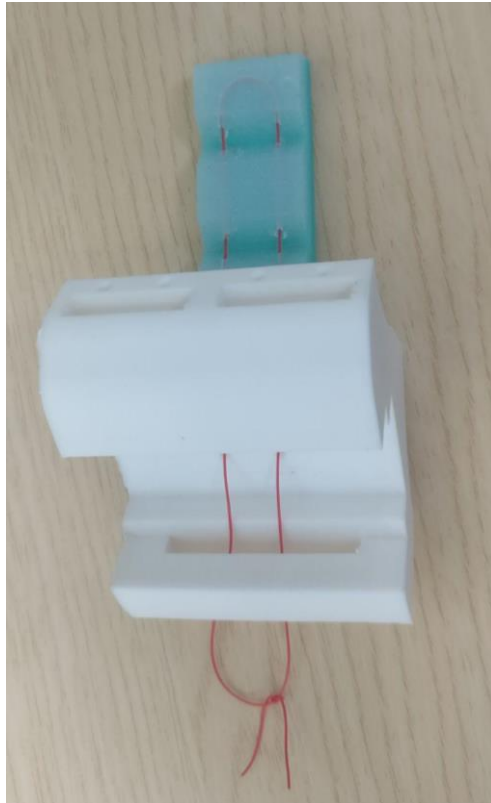
Figure 0.10 'Hand' Prototype with a Single Gripper Installed

To counter the issue of a restrictive grasp width, the angle of the 'thumb' offset was adjusted to 90°, from an initial 45°. The rest of the design remained unchanged. The other print parameters remained the same, with the print again taking approximately 5 hours to complete. The grippers fit securely into the slots and all the cables once again were easily threaded. A series of basic grasping tasks were performed to demonstrate the effectiveness of this design. The wider grasp allows for a far larger range of objects to be grasped. This improved range verifies the design update and it will now be the basis going forward. Whist the design of the hand is basic, it is the intention that the soft-grippers will achieve a level of grasp flexibility that does not necessitate features such as articulated 'thumb'.
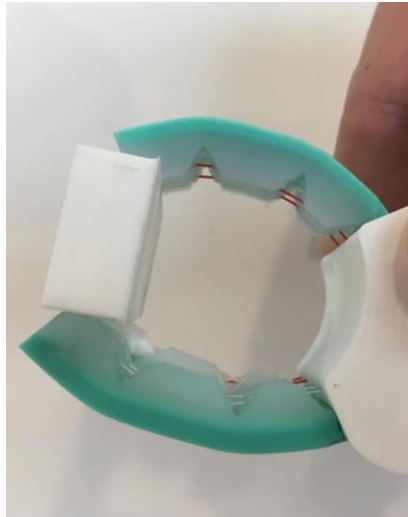
Figure 0.11 Grasping a Plastic Block
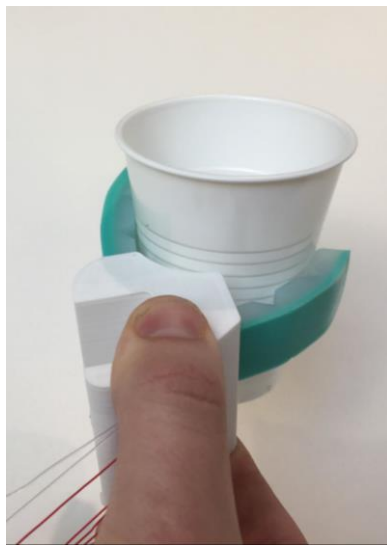
Figure 0.12 Grasping a Disposable Cup
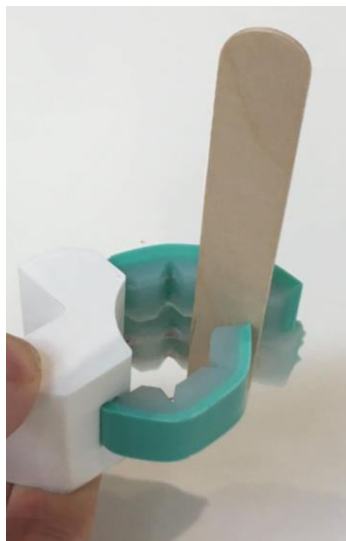
Figure 0.13 Pinch Grasp of a Wooden Stick

Version 1

Using the previously developed hand as a basis, the wrist is constructed of an oval segment, 40mm wide and 50mm high. The 'Sweep' tool is then used with this oval wrist area and a rectangular drawing offset 100mm from the wrist: this forms the forearm of the prosthetic (Figure 0.14). The use of the rectangular shape is to make space for the battery and other components, the 'Sweep' tool automatically smooths the transition and additional fillets are in place to further improve on this.
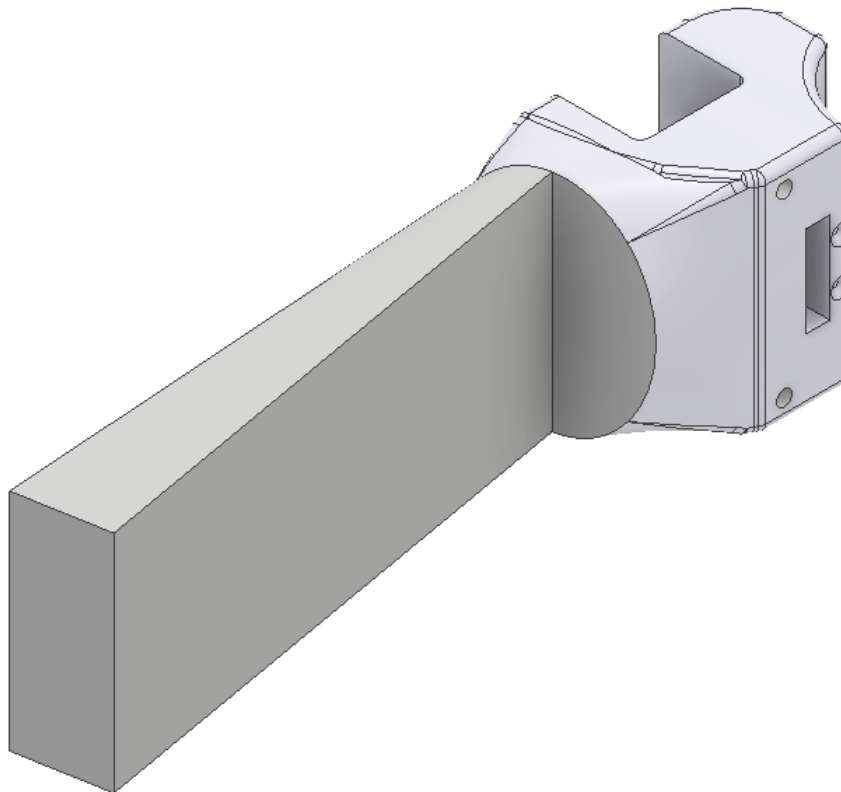
Figure 0.14 Initial Forearm Block
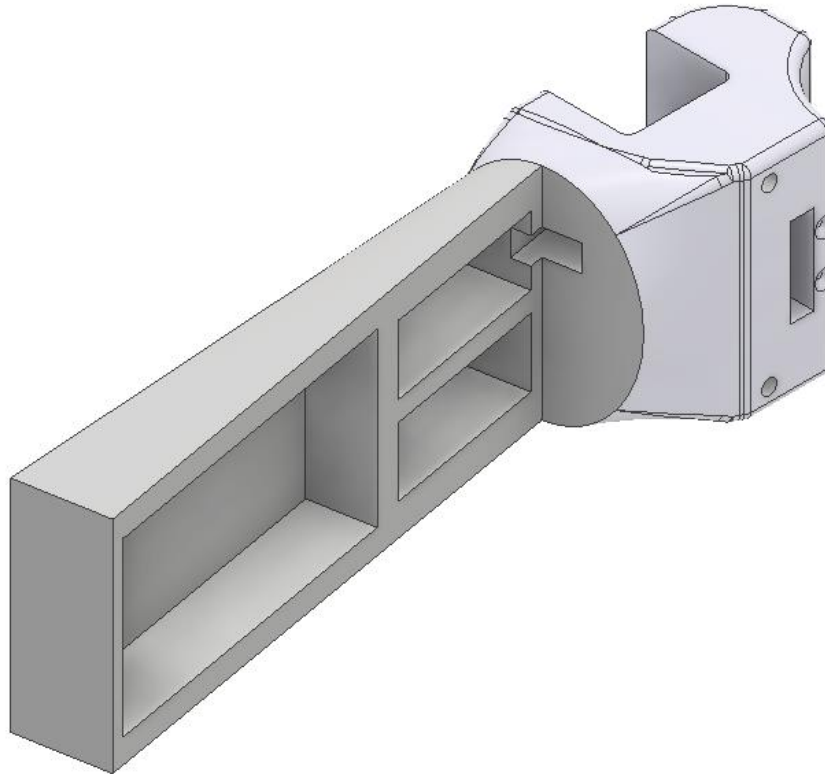
Figure 0.15 Slots for Electrical Components Added

The forearm in its current form is a solid block. Outlines for the motors and battery are drawn on the surface of the forearm and reverse extruded to create slots for these components (Figure 0.15). Additional slots for the cables, fixtures, and actuator shaft are also added to the design. Other design details added include holes and slots for nuts and bolts that will join the three parts together in the final assembly of the arm. These holes and slots are designed for M3 bolts.

The complex nature of the design required the use of support material. Ulitmaker's polyvinyl alcohol (PVA) material was selected as the support, due to it being a water-soluble polymer which can easily be removed by submerging the printed component in water. The use of the material does lead to some added complexity with the 3D-print process, with most of the failures being down to the PVA material becoming jammed midway through printing. The PVA support material is very sensitive to water. If kept incorrectly the material will become saturated and as such will be very difficult to print with.

As with all the previous parts, the CAD design was imported into Cura for slicing. The support was generated automatically anywhere where an overhang is present. The main structure of the arm was also printed in white ABS, just as with the previous prototypes. In order to maximise strength, the print is oriented perpendicular to the load vector. Print orientation is major consideration, due to the non-isotropic structure of the components produced under FDM. The optimisation of print orientation has been explored within literature [130]. At its core, theory dictates that an object expected to be under tension should have layers parallel with the load; conversely a structure under a flexural (bending) or

moment load should have layers perpendicular to the load direction (Figure 0.16). In the case of a prosthetic arm, the load comes from the weight of the object being grasped. This force acts as a moment, centred around the socket of the arm. It is for this reason that the layers are constructed in the way shown in Figure 0.17.
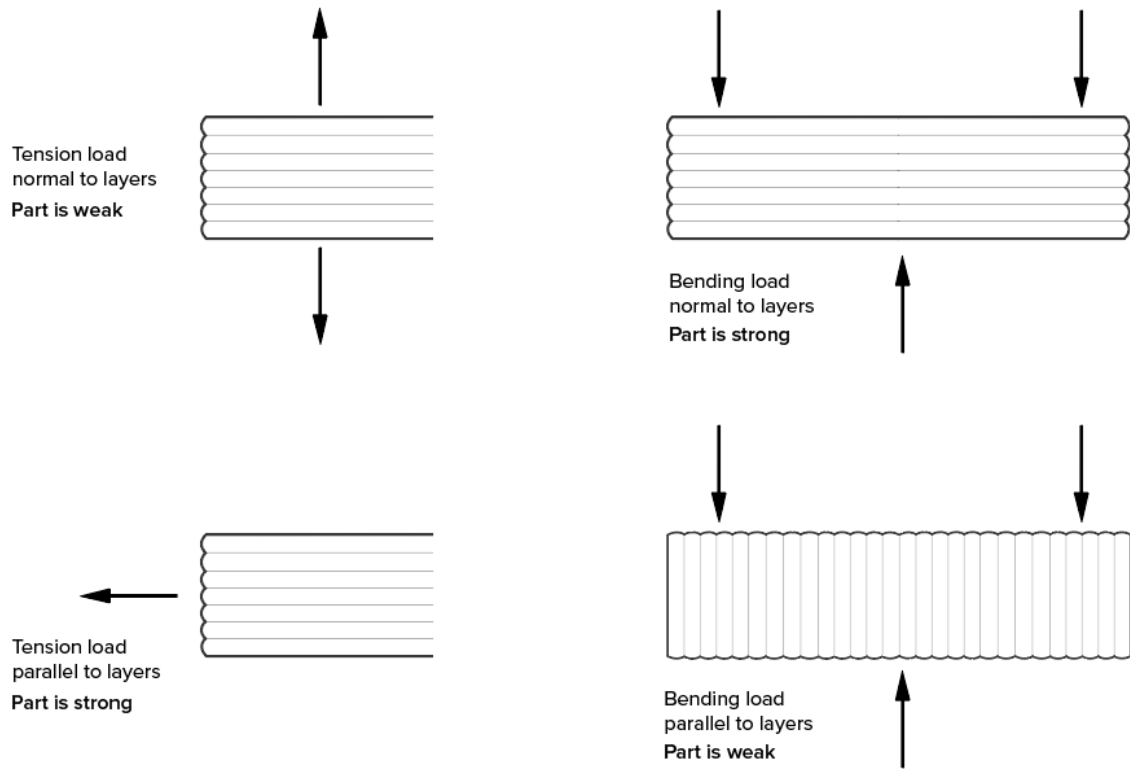
Figure 0.16 FDM Layer Orientation Under Load [131]
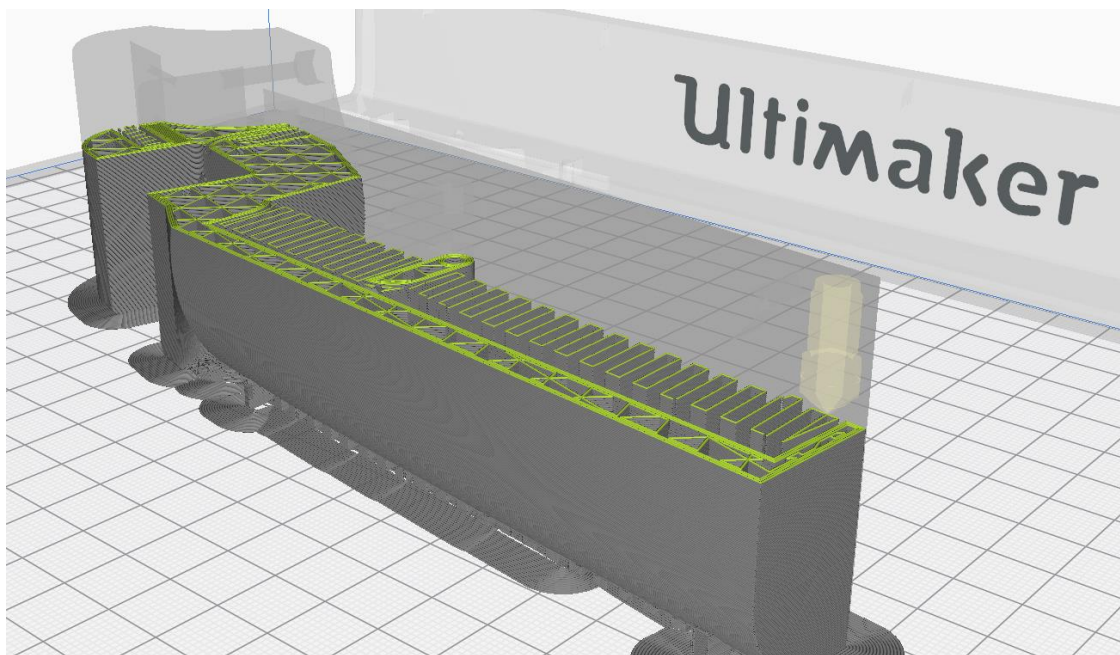
Figure 0.17 CAD Model in Cura with Layer Direction Highlighted

The initial print was successful, with minimal warping or shrinkage. There are some burn mark and warping on the support material, as well as some issues with print bed adhesion; however, the ABS component was still manufactured to an acceptable standard. In order to remove the PVA support, the part was submerged in water for around 24 hours. Most of the material simply dissolves in the water, with some of the larger pieces being removed manually once softened by the water. Cura automatically created a support structure for all overhanging surfaces, this includes the small 2mm channels for the gripper cables. This caused an issue, as the material became jammed within the tight crevasses, even after additional soaking. The 3mm holes likewise had a similar issue (Figure 0.18), though this material was eventually removed.

Figure 0.18 Bolt Hole with PVA Blockage

The grippers all fit securely in their appropriate slots, though due to the tube blockage, they could not be threaded. The battery too fit securely in its appropriate slot. There was however an issue with the installation of the motors due to the actuator shaft slots on the wrist of the device (Figure 0.19). The angle was too tight for the motors to be inserted into their slots, without excessive force that would have likely damaged the actuators. The slot design proved to be an oversight in the initial design. In subsequent versions these slots will be redesigned with the installation of the motor considered.
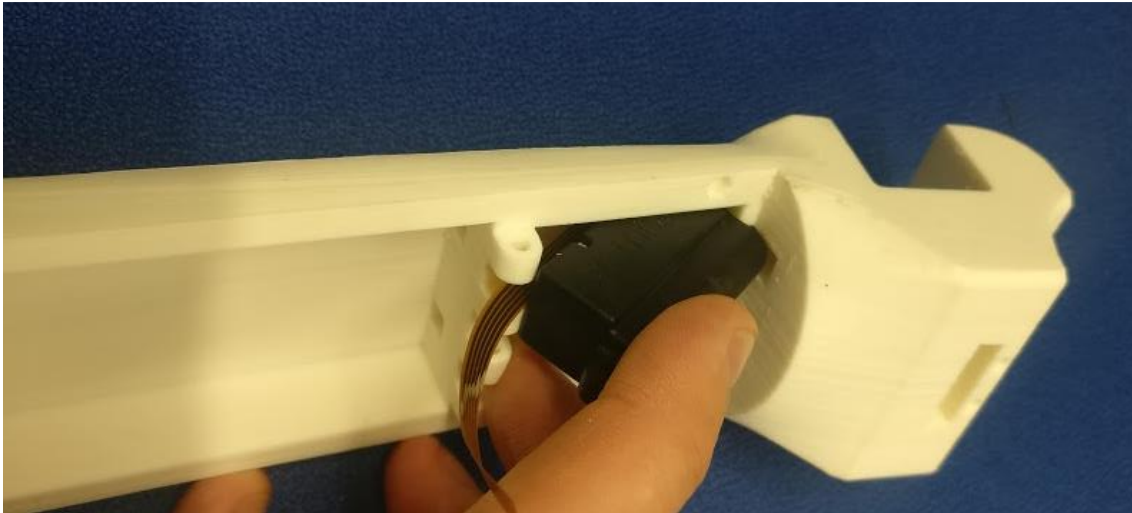
Figure 0.19 Actuator Installation Issue

Version 2

This second version of the arm aims to correct the main issues found in the previous version, primarily the blockages and the installation of the motor. To correct the actuator fitting issues, the slots for the shaft were widened and filleted (Figure 0.20), this allowed the shaft to be angled correctly during the installation of the motors. There are also a few small changes to the design, such as fillets on the battery slots. These were the only design changes made on the CAD model, all the subsequent changes took place on Cura and relate to the manufacturing processes.
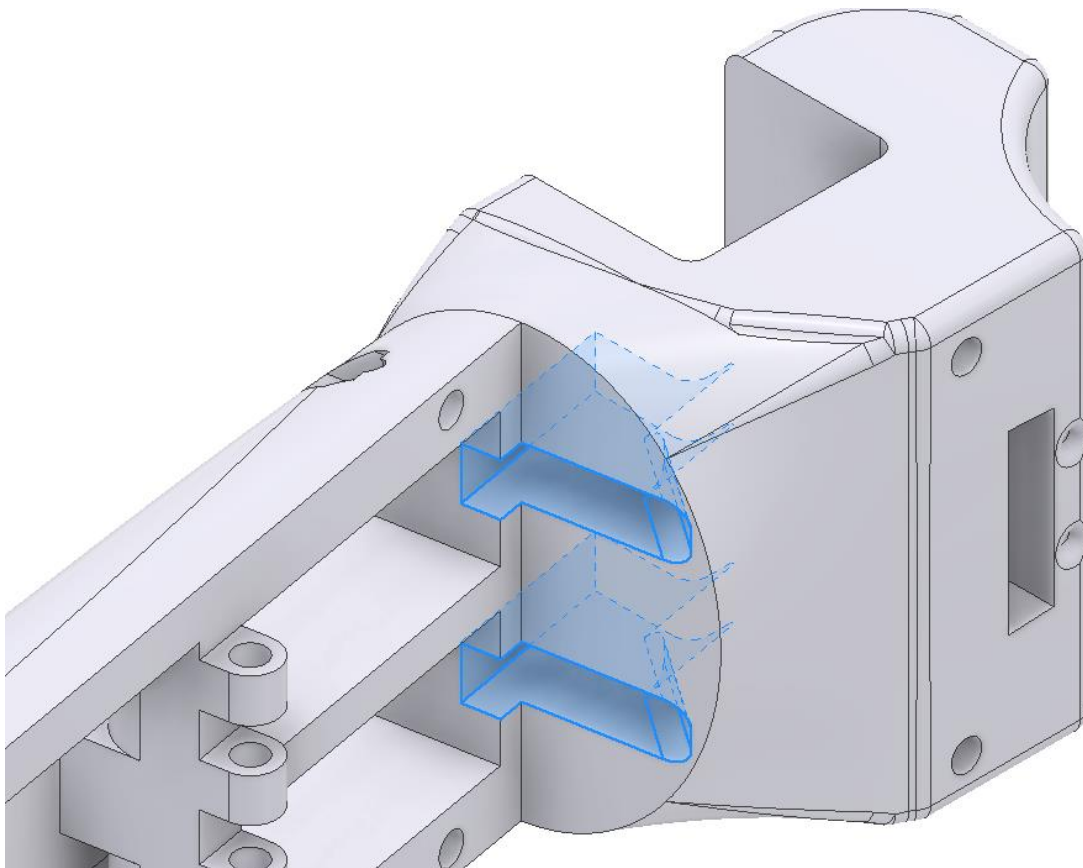
Figure 0.20 Actuator Slot Design Changes

The issues with the tube blockage are due to support material becoming trapped in the narrow holes. In order to avoid this, 'support-blockers' were used in Cura (Figure 0.21). These blockers prevent support material from being printed in the selected region. In the case of the 2mm tubes and the 3mm holes for the bolts, no support material is needed as there is not enough overhang to cause significant issues. For this reason, 'support-blockers' were used in these locations to prevent support material from being printed there.
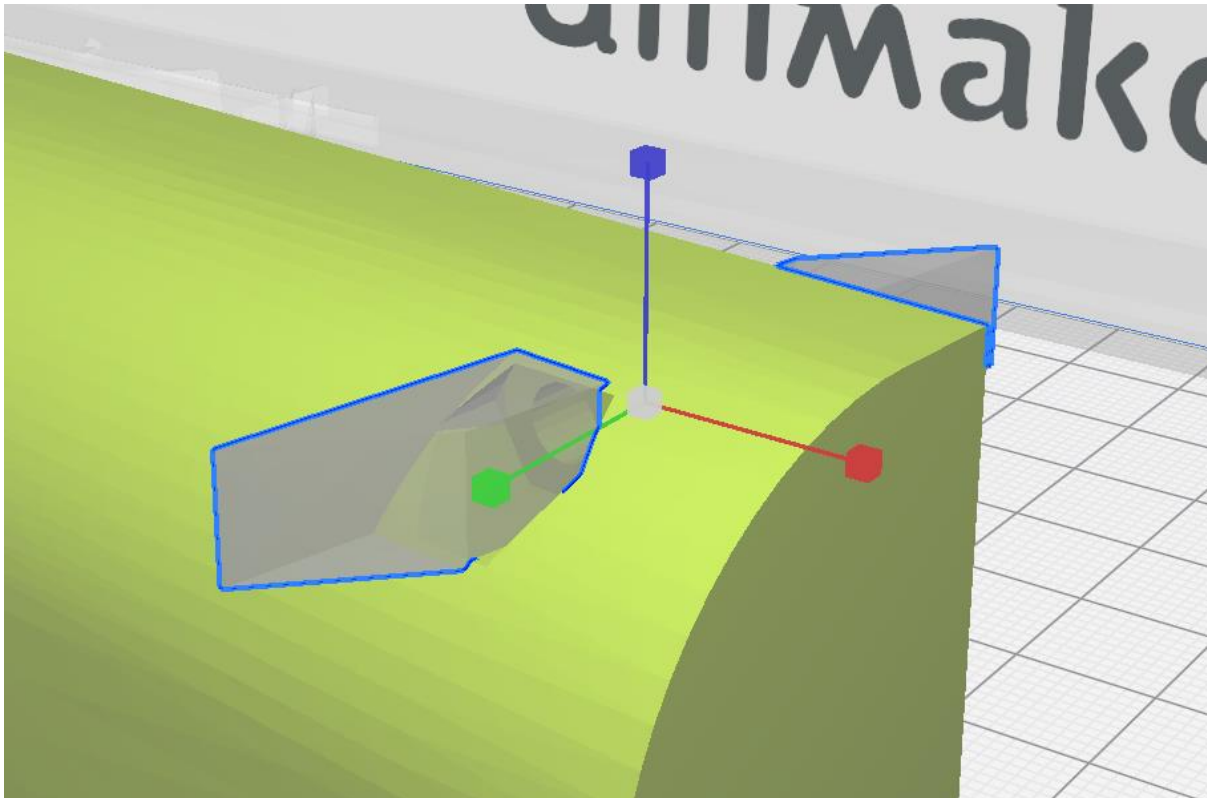
Figure 0.21 Support Blocker on Bolt Fixture

There was an issue during the print process, where the PVA material stopped extruding. The ABS continued to be extruded and the arm was manufactured. However due to an inadequate support structure, the quality of the print was poor. This was particularly concentrated around the actuator and gripper slots, due to their overhang. Some finishing techniques were attempted (filing and sanding), however the quality was still too poor for the device to be functional.
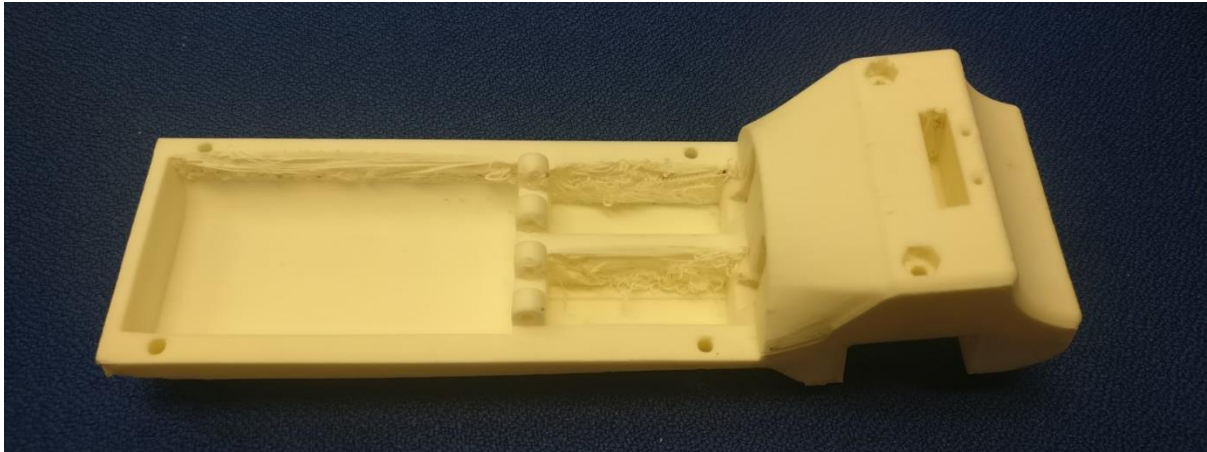
Figure 0.22 Failed Print due to lack of Support Structure

Version 3

This final attempt is the exact same design as in version 2. The issue with the previous print was likely due to the PVA absorbing water due to incorrect storage. This softens the material, causing it to become stuck in the material feeder. Before a second print attempt was conducted, the PVA material was dried out by placing it on the print bed, with the bed temperature set to 50°C. The material was left for 3 hours, with a subsequent hour for cool down. The print process was then repeated, with the same use of support blockers for the tubes and bolt holes.

This print with the now dried PVA support filament was successful. There were minimal flaws present in final component. The support material printed correctly in all the required spots. As intended, the bolt holes and tubes did not have any blockage from the support material. The actuators, with the slot design modification, were able to be installed securely within the 'arm'. The grippers too were secured correctly in the 'hand'. They were then threaded, with the thread tied around the appropriate actuator shaft. By setting up a basic circuit and running a simple extend-retract Arduino script, the performance of the grasp mechanism was verified.
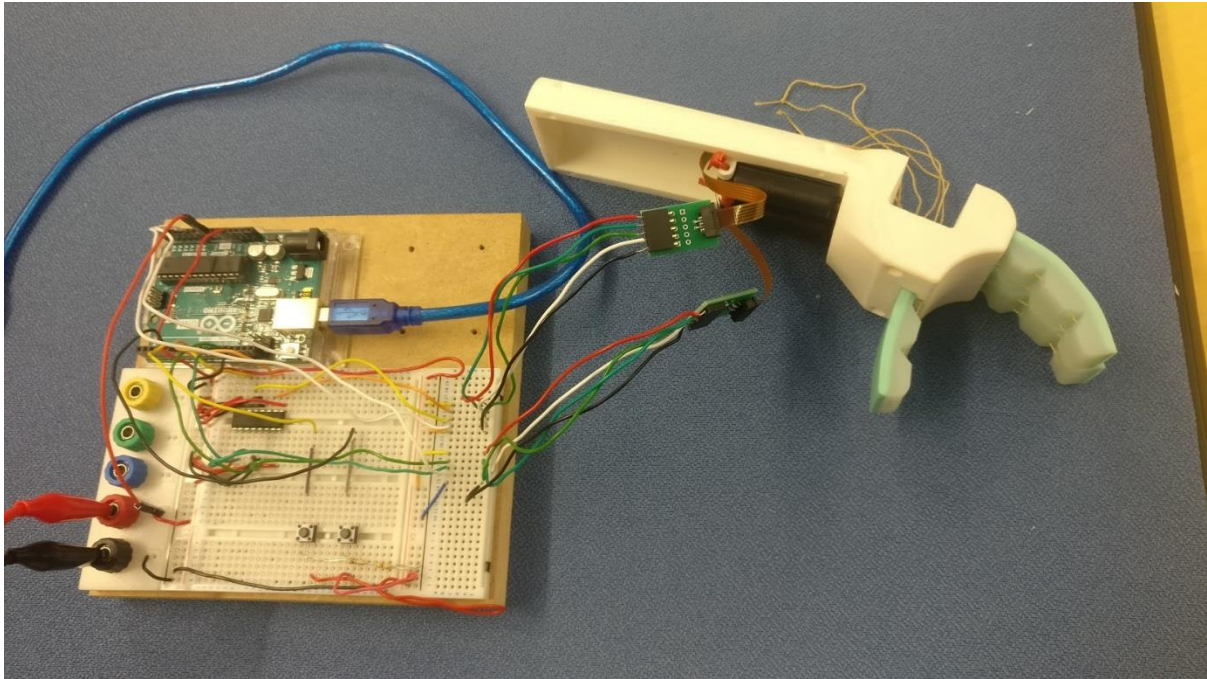
Figure 0.23 Actuator Test

Appendix A3

A circle with a diameter slightly larger than the stump is used as the basic shape (Figure 0.24). This is then extruded into a thin walled cylinder (Figure 0.25). The initial cylinder is made up of an 8 x 8 mesh, which must be extended to cover the entire height of the stump. This process of extending can be performed by adding additional mesh segments or by increasing the size of the pre-existing ones. The level of granularity was considered sufficient to simply increase the segment size in this instance (Figure 0.26), with the option to create a finer mesh in later stages should this be desired.
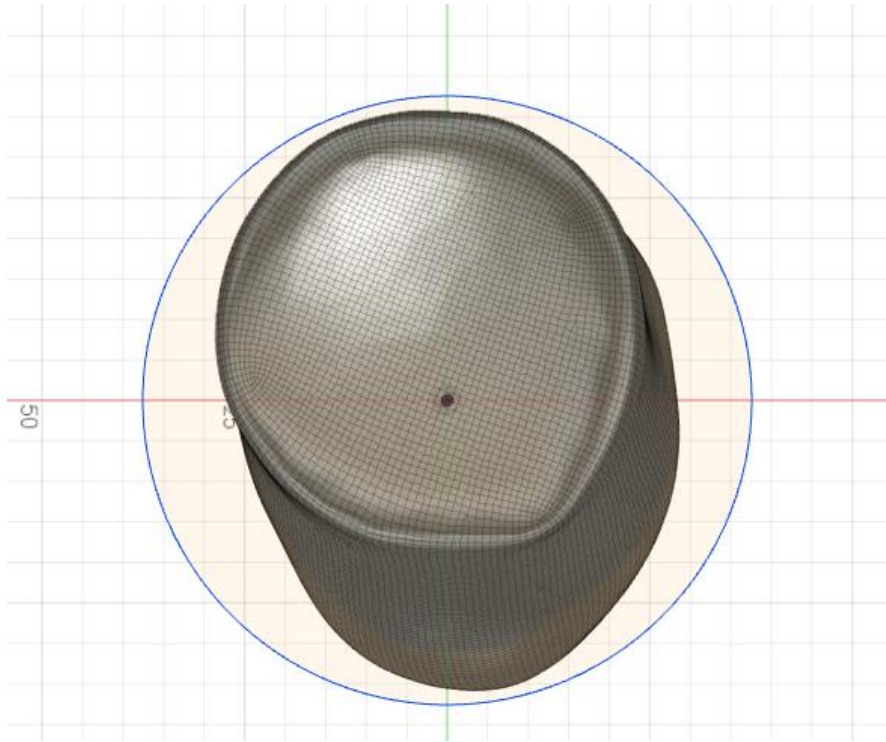
Figure 0.24 Initial Set Drawing for Mesh
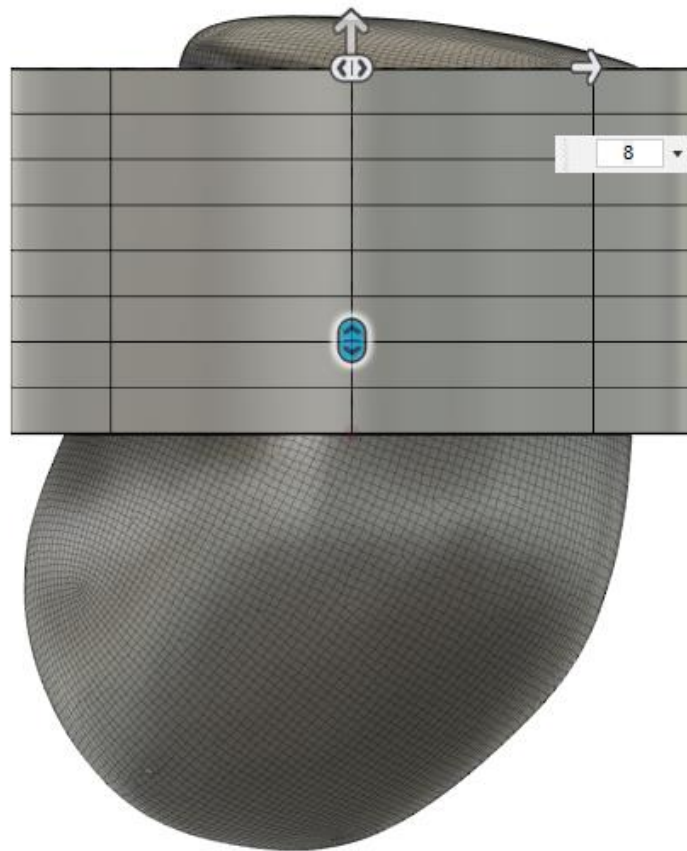
Figure 0.25 Base Cylinder with 8x8 Segmentation
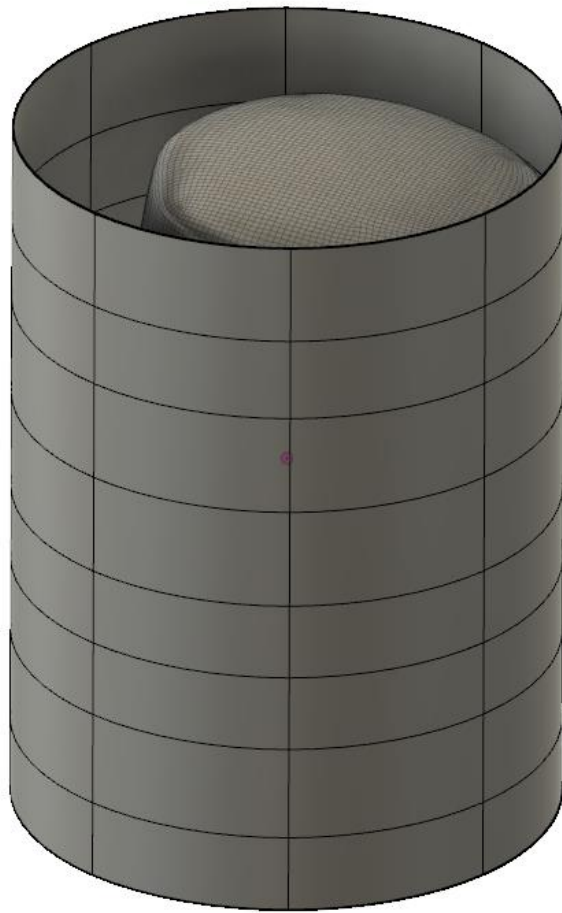
Figure 0.26 Extended Cylinder

With the basic cylinder completed, the shape must now be moulded to match the stump. This can be done completely manually by dragging and resizing the individual points, lines, and segments; however the use of the "pull" tool automatically wraps the base mesh around the scan geometry, as shown in Figure 0.27. From here it is fairly simple process of adjusting the mesh to provide a good fit for the stump, using the drag techniques (Figure 0.28). The base of the stump is automatically sealed using the "fill-hole" tool; this closed region is then adjusted manually to best fit the stump.
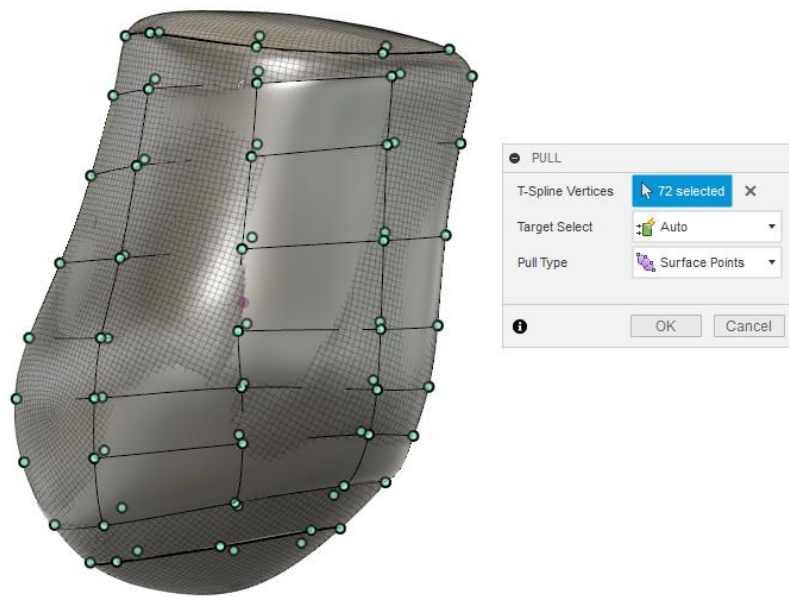
Figure 0.27 Mesh after using the 'Pull' Tool

Figure 0.28 Fine Tuning of the Mesh Structure

Towards the top of the stump, a wide section is created to allow for its insertion during fitting; this too was created with the manual manipulation tools. With this completed, there is no further adjustment required within the mesh environment. When entering the solid model environment, the model shown in Figure 0.29 is displayed. This model is a thin plane model and does not have a defined thickness.

Using the 'thicken' tool allows for the model to be converted into a true 3D-model of the socket. A thickness of 3mm was used in this instance to give the model shown in Figure 0.30.

Figure 0.29 Socket Design in Solid Model Environment

Figure 0.30 Socket with 3mm Wall thickness

Appendix B

Appendix B1
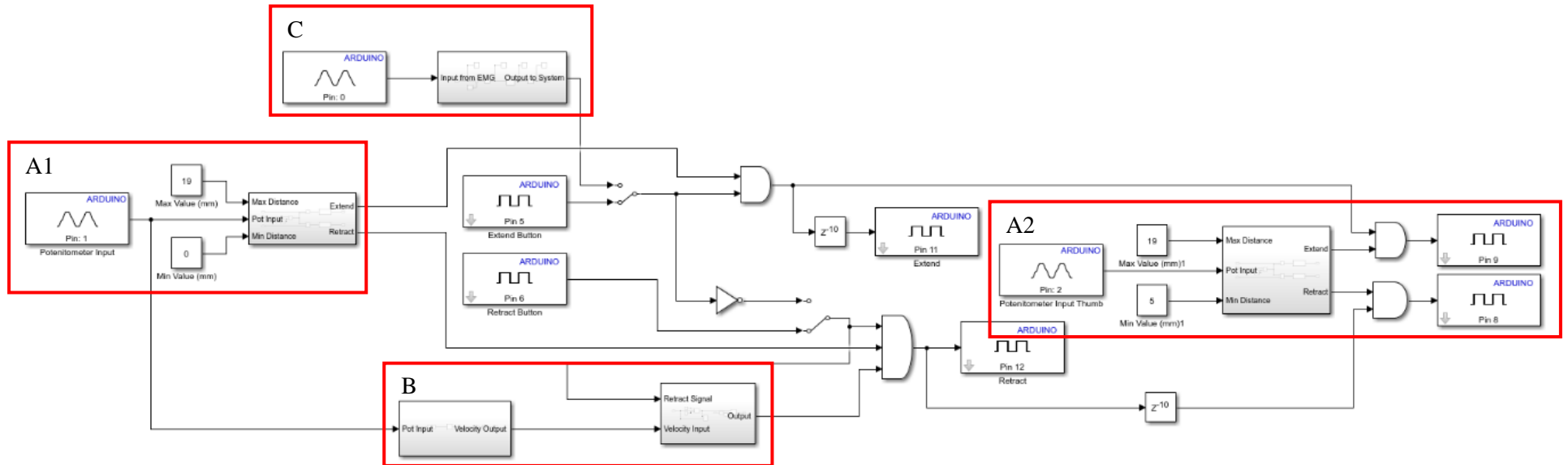
Figure 0.31 Full Simulink™ Model

Appendix B2

The unit conversion takes place within the subsystem (Figure 0.32). The analog input is multiplied by a constant valued at *20(mm)/1023*, to produce a potentiometer reading in millimetres. This potentiometer reading is then subtracted from both maximum and minimum limits.
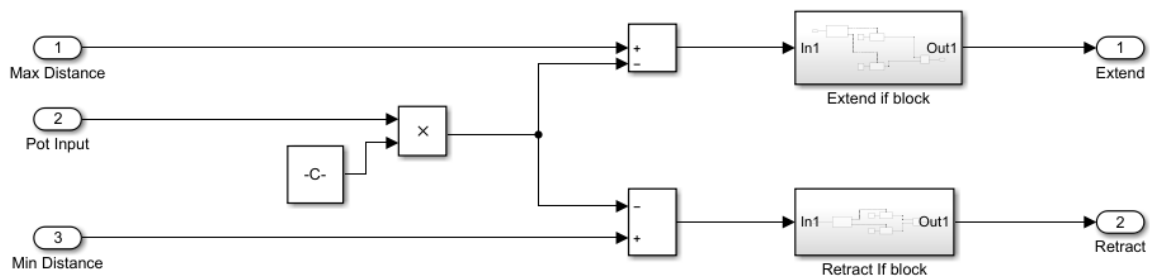
Figure 0.32 Actuator Control Subsystem
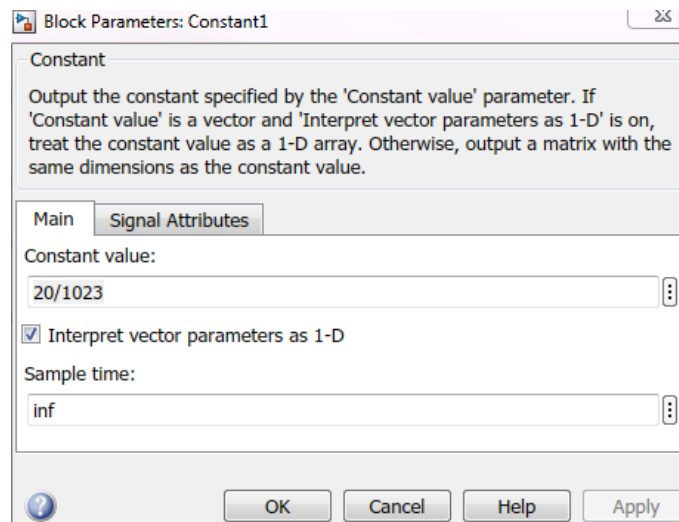
Figure 0.33 Conversion Block Parameters

Within these blocks there is a logic test to determine if the recorded value is within the set limits. The 'if' block determines whether the input signal is greater-than or lower-than 0, a greater-than results in a positive output, whilst the inverse is true for a lower-than or equal-to result.
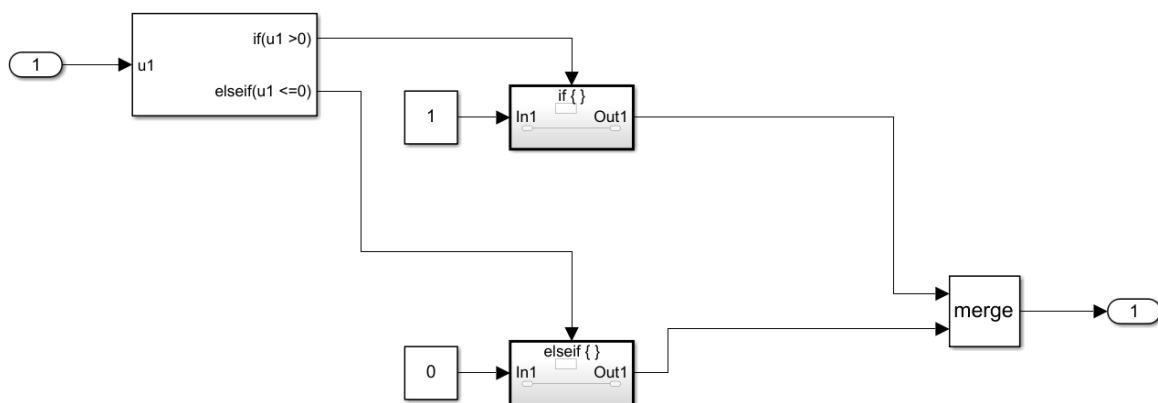
Figure 0.34 Extend/Retract IF Subsystem

The output signal for extend and retract then each respectively join an AND logic gate. If an input signal from the buttons or sEMG is sent to the AND gate and the shaft is within the extension limits, then the actuator will move accordingly. Two digital output pin blocks are used for this and are connected to the motor-driver on the circuit, retracting or extending the actuator accordingly.

Technical Document

RS PRO - ABS PRO

Stock numbers:
174-0013 / 174-0014 / 174-0015 / 174-0016 / 174-0017 / 174-0019 / 174-0020 / 174-0021 / 174-0022 /
174-0023 / 174-0025 / 174-0026 / 174-0027 / 174-0028 / 174-0029 / 174-0031 / 174-0032 / 174-0033 /
174-0034 / 174-0035 / 174-0036 / 174-0037 / 174-0038 / 174-0039

EN

ABS PRO is our take on a next-generation ABS filament. By applying our zero warp technology to the filament we have created a filament with far less cracking, proven near perfect interlayers, reliable bed adhesion (glass, tape & other adhesives) while improving the mechanical properties making ABS PRO extra strong. These properties make ABS PRO the ultimate ABS replacement that prints strong and beautiful parts on any FDM 3D printer without the common headaches associated with regular ABS like warping & horrible bed adhesion. ABS PRO is the perfect material for strong objects that require an high impact tolerance.

Features:
- Zero warp technology
- Excellent interlayer adhesion
- Reliable bed adhesion (Glass, tape & other adhesives)
- Enhanced mechanical properties over regular ABS
- Great strength & aesthetics

Colours:
RS PRO - ABS PRO is available from stock in 12 colours.
Packaging:
RS PRO - ASA PRO is available in 500 grams packaging.

Filament specs.		
Size	Ø tolerance	Roundness
1,75mm	± 0,05mm	≥ 95%
2,85mm	± 0,10mm	≥ 95%

Material properties		
Description	Testmethod	Typical value
Specific gravity	ISO 1183	1,1 g/cc
MFR 260°C/5 kg	ISO 1133	41 gr/10 min
Tensile strength at yield	ISO 527	43,6 Mpa
strain at break	ISO 527	34%
Tensile modulus	ISO 527	2030 Mpa
Impact strength - Charpy notched 23°C	ISO 179	58 kJ/m^2
Printing temp.	Print lab	245±10°C
Melting temp.	ISO 294	235±10°C
Vicat softening temperature	ISO 306	97°C

Additional information:
Recommended temperature for heated bed is ± 80°C.
ABS PRO is printed at high temperatures to make the final product extra strong.
ABS PRO can be used on all common desktop FDM or FFF technology 3D printers.
Storage: Cool and dry (15-25°C). This enhances the shelf life significantly.

rspro.com

Dragon Skin™ Series
Addition Cure Silicone Rubber Compounds

Cured Material Certified Skin Safe!

SMOOTH-ON www.smooth-on.com

PRODUCT OVERVIEW

Dragon Skin™ silicones are high performance platinum cure liquid silicone compounds that are used for a variety of applications ranging from creating skin effects and other movie special effects to making production molds for casting a variety of materials. Because of the **superior physical properties** and flexibility of Dragon Skin™ rubbers, they are also used for medical prosthetics and cushioning applications. Dragon Skin™ rubbers are also used for a variety of industrial applications and have a service temperature range of a constant -65°F to +450°F (-53°C to +232°C).

Great for Making Molds for a Variety of Applications - Available in **Shore 10A, 20A and 30A**, Dragon Skin™ silicones can be used to make exceptionally strong and tear resistant molds for casting plaster, wax, concrete (limited production run), resins and other materials. **Dragon Skin™ 10 AF** is an **anti-fungal** silicone suitable for making a variety of skin-safe cushioning device configurations that resist fungi for orthopedic and orthotic applications.

Time Tested, Versatile Special Effects Material – Soft, super-strong and stretchy, Dragon Skin™ 10 (**Very Fast, Fast, Medium and Slow speeds**) is used around the world to make spectacular skin and creature effects. An infinite number of color effects can be achieved by adding Silc Pig™ silicone pigments or Cast Magic™ effects powders. Cured rubber can also be painted with the Psycho Paint™ system. Cured material is skin safe and certified by an independent laboratory.

Easy To Use – Dragon Skin™ silicones are mixed 1A:1B by weight or volume. Liquid rubber can be thinned with Silicone Thinner™ or thickened with THI-VEX™. Rubber cures at room temperature (73°F/23°C) with negligible shrinkage. *Vacuum degassing is recommended to minimize air bubbles in cured rubber.*

TECHNICAL OVERVIEW

	Mixed Viscosity (ASTM D-2393)	Specific Gravity (g/cc) (ASTM D-1475)	Specific Volume (cu. in./lb.) (ASTM D-1475)	Pot Life (ASTM D-2471)	Cure Time	Shore A Hardness (ASTM D-2240)	Tensile Strength (ASTM D-412)	100% Modulus (ASTM D-412)	Elongation at Break % (ASTM D-412)	Die B Tear Strength (ASTM D-624)	Shrinkage (in./in.) (ASTM D-2566)
Dragon Skin™ 10 Very Fast	23,000 cps	1.07	25.8	4 min.	30 min.	10A	475 psi	22 psi	1000%	102 pli	< .001 in./in.
Dragon Skin™ 10 Fast	23,000 cps	1.07	25.8	8 min.	75 min.	10A	475 psi	22 psi	1000%	102 pli	< .001 in./in.
Dragon Skin™ 10 Medium	23,000 cps	1.07	25.8	20 min.	5 hours	10A	475 psi	22 psi	1000%	102 pli	< .001 in./in.
Dragon Skin™ 10 Slow	23,000 cps	1.07	25.8	45 min.	7 hours	10A	475 psi	22 psi	1000%	102 pli	< .001 in./in.
Dragon Skin™ 10 AF	23,000 cps	1.07	25.8	20 min.	5 hours	10A	475 psi	22 psi	1000%	102 pli	< .001 in./in.
Dragon Skin™ 20	20,000 cps	1.08	25.6	25 min.	4 hours	20A	550 psi	49 psi	620%	120 pli	< .001 in./in.
Dragon Skin™ 30	20,000 cps	1.08	25.7	45 min.	16 hours	30A	500 psi	86 psi	364%	108 pli	< .001 in./in.

Mix Ratio: 1A:1B by volume or weight	**Useful Temperature Range:** -65°F to +450°F (-53°C to +232°C)
Color: Translucent	**Dielectric Strength** (ASTM D-149): >350 volts/mil

PROCESSING RECOMMENDATIONS

*All values measured after 7 days at 73°F/23°C

PREPARATION... Safety – Use in a properly ventilated area ("room size" ventilation). Wear safety glasses, long sleeves and rubber gloves to minimize contamination risk. Wear vinyl gloves only. Latex gloves will inhibit the cure of the rubber.

Store and use material at room temperature (73°F/23°C). Warmer temperatures will drastically reduce working time and cure time. Storing material at warmer temperatures will also reduce the usable shelf life of unused material. These products have a limited shelf life and should be used as soon as possible. Mixing containers should have straight sides and a flat bottom. Mixing sticks should be flat and stiff with defined edges for scraping the sides and bottom of your mixing container.

Cure Inhibition – Addition-cure silicone rubber may be inhibited by certain contaminants in or on the pattern to be molded resulting in tackiness at the pattern interface or a total lack of cure throughout the mold. Latex, tin-cure silicone, sulfur clays, certain wood surfaces, newly cast polyester, epoxy, tin cure silicone rubber or urethane rubber may cause inhibition. If compatibility between the rubber and the surface is a concern, a small-scale test is recommended. Apply a small amount of rubber onto a non-critical area of the pattern. Inhibition has occurred if the rubber is gummy or uncured after the recommended cure time has passed.

Because no two applications are quite the same, a small test application to determine suitability for your project is recommended if performance of this material is in question.

Smooth-Sil™ Series

Addition Cure Silicone Rubber Compounds

SMOOTH-ON
www.smooth-on.com

PRODUCT OVERVIEW

Smooth-On **Smooth-Sil™** Platinum Silicones cure at room temperature with negligible shrinkage. With different hardnesses to choose from, **Smooth-Sil™** products offer tremendous versatility and are suitable for making production molds of any configuration, large or small. These silicones exhibit good chemical, abrasion and heat resistance. Materials such as plasters, concrete, wax, low-melt metal alloys or resins (urethane, epoxy or polyester) can then be cast into these silicone rubbers without a release agent.

Smooth-Sil™ 936 is a lower viscosity version of Smooth-Sil® 935 platinum silicone rubber (21,000 cps vs. 40,000 cps). It is easier to mix, vacuum degas and pour. **Smooth-Sil™ 945** offers the convenience of a **1A:1B by volume** mix ratio and a fast **6 hour cure time.**

Smooth-Sil™ Platinum Silicones are used for rapid prototyping, wax casting (foundries and candle makers), architectural restoration and for casting concrete. Smooth-Sil™ 940, 950 and 960 are suitable for food related applications. (See separate technical bulletin for usage instructions available at www.smooth-on.com).

TECHNICAL OVERVIEW

	Mixed Viscosity (ASTM D-2393)	Specific Gravity (g/cc) (ASTM D-1475)	Specific Volume (cu. in./lb.) (ASTM D-1475)	Color	Pot Life (ASTM D-2471)	Cure Time	Mix Ratio	Shore A Hardness (ASTM D-2240)	Tensile Strength (ASTM D-412)	100% Modulus (ASTM D-412)	Elongation @ Break % (ASTM D-412)	Die B Tear Strength (ASTM D-624)
Smooth-Sil™ 935	40,000 cps	1.18	23.5	Blue	45 min.	24 hrs.	100A:10B by weight	35A	650 psi	170 psi	300%	115 pli
Smooth-Sil™ 936	21,000 cps	1.21	22.9	Blue	60 min.	24 hrs.	100A:10B by weight	36A	550 psi	180 psi	500%	110 pli
Smooth-Sil™ 940	35,000 cps	1.18	23.4	Pink	30 min.	24 hrs.	100A:10B by weight	40A	600 psi	200 psi	300%	100 pli
Smooth-Sil™ 945	30,000 cps	1.24	22.3	Purple	25 min.	6 hrs.	1A:1B by weight or volume	45A	700 psi	260 psi	320%	120 pli
Smooth-Sil™ 950	35,000 cps	1.24	22.3	Blue	45 min.	18 hrs.	100A:10B by weight	50A	725 psi.	272 psi	320%	155 pli
Smooth-Sil™ 960	30,000 cps	1.25	22.2	Green	45 min.	16 hrs.	100A:10B by weight	60A	650 psi.	280 psi.	270%	110 pli

Useful Temperature Range: -65°F to 450°F (-53°C to 232°C)
Dielectric Strength (ASTM D-147-97a): >350 volts/mil

*All values measured after 7 days at 73°F/23°C
Shrinkage* (in./in.) (ASTM D-2566): < .001

PROCESSING RECOMMENDATIONS

PREPARATION... Safety – Use in a properly ventilated area ("room size" ventilation). Wear safety glasses, long sleeves and rubber gloves to minimize contamination risk. Wear vinyl gloves only. Latex gloves will inhibit the cure of the rubber.

Store and use material at room temperature (73°F/23°C). Warmer temperatures will drastically reduce working time and cure time. Storing material at warmer temperatures will also reduce the usable shelf life of unused material. These products have a limited shelf life and should be used as soon as possible.

Cure Inhibition – Addition-cure silicone rubber may be inhibited by certain contaminants in or on the pattern to be molded resulting in tackiness at the pattern interface or a total lack of cure throughout the mold. Latex, tin-cure silicone, sulfur clays, certain wood surfaces, newly cast polyester, epoxy or urethane rubber my cause inhibition. If compatibility between the rubber and the surface is a concern, a small-scale test is recommended. Apply a small amount of rubber onto a non-critical area of the pattern. Inhibition has occurred if the rubber is gummy or uncured after the recommended cure time has passed.

Because no two applications are quite the same, a small test application to determine suitability for your project is recommended if performance of this material is in question.

To prevent inhibition, one or more coatings of a clear acrylic lacquer applied to the model surface is usually effective. Allow any sealer to thoroughly dry before applying rubber. Note: Even with a sealer, platinum silicones will not work with modeling clays containing heavy amounts of sulfur. Do a small scale test for compatibility before using on your project.

Applying A Release Agent - Although not usually necessary, a release agent will make demolding easier when pouring into or over most surfaces. Ease Release™ 200 is a proven release agent for making molds with silicone rubber. Mann Ease Release™ products are available from Smooth-On or your Smooth-On distributor.

Miniature Linear Motion Series · PQ12

Actuonix Motion Devices unique line of Miniature Linear Actuators enables a new generation of motion-enabled product designs, with capabilities that have never before been combined in a device of this size. These tiny linear actuators are a superior alternative to designing your own push/pull mechanisms. Their low cost and easy availability make them attractive to hobbyists and OEM designers alike.

The PQ12 actuators are complete, self contained linear motion devices with position feedback for sophisticated position control capabilities, or end of stroke limit switches for simple two position automation. Driving them couldn't be easier, simply apply a DC voltage to extend the actuator, and reverse the polarity to retract it. Several gear ratios and voltage options are available to give you varied speed/force configurations.

PQ12 Actual Size

Benefits
→ Compact miniature size
→ Precise position feedback
→ Limit switches
→ Simple control
→ Low voltage
→ Equal push/pull force
→ Easy mounting

Applications
→ Robotics
→ Consumer appliances
→ Toys
→ RC vehicles
→ Automotive
→ Industrial Automation

PQ12 Specifications

Gearing Option	30:1	63:1	100:1
Peak Power Point	15N@15mm/s	30N @ 8mm/s	40N @ 6mm/s
Peak Efficiency Point	8N @ 20mm/s	12N@12mm/s	20N @ 8mm/s
Max Speed (no load)	28mm/s	15mm/s	10mm/s
Max Force (lifted)	18N	45N	50N
Max Side Load	5N	10N	10N
Back Drive Force	9N	25N	35N

Stroke	20 mm
Input Voltage	6 or 12 VDC
Stall Current	550mA @ 6V, 210mA @ 12V
Mass	15g
Operating Temperature	-10°C to +50°C
Positional Repeatability	±0.1mm
Mechanical Backlash	0.25 mm
Audible Noise	55dB @ 45cm
Ingress Protection	IP-54
Feedback Potentiometer	5kΩ±50%
Limit Switches	Max. Current Leakage: 8uA
Maximum Duty Cycle	20%

Basis of Operation

The PQ12 is designed to push or pull a load along its full stroke length. The speed of travel is determined by the load applied (see load curves). When power is removed the actuator will hold its position, unless the applied load exceeds the back drive force. Repeated stalling of the actuator against a fixed load will shorten the life of the actuator. Since application conditions (Environmental, loading, duty cycle, vibration, etc) vary so widely, we advise application specific testing to determine the expected life of the actuator.

Ordering

Small quantity orders can be placed directly online at www.Actuonix.com. Each actuator ships with two mounting brackets, M3 mounting hardware, and one FPC ribbon cable connector. To extend the length of the ribbon cable you can purchase one of our PQ12 cable adapters and extension cable, or solder wires directly to the ribbon cable. Contact sales@Actuonix.com for volume quotes and customization options for OEM's.
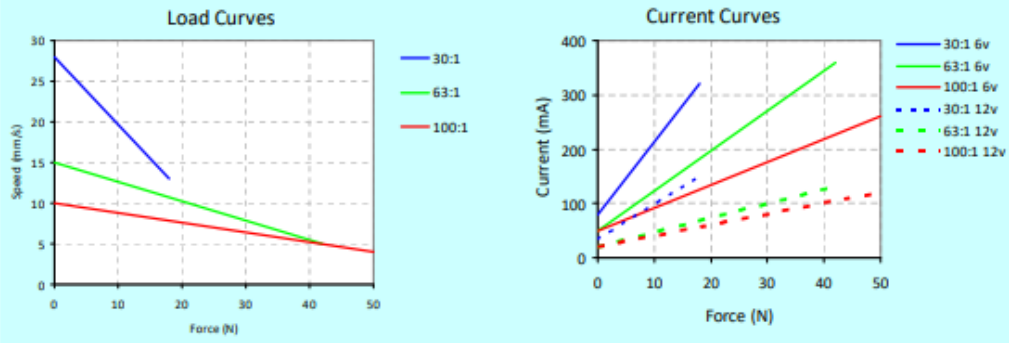
ACTUONIX MOTION DEVICES INC.

Actuonix Motion Devcies Inc.   1 (206) 347-9684 Phone   sales@actuonix.com
Unit 201-1753 Sean Heights   1 (888) 225-9198 Toll Free   www.actuonix.com
Saanichton, BC Canada   1 (206) 347-9684 Fax
V8M 0B3

PQ12 Specifications

Load Curves

Current Curves

Model Selection

The PQ12 has 3 configuration choices: Gear Ratio, Voltage and Controller. PQ12 options are identified according to the following scheme:

PQ12-GG-VV-C

feature	options
GG: Gear reduction ratio (refer to load curves above)	**30, 63, 100** (lower ratios are faster but push less force, and vice versa)
VV: Voltage	**6, 12** (DC volts)
C: Controller	**P** Potentiometer Feedback **S** Limit Switches **R** RC Linear Servo (6V Only)

PQ12 Controller Options

Option S – End of Stroke Limit Switches

WIRING: (see next page for pin numbering)
1- Limit Switch Detection (Optional)
2- Actuator Motor Power
3- Actuator Motor Power
4- Not Connected
5- Not Connected

The –S actuators have limit switches that will turn off power to the motor when the actuator reaches within 1mm of the end of stroke. Internal diodes allow the actuator to reverse away from the limit switch. The limit switches cannot be moved. While voltage is applied to the motor power pins (2 & 3) the actuator extends. Reverse the polarity and the actuator retracts. This can be accomplished manually with a DPDT switch or relay, or using an H-Bridge circuit. The –S model cannot be used with the LAC control board. Pin #1 can be used to sense when the actuator has reached the end limits. See our FAQ page for a simple schematic to light an LED when the limits are reached.

Option P – Potentiometer Position Feedback

WIRING: (see next page for pin numbering)
1 – Feedback Potentiometer negative reference rail
2 – Actuator Motor Power
3 – Actuator Motor Power
4 – Feedback Potentiometer positive reference rail
5 – Feedback Potentiometer wiper

The –P actuators have no built in controller, but do provide analog position feedback. While voltage is applied to the motor power pins (2 & 3) the actuator extends. Reverse the polarity and the actuator retracts. Position of the actuator stroke can be monitored using the internal linear potentiometer. Provide any stable low and high reference voltage on pins 1 & 4, then read the position signal on pin 5. The voltage on pin 5 will vary linearly between the two reference voltages in proportion to the position of the actuator stroke. Connect to an LAC board for easy interface with any of the following control signals: Analog 0-5V or 4-20mA, or Digital 0-5V PWM, 1-2ms Standard RC, or USB.

Option R – RC Linear Servo

WIRING: (see last page for pin numbering)
1 - RC input signal (RC-servo compatible)
2 - Power (+6 VDC)
3 - Ground
Note: Reversing polarity on pins 2 and 3 may cause damage

-R actuators are ideally suited to use in robotics and radio control models. The –R actuators or 'linear servos' are a direct replacement for regular radio controlled hobby servos. The desired actuator position is input to the actuator on lead 1 as a positive 5 Volt pulse width signal. A 2.0 ms pulse commands the controller to fully retract the actuator, and a 1.0 ms pulse signals it to fully extend. If the motion of the actuator, or of other servos in your system, seems erratic, place a 1–4Ω resistor in series with the actuator's red V+ lead wire. The PQ12–R Linear Servos are designed to work with typical RC receivers and battery packs. Consequently, they also are compatible with Arduino control boards, VEX Microcontrollers and many other similar boards designed for robotics.

PURCHASE REQUISITION
FOR INTERNAL USE ONLY
School of Engineering

UNIVERSITY OF
LINCOLN

Reference:		Delivery address:	
Date:	10/02/2019		
Suggested Supplier:			
		Delivery address:	University of Lincoln
Requisitioned by:	Daniel De Barrie (ddebarrie@lincoln.ac.uk)		University of Lincoln
PI Approval:			School of Engineering
Facilities/H&S Approval (If relevant):			Brayford Pool
Business Manager Approval:			Lincoln, LN6 7TS
Authorised by Head of School or Equivalent:			Delivery date required: 15/02/2019

Project	Account	Description of Goods/Services	Qty	Unit Price (excl VAT)	Line Value (excl VAT)	
		Emmakites 100lb Braided Kevlar String Utility Cord 60M	1	£7.46	£7.46	https://www.amazon.co.uk/dp/B01
		1MM I.D X 2MM O.D CLEAR TRANSULCENT SILICONE HOSE PIPE TUBING	3	£1.00	£3.00	https://www.advancedfluidsolution
		600ml Clear Plastic Mixing Cup - 10pk - No Lid	1	£4.52	£4.52	https://www.amazon.co.uk/600ml-
		Bond It Silicone Release Spray - 500ml	1	£4.57	£4.57	https://www.amazon.co.uk/Bond-S
		Giant Lollipop Sticks Natural Wood (Pack of 100) by Choice DIY	1	£1.61	£1.61	https://www.amazon.co.uk/Giant-l
		100 x Latex Disposable Gloves Multi Purpose Medical Examination Garage Single Use	1	£6.09	£6.09	https://www.amazon.co.uk/Dispos
		Sealapack premium quality Greaseproof Paper - 37centimeter wide x 10 metre long	1	£2.56	£2.56	https://www.amazon.co.uk/Sealap
		Smooth-Sil 950 - Gallon Unit (4.99Kg)	1	£158.78	£158.78	https://www.benam.co.uk/products
		Dragon Skin 30 - Gallon Unit (7.2Kg)	1	£153.07	£153.07	https://www.benam.co.uk/products
					£0.00	
					£0.00	

Is a Risk Assessment required for this purchase?		NO	Total excl. VAT:	£341.66
Are special handling/storage requirements necessary?		NO	VAT (20%):	£68.33
s a copy of this form to the Senior Experimental Officer			Total Value incl. VAT:	£409.99

This box to be completed by Purchaser and copy returned to Originator.

Agresso Purchase Order Number: PO Date:

PURCHASE REQUISITION
FOR INTERNAL USE ONLY
School of Engineering

UNIVERSITY OF
LINCOLN

Reference:	
Date:	02/04/2019
Suggested Supplier:	

		Delivery address:
Requisitioned by:	Daniel De Barrie (ddebarrie@lincoln.ac.uk)	University of Lincoln
PI Approval:		School of Engineering
Facilities/H&S Approval (If relevant):		Brayford Pool
Business Manager Approval:		Lincoln, LN6 7TS
Authorised by Head of School or Equivalent:		Delivery date required: 07/04/2019

Project	Account	Description of Goods/Services	Qty	Unit Price (excl VAT)	Line Value (excl VAT)	
		SEN0240 - Gravity: Analog EMG Sensor by OYMotion	1	£28.61	£28.61	https://www.mouser.co.uk/Product
		SparkFun RedBoard Edge	1	£15.71	£15.71	https://www.robotshop.com/uk/spa
		Pololu Dual DC Motor Driver 1A, 4.5V-13.5V- TB6612FNG	2	£2.62	£5.24	https://www.robotshop.com/uk/pol
		Break Away Headers - Straight	1	£1.18	£1.18	https://www.robotshop.com/uk/sfe
		RS PRO 2.85mm White ABS 3D Printer Filament, 500g	1	£21.33	£21.33	https://uk.rs-online.com/web/p/3d-
		Breadboard Prototyping Solderless Breadboard 83 x 147 x 19mm	1	£20.16	£20.16	https://uk.rs-online.com/web/p/bre
		ROHM BA60BC0FP-E2, LDO Regulator, 1A, 6 V, ±2% 3-Pin DPAK	10	£0.42	£4.16	https://uk.rs-online.com/web/p/low
		KEMET 330nF Polyester Capacitor PET 40 V ac, 63 V dc ±5% R82 Series Through Hole	10	£0.16	£1.64	https://uk.rs-online.com/web/p/pol
		Panasonic 22µF 50V dc Aluminium Electrolytic Capacitor, Through Hole 5 (Dia.) x 11mm +105°C 5mm 2mm	5	£0.23	£1.16	https://uk.rs-online.com/web/p/alu
		ENIX Energies 7.5V Wire Lead Terminal Lithium Rechargeable Battery, 2200mAh 2	1	£23.75	£23.75	https://uk.rs-online.com/web/p/lithi
		PQ12 Cable Adapter	2	£2.36	£4.72	https://www.robotshop.com/uk/pq1
		PQ12 Linear Actuator 20mm, 100:1, 6V, Potentiometer	2	£51.18	£102.36	https://www.robotshop.com/uk/firg
					£0.00	
					£0.00	
					£0.00	
					£0.00	

Is a Risk Assessment required for this purchase?	NO	Total excl. VAT:	£230.02
Are special handling/storage requirements necessary?	NO	VAT (20%):	£46.00
s a copy of this form to the Senior Experimental Officer		Total Value incl. VAT:	£276.02

This box to be completed by Purchaser and copy returned to Originator.

Agresso Purchase Order Number: PO Date:

Appendix E

ID	Task Mode	Task Name	Duration	Start	Finish	Predecessors
1		Logbook	261 days	Mon 08/10/18	Mon 07/10/19	
2		Research proposal	51 days	Mon 08/10/18	Mon 17/12/18	
3		Proposal feedback and revision	20 days	Tue 18/12/18	Mon 14/01/19	2
4		Final proposal write-up	5 days	Tue 15/01/19	Mon 21/01/19	3
5		Concept designs	50 days	Tue 22/01/19	Mon 01/04/19	4
6		Design review	5 days	Tue 02/04/19	Mon 08/04/19	5
7		Prototyping	15 days	Tue 09/04/19	Mon 29/04/19	6
8		Further design revision	15 days	Tue 30/04/19	Mon 20/05/19	7
9		Final prototyping	15 days	Tue 21/05/19	Mon 10/06/19	8
10		Control system design	40 days	Tue 21/05/19	Mon 15/07/19	8
11		Testing	10 days	Tue 16/07/19	Mon 29/07/19	10
12		Thesis draft	20 days	Tue 30/07/19	Mon 26/08/19	11
13		Thesis revisoin	30 days	Tue 27/08/19	Mon 07/10/19	12
14		Biorobotics group presentation	0 days	Fri 16/11/18	Fri 16/11/18	
15		Proposal submission	0 days	Fri 18/01/19	Fri 18/01/19	
16		Final thesis submission	0 days	Mon 07/10/19	Mon 07/10/19	
17		ICRA 2019 - Montreal	0 days	Mon 20/05/19	Mon 20/05/19	
18		IROS 2019 Deadline	0 days	Wed 31/07/19	Wed 31/07/19	
19		CLAWAR 2019 - KL	0 days	Mon 02/09/19	Mon 02/09/19	
20		ICRA 2020 Deadline	0 days	Sun 15/09/19	Sun 15/09/19	
21		IROS 2019 - Macau	0 days	Sun 03/11/19	Sun 03/11/19	

Project: Project plan (first draft)
Date: Wed 12/12/18

Task		Inactive Task		Manual Summary Rollup	External Milestone
Split		Inactive Milestone		Manual Summary	Deadline
Milestone		Inactive Summary		Start-only	Progress
Summary		Manual Task		Finish-only	Manual Progress
Project Summary		Duration-only		External Tasks	

Page 1

ID	ⓘ	Task Mode	Task Name	Duration	Start	Finish	Predecessors
1		📌	Logbook	261 days	Mon 08/10/18	Mon 07/10/19	
2		🖥	Research proposal	51 days	Mon 08/10/18	Mon 17/12/18	
3		🖥	Proposal feedback and revision	20 days	Tue 18/12/18	Mon 14/01/19	2
4		🖥	Final proposal write-up	5 days	Tue 15/01/19	Mon 21/01/19	3
5		🖥	Concept designs	50 days	Tue 22/01/19	Mon 01/04/19	4
6		🖥	Design review	5 days	Tue 02/04/19	Mon 08/04/19	5
7	▦	🖥	Prototyping	15 days	Tue 30/04/19	Mon 20/05/19	6
8	▦	🖥	Further design revision	34 days	Tue 21/05/19	Fri 05/07/19	7
9		🖥	Final prototyping	15 days	Mon 08/07/19	Fri 26/07/19	8
10	▦	🖥	Control system design	30 days	Mon 08/07/19	Fri 16/08/19	8
11		🖥	Testing	10 days	Mon 19/08/19	Fri 30/08/19	10
12		🖥	Thesis draft	40 days	Mon 02/09/19	Fri 25/10/19	11
13		🖥	Thesis revision	30 days	Mon 28/10/19	Fri 06/12/19	12
14		📌	Biorobotics group presentation	0 days	Fri 16/11/18	Fri 16/11/18	
15		📌	Proposal submission	0 days	Fri 18/01/19	Fri 18/01/19	
16		📌	Final thesis submission	0 days	Fri 31/01/20	Fri 31/01/20	
17		📌	Prepare ICRA Paper	22 days	Thu 01/08/19	Fri 30/08/19	
18		📌	Prepare CLAWAR Paper	22 days	Fri 01/03/19	Sun 31/03/19	
19		📌	CLAWAR 2019 - KL	3 days	Mon 26/08/19	Wed 28/08/19	
20		📌	ICRA 2020 Deadline	0 days	Sun 15/09/19	Sun 15/09/19	

Project: Project plan (final)
Date: Thu 30/01/20

Task		Inactive Task		Manual Summary Rollup	External Milestone
Split		Inactive Milestone		Manual Summary	Deadline
Milestone		Inactive Summary		Start-only	Progress
Summary		Manual Task		Finish-only	Manual Progress
Project Summary		Duration-only		External Tasks	